8-2010

THE GLYCOPROTEINS OF PORCINE REPRODUCTIVE AND RESPIRATORY SYNDROME VIRUS AND THEIR ROLE IN INFECTION AND IMMUNITY

Phani B. Das
University of Nebraska-Lincoln, pdas2@unl.edu

THE GLYCOPROTEINS OF PORCINE REPRODUCTIVE AND RESPIRATORY SYNDROME VIRUS AND THEIR ROLE IN INFECTION AND IMMUNITY

by

Phani Bhusan Das

A DISSERTATION

Presented to the Faculty of

The Graduate College at the University of Nebraska

In Partial Fulfilment of Requirements

For the Degree of Doctor of Philosophy

Major: Integrative Biomedical Sciences

Under the Supervision of Professor Asit K. Pattnaik

Lincoln, Nebraska

August, 2010

THE GLYCOPROTEINS OF PORCINE REPRODUCTIVE AND RESPIRATORY SYNDROME VIRUS AND THEIR ROLE IN INFECTION AND IMMUNITY

Phani Bhusan Das, Ph.D.

University of Nebraska, 2010

Adviser: Asit K. Pattnaik

The porcine reproductive and respiratory syndrome virus (PRRSV) is an economically important pathogen of swine and is known to cause abortion and infertility in pregnant sows and respiratory distress in piglets. PRRSV contains a major glycoprotein (GP5) and three minor glycoproteins (GP2a, GP3, and GP4) on the virion envelope, all of which are required for infectious virus production. To study their interactions amongst each other and with a cellular receptor for PRRSV, CD163, I cloned each of the viral glycoproteins and CD163 in various expression vectors. My studies have shown that while the GP2a, GP3, and GP4 are co-translationally glycosylated, the GP5 is post-translationally glycosylated. By using co-immunoprecipitation (co-IP) assays, strong interaction was demonstrated between GP4 and GP5 proteins, although weak interactions among the other envelope glycoproteins were also detected. Further, GP4 was found to mediate interactions leading to formation of multiprotein glycoprotein complex. My results also show that GP2a and GP4 proteins are the only two GPs that specifically interact with the CD163 molecule and that glycosylation of these GPs is required for efficient interaction. Based on these studies, I have developed an interactome map of the viral GPs and CD163 and have proposed a model of the viral glycoprotein complex and

its interaction with CD163. Studies reported here also show that glycan addition at residue 184 (N184) of GP2a, and residues N42, N50, and N131 of GP3 is essential for recovery of infectious virus. Although single site glycosylation mutants of GP4 had no effect on infectious virus production, introduction of double mutations was lethal. The loss of glycan moieties of GP2a, GP3, and GP4 proteins had no effect on host neutralizing antibody production. Overall, I conclude that the PRRSV glycoproteins are co-translationally and post-translationally glycosylated, the GP4 protein is central to mediating interglycoprotein interactions, and along with GP2a, serves as the viral attachment protein that is responsible for interactions with the viral receptor, CD163. Further, glycosylation of GP2a, GP3, and GP4 proteins is required for infectious virus production, efficient interaction with CD163, but does not play any role in neutralizing antibody response in infected animals.

ACKNOWEDGMENTS

It is a pleasure to thank those who made this thesis possible.

It is difficult to overstate my gratitude to my PhD adviser, Dr. Asit K. Pattnaik. With his enthusiasm and inspiration, he made research an enjoyable experience for me. Throughout out my graduate study period he provided sound advice, encouragement, and lots of interesting ideas. He taught me how to design experiments and write manuscripts. Also, he taught me to be patient and persistent while solving research related problems.

I would like to thank my committee members, Dr. Fernando A. Osorio, Dr. Luwen Zhang, and Dr. Clinton Jones for providing several suggestions for improvement in research. I want to specially thank Dr. Osorio for his contributions during my manuscript preparations.

I am indebted to my current and former lab members for providing a stimulating and fun environment in which to learn and grow. I am grateful to Israrul H. Ansari, Jonathan Cooney, Jackson Turner, Phat Dinh, Debasis Nayak, Subash Das, Debasis Panda, and Zhi Hong Gill. Israrul was especially helpful for patiently teaching me different laboratory techniques.

I want to thank my best friend in life (Laxmi P. Nayak) and other friends: Derek Gyllenhammer, Bhopal Mohapatra, Shantibhusan Senapati, Prasanta Dash, Arabinda

Nayak, Pradyot Dash, Lalit Beura, Rajeshwari Parida, Trista Fuchs, Ashley Haile, and Adam Rogers for helping me to get through the difficult times and providing encouragement throughout my graduate study.

Lastly, and most importantly, I want to thank my parents, brothers, and other family members for providing unconditional support to pursue my interests and providing me wise advice in several circumstances. I dedicate the thesis to my parents.

Phani B. Das

University of Nebraska-Lincoln

August 2010

Table of Contents

Table of Contents (continued)

Table of Contents (continued)

Table of Contents (continued)

Table of Contents (continued)

Table of Contents (continued)

Table of Contents (continued)

List of Figures

List of Figures (continued)

List of Figures (continued)

List of Figures (continued)

List of Figures (continued)

List of Tables

Abbreviations

A	Alanine
CBP	CREB binding protein
Co-IP	Co-immunoprecipitation
CPE	Cytopathic effect
CTE	Carboxy terminal of extension
dsRNA	Double stranded RNA
EAV	Equine arteritis virus
ER	Endoplasmic reticulum
GP	Glycoprotein
h	Hour (s)
HIV	Human immunodeficiency virus
IFN	Interferon
kDa	Kilodaltons
LDV	Lactate dehydrogenase-elevating virus
M protein	Matrix protein
min	Minutes(s)
MOI	Multiplicity of infection
N	Asparagine
N protein	Nucleocapsid protein
NendoU	Nidoviral endonucleae specific for U

Abbreviations (continued)

NLS	Nuclear localization signal
NSP	Non-structural protein
ORF	Open reading frame
OST	Oligosaccharyl transferase
OTU	Ovarian tumor
PAM	Porcine alveolar macrophage
PCP	Papain like cysteine protease
PFU/ml	Plaque forming unit/milliliter
PRRSV	Porcine reproductive and respiratory syndrome virus
RdRp	RNA dependent RNA polymerase
SDS-PAGE	Sodium dodecyl sulfate-polyacrylamide gel electrophoresis
sg mRNA	Sub-genomic messenger RNA
SRCR	Scavenger receptor cysteine-rich
SHFV	Simian hemorrhagic fever virus
SIV	Simian immunodeficiency virus
$TCID_{50}$	Tissue culture infectious dose 50
TRS	Transcription regulating sequences
UTR	Untranslated region
WT	Wild type

Chapter I: INTRODUCTION

1.1 Economic importance and pathogenesis of PRRSV

Porcine reproductive and respiratory syndrome virus (PRRSV) is endemic in pork producing countries worldwide. Infection of pigs with the virus can result in PRRS disease leading to significant economic losses to the swine industry. PRRSV causes respiratory disorders leading to pneumonia and is responsible for mortality observed in young piglets. The virus also infects pregnant sows causing several reproductive disorders resulting in abortion, infertility, mummified fetuses, stillborn piglets etc. Initially, this disease was reported in USA and later discovered in Netherlands and other parts of the world (Benfield et al., 1999; Paton et al., 1991).

PRRSV replication occurs in macrophages and the infected pigs show prolonged viremia and continue to shed the virus for long period (up to 2-5 months) (Snijder & Spaan, 2007). But, the virus does not enter a latent stage (Kimman et al., 2009). In case of postnatally infected pigs, the virus persists up to 150 days whereas in congenitally infected pigs, it persists up to 210 days (Cho & Dee, 2006). Persistent infection of PRRSV is observed in lungs, tonsils, and lymphoid organs of pigs (Lamontagne et al., 2003).

1.2 Ultrastructure and morphology of PRRSV

Mature PRRSV particles are enveloped and pleomorphic. They have spherical to oval shape with a diameter of 50-65 nm (Spilman et al., 2009). The cryoelectron microscopy tomographic studies have shown a smooth outer surface of the virion with few protruding structures. The virion has a double layer hollow core of ~ 40 nm in

diameter, which remains separated from the envelope by 2-3 nm gap (Spilman et al., 2009).

1.3 Classification of PRRSV

PRRSV along with equine arteritis virus (EAV), simian hemorrhagic fever virus (SHFV) and lactate dehydrogenase-elevating virus (LDV) is grouped under family *Arteriviridae* and the order *Nidovirales* based on their similar genome organization and replication strategy (Snijder & Meulenberg, 1998). PRRSV is classified into two genotypes: genotype I (European genotype) and genotype II (North American genotype). These two genotypes share approximately 60% of genome sequence homology (Forsberg, 2005; Hanada et al., 2005) and are serologically distinct (Kim & Yoon, 2008). The European and North American strains of PRRSV can also be differentiated from each other based on common and type specific antigenic determinants present on the structural proteins (Dea et al., 2000).

1.4 Genome organization and proteins of PRRSV

The genome of PRRSV is approximately 15.4 kb in length. The genome contains a methylated cap structure at the 5' end, the 3' end is polyadenylated, and untranslated regions (UTRs) are present at both termini (Meulenberg *et al.*, 1993; Snijder & Meulenberg, 1998; Wootton *et al.*, 2000). It has nine open reading frames (ORFs) (Fig. 1.1A). All the ORFs overlap with each other except between ORF1b and ORF2a. ORF1a and ORF1ab, which is accessed by ribosomal frame-shifting during protein synthesis (Snijder & Meulenberg, 1998) together span approximately 75% of the genome from the 5'-end. These ORFs produce polyproteins that are processed by different viral proteases encoded in the ORF1a region to generate a total thirteen to fourteen non-structural

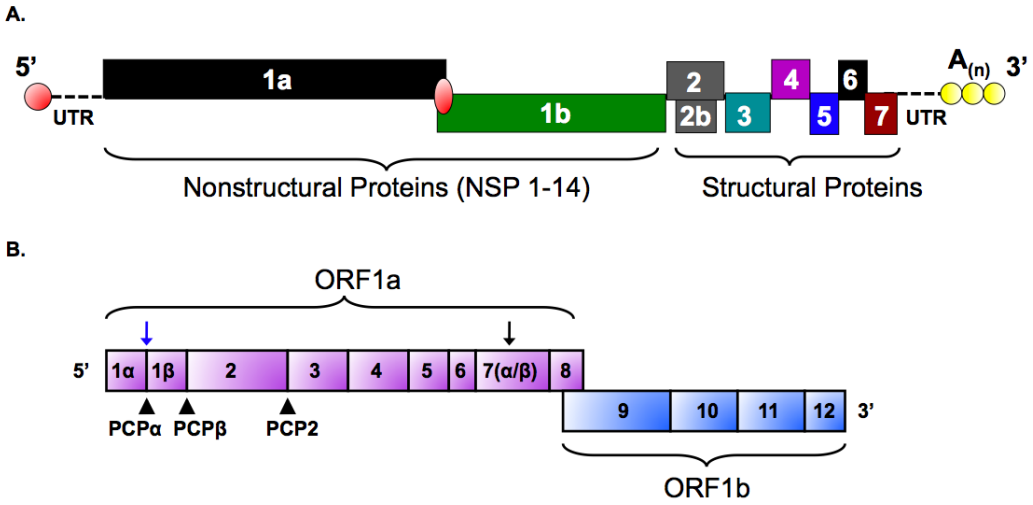

Figure 1.1 Schematic representation of PRRSV genome organization. (A) Overview of the genome organizations. The ORFs are shown as solid rectangles from 5' to 3' end with the appropriate ORF named on it. The ORF encoding NSPs and structural proteins are labeled accordingly. The replicase ORFs (ORF1a and ORF1b) are followed by ORF encoding 2b protein and three ORFs encoding three minor envelope glycoproteins (GP2a, GP3, and GP4), and ORFs encoding major structural proteins (GP5, M, and N). The 5' cap and 3' poly (A) tail is shown. The 5' and 3' UTRs are shown as dotted lines in each end of the genome. (B) Overview of the ORFs encoding NSPs of PRRSV. ORF1a and ORF1b are labelled and NSPs encoded by each of the ORFs are shown. The cleavage site of NSP1 to NSP1α and NSP1β are indicated by blue downward arrow where as the predicted cleavage site of NSP7 to NSP7α and NSP7β are shown as black downward arrow. The cleavage site of PLPα, PLPβ, and PLP2 are indicated by black upward arrow.

proteins (NSPs), named NSP1α, NSP1β, and NSP 2-6, NSP7α, NSP7β, and NSP8-12 (Kroese et al., 2008; Meulenberg, 2000; van Aken et al., 2006). The NSPs are involved in processing of the viral polyproteins, genome replication, and transcription (Meulenberg, 2000). The ORFs 2a, 2b, 3-7 encompass approximately 25% of the genome at the 3'-end and they produce the viral structural proteins, namely, the glycoprotein (GP) 2a (GP2a), non-glycosylated protein 2b (or E), GP3, GP4, GP5, the matrix protein (M), and the nucleocapsid protein (N), respectively (Wu et al., 2005).

1.5 Non-structural proteins of PRRSV

The ORF1a and ORF1b are connected with each other by -1 ribosomal frame shift site and upon translation it produces a large polyprotein (Fig. 1.1A). Ribosomal frame shifting is regulated by specific RNA signals called 'slippery sequence' (at the actual frame shift site) and a pseudoknot structure downstream of the frame shift site in the virion (Godeny *et al.*, 1993; Meulenberg *et al.*, 1993; Snijder & Meulenberg, 1998). It results in carboxy terminal extension of a relatively small fraction of ORF1a gene product (polyprotein-1a) with ORF1b gene product producing polyprotein-1ab. This protein is further cleaved by the four autoproteanases (NSP1α, NSP1β, NSP2, and NSP4) to produce 13 to 14 non-structural proteins (Fig 1.1B). The NSP1 cleaves to form NSP1α and NSP1β (den Boon et al., 1995; Kroese et al., 2008; Sun et al., 2009). The cleavage of NSP7 to NSP7α and NSP7β for PRRSV was predicted based on the similar observation in its counterpart of EAV (van Aken et al., 2006). The NSP1α, NSP1β, and NSP2 release from polyprotein-1a (or, polyprotein-1ab) first and then NSP4 (3C like protease) cleaves each of the rest 7 to 8 NSPs from the polyprotein (Sun *et al.*, 2009; Ziebuhr *et al.*, 2000).

The NSP1α and NSP1β cleavage site is important for PRRSV genome replication. The NSP1α of PRRSV is important for subgenomic mRNA synthesis whereas, NSP1β is mostly required for genome replication (Kroese et al., 2008). Both NSP1α and NSP1β have papain like cysteine protease (PCP) domain known as PCPα and PCPβ respectively which are required for their autoproteinase activity (Kroese et al., 2008; Xue et al., 2010). The NSP1α-NSP1β cleavage occurs between Met and Ala amino acids of putative cleavage sites Cys-Ala-**Met^{180}-Ala-**Asp-Val and the carboxy terminal PCP domain are required for this cleavage (Kroese et al., 2008; Xue et al., 2010). The crystal structure of analysis of NSP1α shows existence of zinc finger domain in its amino terminus, PCP domain, and carboxy terminal of extension (CTE). Also, NSP1α was shown to exist as a dimer (Sun et al., 2009). The zinc binding domain is present in the active site of PCPα (Sun et al., 2009). The crystal structure of NSP1β was recently solved (Xue et al., 2010). The amino terminus of NSP1β has divalent cation (Mg^{2+} and Mn^{2+}) dependent nuclease activity (Xue et al., 2010). The NSP1β cleaves between NSP1β and NSP2 at Gly and Ala of putative cleavage site Trp-Trp-**Gly^{203}-Ala-**Gly-Lys (Kroese et al., 2008; Xue et al., 2010).

The NSP2 protein of PRRSV contains an amino terminus cysteine protease domain which is required for NSP2 and NSP3 cleavage. Also, NSP2 functions as cofactor in the protease activity of NSP4 for cleavage of the polyprotein-1a and polyprotein-1b (Snijder *et al.*, 1994; Snijder *et al.*, 1995; Wassenaar *et al.*, 1997). B cell epitope mapping studies (de Lima et al., 2006) have shown the existence of more immunodominant epitopes in the NSP2 in comparison to other structural proteins of

PRRSV. Also, NSP2 region is more tolerant to larger amino acid deletions and insertions (Fang et al., 2008; Han et al., 2007; Ran et al., 2008; Shen et al., 2000).

Out of all 14 NSPs, NSP9 (RNA dependent RNA polymerase, RdRp), NSP10 (helicase), NSP11 (a *Xenopus laevis* homolog poly [U] specific endoribinuclease known as nidoviral endonucleae specific for U [NendoU]), and NSP12 are encoded by ORF1b of PRRSV (Fig.1.1B). The RdRP and helicase are required replication and transcription of PRRSV RNA genome (Snijder & Meulenberg, 1998). The NendoU protein possesses pyrimidine specific endoribonuclease activity. This protein of PRRSV is required for cleavage of U stretches in the RNA substrate in divalent cations (Mn^{2+}) independent manner releasing 2'-3'-cyclic phosphodiester products (Nedialkova et al., 2009).

Besides role of different NSPs of PRRSV in RNA genome transcription and replication, recent reports also emphasized their role in suppression of host innate immune response. NSP1α, NSP1β, NSP2, NSP4, and NSP11 antagonize IFN response and inhibit activation of IFN-β promoter activity (Beura et al., 2010; Chen et al., 2010; Kim et al., 2010). NSP1β inhibits double stranded RNA (dsRNA) induced phosphorylation and nuclear translocation of IRF3 (Beura et al., 2010). NSP1 also degrades CREB binding protein (CBP) and downregulates enhanceosome assembly. This in turn inhibits IFN response in PRRSV infected cells (Kim et al., 2010). The cysteine protease of NSP2 of PRRSV belongs to ovarian tumor (OTU) protease superfamily which is required for inhibition of ubiquitin mediated and ISG15 mediated host innate immune response (Frias-Staheli et al., 2007).

1.6 Structural proteins of PRRSV

PRRSV has seven structural proteins. They are GP2a, 2b (E), GP3, GP4, GP5, M, and N protein (Fig. 1.2). GP2a, GP3, GP4, and GP5 are N-glycosylated and are present on the viral envelope (Dea et al., 2000) as are the non-glycosylated M protein and 2b proteins. GP5, M, and N proteins are known as major structural proteins whereas, GP2a, 2b (E), GP3, and GP4 proteins are regarded as minor structural proteins. All the major and minor envelope proteins are required for generation of infectious PRRSV (Wissink et al., 2005).

1.6.1 Nucleocapsid (N) protein

In the infected cells, the N protein is the most abundant viral protein (Dea *et al.*, 2000; Snijder & Meulenberg, 1998). It constitutes 40% of the total mass of the virion. It is a basic protein with an isoelectric point of 10.4 (Snijder & Meulenberg, 1998; Wootton *et al.*, 2002) and molecular mass of approximately 15kDa. It is encoded by ORF7 and exists as a dimer (Dea *et al.*, 2000; Mardassi *et al.*, 1996; Meulenberg *et al.*, 1995). Homodimerization of the N protein occurs in the endoplasmic reticulum (ER) and the Golgi complex through disulfide linkage via cysteine residue at position 23 in North American strain and cysteine-27 in European isolates (Wootton & Yoo, 2003). Cysteine-23 position is required for infectious virus production and replication of viral genome (Lee et al., 2005). PRRSV replicates in the cytoplasm. Besides localization of the N protein in the cytoplasm and perinuclear region, nuclear localization of this protein has also been observed due to presence of a nuclear localization signal (NLS). Dimerization of the N protein does not appear to be required for nuclear translocation

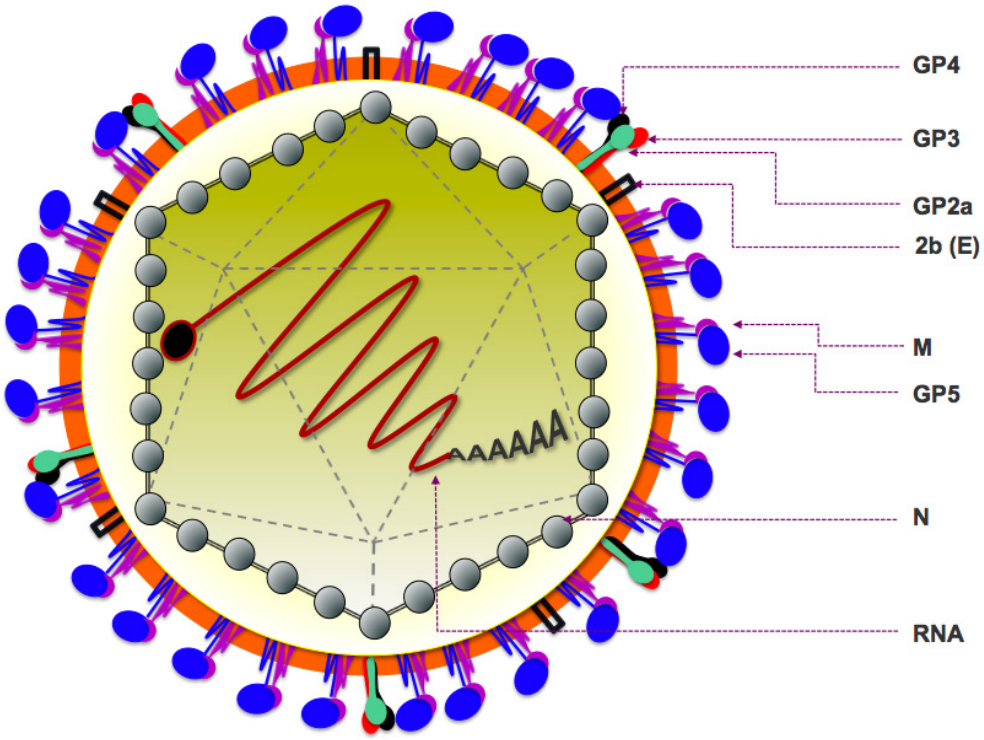

Figure 1.2 Schematic representation of PRRSV particle. The location of structural proteins GP2a, 2b (E), GP3, GP4, GP5, M, and N are shown. GP5 and M are shown to exist as heterodimeric complexes. GP2a, GP3, and GP4 are shown as heterotrimers. The PRRSV RNA genome with 5' cap and 3' poly (A) tail is shown. The RNA is encapsidated by N protein.

(Lee et al., 2005). For efficient virus genome replication, nuclear localization of the N protein is not required (Lee et al., 2006). Out of two NLS at amino acid positions 10-13 (NLS-1) and 41-47 (NLS-2) of the N protein, NLS-2 is required for nuclear localization (Rowland & Yoo, 2003). The N protein probably localizes to the nucleus because of an interaction between NLS and nuclear transporters, importin-α and importin-β (Rowland et al., 2003). The N protein has a role in ribosome biogenesis because it binds to the 28S and 18S ribosomal RNA (Yoo et al., 2003). The N protein of the North American strain of PRRSV has 123 amino acids and the European strain has 128 amino acids (Snijder & Meulenberg, 1998; Wootton *et al.*, 2002). The N protein of both North American and European strains of PRRSV has a common antigenic region between amino acids 52 and 69 (Meulenberg et al., 1998; Rodriguez et al., 1997). The N protein is a serine phosphoprotein and is highly immunogenic, but it does not produce neutralizing antibodies (Kimman *et al.*, 2009; Wootton *et al.*, 2002). Overall, the N protein promotes virus assembly in the cytoplasm and its role in the nucleus (and nucleolus) in the infected cell is not known (Lee et al., 2006).

1.6.2 GP5

The GP5 is the most abundant glycoprotein found on the surface of the virion. It has a predicted signal sequence at its amino terminus. The protein has a ectodomain of 40 amino acids, cytoplasmic domain of 50-72 amino acid, and spans the membrane three times (Kimman *et al.*, 2009; Mardassi *et al.*, 1996; Meulenberg *et al.*, 1995). The M and GP5 proteins form heterodimers within the ER (Mardassi *et al.*, 1996). In EAV, it has been shown that heterodimerization of M and GP5 is important for envelope assembly and virus infectivity (Snijder *et al.*, 2003) and by analogy, heterodimerization of these

proteins in PRRSV is also presumed to play a similar role. GP5 has three N-glycosylation sites in North American strains (Fig. 1.3) whereas European strains of PRRSV have two N-glycosylation sites (Ansari et al., 2006; Wissink et al., 2004). Previous studies have shown that the glycan moities are required for protection against host neutralizing antibody response and virus production (Ansari et al., 2006).

1.6.3 Matrix (M) protein

M protein is unglycosylated and is the most conserved structural proteins among the Arteriviruses (Kimman et al., 2009). It has a molecular weight of 18 to 19 kDa (Dea et al., 2000), a short ectodomain of 10-18 amino acids, and amino terminal domains span the membrane three times. As described previously, the M protein is involved in heterodimer formation with GP5 through disulfide linkage in the amino terminus of both the proteins in the ER (Mardassi *et al.*, 1996). Though it is not clear, M protein was predicted to play an important role in virus assembly and budding.

1.6.4 GP2a

The GP2a protein of PRRSV has two N-glycosylation sites (Fig. 1.3) and has a molecular size of 29-30 kDa (Dea et al., 2000). This protein along with 2b protein are synthesized from the same bicistronic mRNA2 (Fig. 1.4) (Lee & Yoo, 2006). Both the glycosylation sites of European strains of PRRSV are dispensable or virus production (Wissink et al., 2004). However, my recent studies with type II North American isolate of PRRSV (reported in this thesis in chapter V) have revealed that the glycan addition at amino acid position 184 of GP2a is important for production of infectious virus. In addition, this protein also interacts with the PRRSV receptor CD163 (Das et al., 2010).

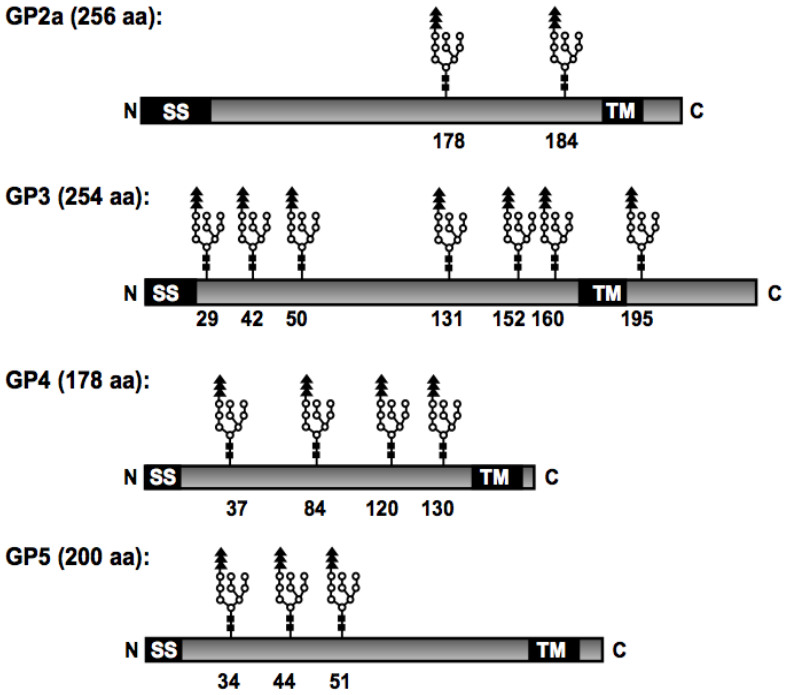

Figure 1.3 schematic representations of GP2a, GP3, GP4, and GP5 proteins. The proteins with their size in amino acids shown. Potential N-linked glycosylation sites (with residue number on bottom of the rectangular boxes), predicted signal sequences (SS) and transmembrane regions (TM) are shown. The amino (N) - and the carboxy (C) - termini are identified.

1.6.5 E (2b)

It is a non-glycosylated, hydrophobic protein of 73 amino acids in case of North American strain and 70 amino acids in case of European strain. This protein is encoded from the internal ORF starting at +6 nucleotide position of the bicistronic mRNA2 (mRNA for GP2a protein) (Lee & Yoo, 2006). The 2b protein of PRRSV also forms homo-oligomers by non-covalent interactions (Lee & Yoo, 2005; 2006). Though this protein is dispensable for virus assembly and particle formation, it is required for virus infectivity (Lee & Yoo, 2006). The 2b (or E) protein possesses ion-channel like properties and may function as a viroporin on the envelope (Lee & Yoo, 2006). After entry and transport of virus particle to the endosome, conformational changes occur due to the lower pH. This further exposes 2b and let it function as ion channel. The 2b protein is required for virus uncoating because it allows ions to enter the virion, triggers internal capsid disassembly, and promotes virus release into the cytoplasm (Lee & Yoo, 2006). The 2b protein associates with intracellular membranes and localizes around perinuclear regions including ER and the Golgi complex (Lee & Yoo, 2006).

1.6.6 GP3

It is highly N-glycosylated envelope protein with seven predicted glycosylation sites (Fig. 1.3) (Dea et al., 2000), but studies reported in this thesis (chapter V) show that only six of these glycosylation sites are used for glycan addition. It has a molecular mass of 42-45 kDa (de Lima et al., 2009; Dea et al., 2000). The coding sequence of GP3 is highly variable among different strains of PRRSV and most of the variability occurs at the amino terminus of the protein (Katz *et al.*, 1995; Mardassi *et al.*, 1995; Murtaugh *et al.*, 1995). Although early studies reported that the GP3 protein is not a structural

component of the North American (genotype II) PRRS virions (Gonin et al., 1998; Mardassi et al., 1998), recent studies from our laboratory have shown that it is present on the virion envelope (de Lima et al., 2009), an observation consistent with the European (genotype I) PRRS virions (van Nieuwstadt et al., 1996).

1.6.7 GP4

It has four N-glycosylation sites (Fig. 1.3) and has a molecular mass of 29-35 kDa (Das et al., 2010; Meulenberg et al., 1997). The neutralizing epitopes of GP4 protein in North American and European strains are not well conserved (Dea et al., 2000).The most variable region for neutralizing epitopes of GP4 for Lelystad virus is between amino acids 40 and 79 (Meulenberg et al., 1997). Recent studies from our laboratory (Das et al., 2010), demonstrated that GP4 interacts with the PRRSV receptor CD163. A detailed description of this interaction is described in this thesis (chapter IV).

1.7 Multimeric complex formation of PRRSV envelope proteins

Previous studies with both PRRSV and EAV have shown that the minor envelope glycoproteins GP2a, GP3 and GP4 and the unglycosylated 2b protein form a heterotetrameric complex in infected cells and formation of such a complex is required for the transport of these proteins from the endoplasmic reticulum (ER) to the Golgi apparatus in infected cells prior to virion assembly (Wieringa et al., 2004; Wissink et al., 2005). Furthermore, the GP5 and M proteins of EAV and the homologous proteins of LDV form a heterodimer through disulfide bonds, which is required for viral infectivity (Balasuriya & MacLachlan, 2004; Faaberg *et al.*, 1995; Snijder *et al.*, 2003; Snijder & Meulenberg, 1998). This heterodimeric GP5-M protein interaction is required for proper post-translational processing of the proteins and the N-linked glycosylation of GP5 is not

required for GP5-M heterodimer formation (Mardassi *et al.*, 1996). Although the envelope glycoproteins form multimeric complexes, the specific interactions among these glycoproteins and how the interactions result in formation of the large multimeric complex is currently unknown.

1.8 Cell tropism and receptors of PRRSV

PRRSV infects mostly alveolar macrophages of the lung. But, it does not replicate in nonactivated monocytes (Thanawongnuwech et al., 2001). The virus also infects other cells of monocyte and macrophage lineage including pulmonary intravascular macrophages, intravascular macrophages of placenta and umbilical cord, and subsets of macrophages in lymph nodes and spleen (Duan *et al.*, 1997; Lawson *et al.*, 1997).

PRRSV has tropism for porcine alveolar macrophage (PAM) cells and sialoadhesin expressed on the surface of these cells is a receptor for PRRSV (Delputte *et al.*, 2005; Delputte & Nauwynck, 2004; Delputte *et al.*, 2007). PRRSV has only been found to infect and replicate to high levels in MARC-145 cells (Kim et al., 1993), a derivative of the African green monkey kidney cell line MA-104. However, MARC-145 cells do not express sialoadhesin, indicating that molecules other than sialoadhesin promote entry of PRRSV in MARC-145 cells. Although several other molecules like vimentin, CD151, heparan sulfate have been identified as potential entry molecules for PRRSV (Kim *et al.*, 2006; Shanmukhappa *et al.*, 2007), recently porcine CD163 isolated from PAM cells was found to confer susceptibility to PRRSV infection to non-permissive cells (Calvert et al., 2007). A detailed description of different receptors and cofactors identified for PRRSV infection is described below:

1.8.1 Heparan sulfate

Heparan sulfate was reported as the receptor for PRRSV in MARC-145 cells (Jusa et al., 1997) and PAM cells (Delputte et al., 2002; Vanderheijden et al., 2001). Either incubation of PRRSV with heparin or treatment of cells with heparinase I (an enzyme that cleaves heparin and heparan sulfate) before inoculation with the virus decreased virus infectivity (Delputte et al., 2002; Jusa et al., 1997; Vanderheijden et al., 2001). But, complete block to viral infection was not achieved indicating that this receptor is not the only receptor. Heparan sulfate is not macrophage specific and found in different animal tissues. It is assumed that the heparan sulfate molecules present on the surface of macrophage act as PRRSV attachment factors that helps in concentration of virion on the cell surface (Delputte *et al.*, 2005). The M and N proteins of PRRSV can interact with heparan sulfate. The M protein binds with heparan sulfate mainly as a complex with GP5 whereas the N protein binds with heparan sulfate as a homodimer (Delputte et al., 2002).

1.8.2 Sialoadhesin

It is a macrophage specific type I transmembrane glycoprotein of 210 kDa in molecular mass. It is a prototype member of family of sialic acid binding lectins known as siglecs (Munday *et al.*, 1999). Porcine sialoadhesin is considered as the attachment and internalization receptor since expression of this protein in non-permissive mammalian cells lead to binding and internalization of PRRSV but not productive viral infection (Vanderheijden et al., 2003). The sialic acid binding activity of porcine sialoadhesin is important for its function as the receptor for PRRSV. The amino terminal immunoglobulin like V-set domain of porcine sialoadhesin is important for its binding

with PRRSV (Delputte et al., 2007). Mostly α2-3 linked and to a lesser extend α2-6 linked sialic acids present on the PRRSV envelope are required for binding of the virus with sialoadhesin (Delputte et al., 2007). The M and GP5 heterodimeric complex of PRRSV interacts with porcine sialoadhesin receptor (Van Breedam et al., 2010).

1.8.3 Cellular proteases

Aspartic proteases cathepsin E and unidentified serine proteases are implicated in PRRSV infection of macrophages (Misinzo *et al.*, 2008). Their role in the virus life cycle is predicted to enhance virus uncoating (Misinzo *et al.*, 2008). PRRSV partially colocalizes with cathepsin E and there is existence of positive correlation between cathepsin E and PRRSV infection (Misinzo *et al.*, 2008). Expression of cathepsin E is restricted to certain cell types and generally it is found in non-lysosomal compartments such as endosomes, ER, and Golgi complex (Maric *et al.*, 1994; Rawlings & Barrett, 1995; Sastradipura *et al.*, 1998). These proteases probably do not act as receptor of PRRSV, but their protease activity may be needed to cleave yet unidentified PRRSV GPs for uncoating as observed for Ebola virus (Chandran *et al.*, 2005; Kaletsky *et al.*, 2007).

1.8.4 Simian Vimentin

Vimentin is associated with cytoskeletal component of cells. Simian vimenin is present both in the cytoplasm as well as in the plasma membrane of MARC-145 cells (Kim et al., 2006) and appears to be a receptor for PRRSV in these cells. It also interacts with the N protein of PRRSV and may regulate virus association with other cytoskeletal components and enhance transport in the cytoplasm (Kim et al., 2006).

1.8.5 CD151

CD151 is a member of the tetraspanin superfamily and has important roles in cell signalling and platelet aggregation (Fitter et al., 1999; Hasegawa et al., 1998; Roberts et al., 1995; Sincock et al., 1999). It interacts with the 3' UTR of the virus and is an important cofactor for PRRSV infection in MARC-145 cells (Shanmukhappa *et al.*, 2007).

1.8.6 CD163

Recently, porcine CD163 isolated from PAM cells was found to confer susceptibility for PRRSV infection to non-permissive cells (Calvert et al., 2007; Das et al., 2010). Additionally, CD163 is also expressed in MARC-145 cells, suggesting that it facilitates entry of PRRSV in these cells. CD163 is a type I transmembrane protein that belongs to a scavenger receptor super family. It is mostly expressed in cells of monocyte and macrophage lineage. It was earlier reported that porcine sialoadhesin and CD163 act co-operatively for productive virus infection (Van Gorp et al., 2008). The major role of CD163 was predicted to be in virus uncoating and genome release instead of attachment (Van Gorp et al., 2008). Out of nine scavenger receptor cysteine-rich (SRCR) domains of porcine CD163, the 5^{th} SRCR domain is the most important for PRRSV infection (Van Gorp et al., 2010). The 6^{th} SRCR domain and two proline-serine-threonine (PST) rich interdomains of porcine CD163 also positively influence PRRSV infection (Van Gorp et al., 2010). Additionally, I have observed that the carboxy terminus 223 amino acids are required for PRRSV entry (chapter IV) (Das et al., 2010).The GPs on the virion envelope may interact with CD163 to mediate virus entry into these cells. At the present time, it is unknown which of the viral envelope glycoproteins directly interact with CD163 to

mediate virus entry into susceptible cells. Studies reported in this thesis (chapter IV) demonstrated that GP2a and GP4 proteins of PRRSV interact directly with CD163 (Das et al., 2010).

Since GP5 protein is an abundant protein within the PRRSV envelope, it may play a role in interacting with the cell surface receptor for PRRSV entry. However, studies in which the ectodomains of the GP5 and M proteins of EAV were replaced with the ectodomains of the corresponding proteins from PRRSV or LDV in EAV infectious clone, the resulting chimeric EAV did not exhibit the altered tissue tropism, indicating that the GP5 protein may not be the PRRSV envelope protein that interacts with the receptor (Dobbe et al., 2001; Verheije et al., 2002). This finding suggests that other PRRSV envelope glycoproteins, especially, the minor envelope glycoproteins of PRRSV, also mediate receptor interaction and virus entry.

1.9 Entry and uncoating of PRRSV

Upon PRRSV binding with specific receptor(s), the virus internalizes via clathrin mediated endocytosis (Nauwynck et al., 1999). Release of the virus genome depends on the low pH of the endocytic compartment (Kreutz & Ackermann, 1996). After PRRSV entry, it enters early endosomes (pH 6-6.5) and releases its genome (Kreutz & Ackermann, 1996; Nauwynck *et al.*, 1999).

1.10 Replication and Transcription of PRRSV

PRRSV genome replication occurs in the cytoplasm of the infected cell. A schematic of PRRSV genome replication and transcription is shown in Fig. 1.4. This is derived from the current knowledge of *Nidovirales* genome transcription and replication (Snijder & Spaan, 2007). The RdRp enzyme complex recognises the RNA signals near

the 3' end of the positive stranded viral genome and initiates replication to generate the full-length minus strand anti-genome (Pasternak *et al.*, 2006). The minus-strand again acts as template for genomic RNA synthesis. Specific cis-signals present on the 3' end of both the genomic and the anti-genomic RNA are required for replication (Godeny *et al.*, 1993; Meulenberg *et al.*, 1993; Snijder & Meulenberg, 1998). The newly synthesized genomic RNA acts as the template for both synthesis of more anti-genome RNA as well as sub-genomic length minus-strands (Snijder & Meulenberg, 1998). PRRSV RNA synthesis is asymmetric. During genome replication, more plus stranded RNA is synthesized than minus stranded RNA (Sawicki *et al.*, 2001). Sub-genomic messenger RNA (sg mRNA) is mostly synthesized from full-length minus-strand anti-genome in non-equimolar but constant amounts (Fig. 1.4, step 6). But, there are also reports of sg mRNA synthesis from sub-genomic length minus strand templates (Pasternak *et al.*, 2006; Sawicki *et al.*, 2001; Sawicki & Sawicki, 2005). The ratio of synthesis of genomic RNA to sg mRNAs remains constant throughout the replication cycle. The sg mRNAs of PRRSV have 3' co-terminal sequences (nested set of mRNAs) and common 5' leader sequence of 65-100 nucleotides in length (Lai *et al.*, 1983; Lai *et al.*, 1982). All of the sg mRNAs of PRRSV except the smallest one (sg mRNA for N protein) are polycistronic. But, during translation only the 5' ORF of the genome gets translated (Pasternak *et al.*, 2006).

For PRRSV sg mRNA synthesis, discontinuous transcription occurs in which case the leader sequences of mRNA fuses co-transcriptionally with the body of mRNA (Pasternak *et al.*, 2006). Transcription regulating sequences (TRS) play an important role for fusion of leader and body sequences of mRNA

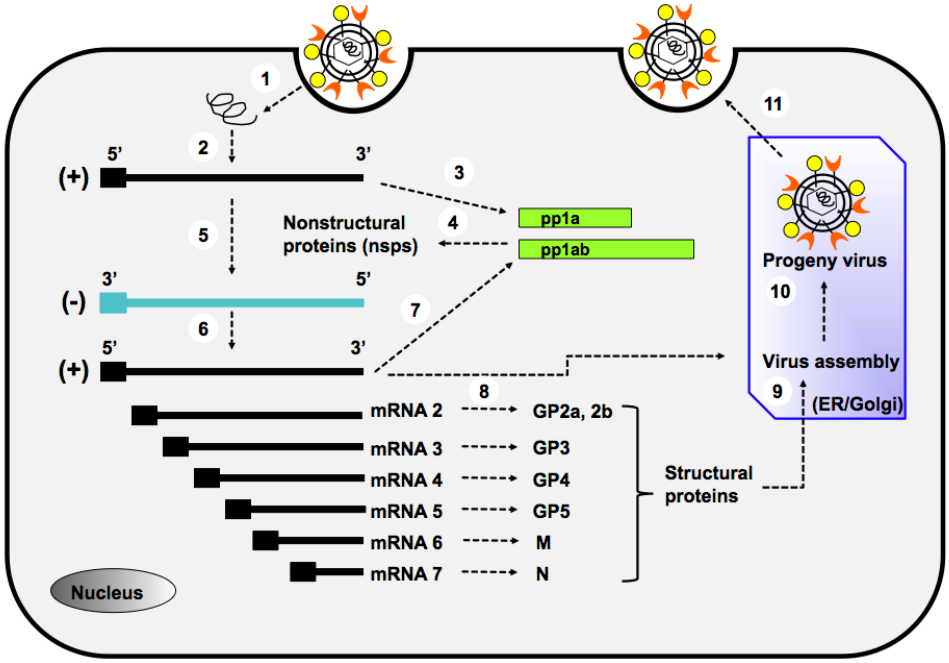

Figure 1.4 Overview of life cycle of PRRSV. After entry (by receptor mediated endocytosis) and uncoating (step 1), the + sense genomic RNA acts as mRNA for synthesis of NSP polyprotein complex polyprotein-1a and polyprotein-1b (step 2 and 3), which further gets cleaved by viral proteases to produce 13-14 NSPs (step 4). The NSPs (especially RdRp) catalyses replication of genomic RNA to produce full-length antigenomic RNA (step 5) and transcription to produce 8 sub-genomic mRNAs (sg mRNAs) (step 6). The longest sg mRNA (+ sense genome) can be used either as mRNA template for NSP polyprotein synthesis (step 7) or as genomic RNA for packaging (step 8). The different sg mRNAs are translated to produce seven structural proteins – GP2a, 2b, GP3, GP4, GP5, M, and N. All the structural proteins are required for virus packaging. Virus assembly occurs in the ER and Golgi complex (step 9). Budding of progeny virus occurs in intra cellular membranes in ER and Golgi complex (step 10) followed by release of the virion particle (step 11).

(Pasternak et al., 2001; van Marle et al., 1999; Zuniga et al., 2004). TRSs are AU-rich sequences of 5 to 8 nucleotides long (Pasternak *et al.*, 2006) which are located at either the 3' end of the leader sequences of sg mRNA, the 5' end of body segment of sg mRNA, or at the leader-body fusion site of sg mRNA (Pasternak *et al.*, 2006; Spaan *et al.*, 1983). Two mechanisms proposed for transcription of PRRSV sg mRNA are (a) leader primed transcription and (b) discontinuous extension of minus strand RNA synthesis (Pasternak *et al.*, 2006; Snijder & Meulenberg, 1998). In the case of "leader primed transcription" model (Fig. 1.5A) (Baric *et al.*, 1983; Lai *et al.*, 1984; Spaan *et al.*, 1983), the leader primer is initially synthesized by transcription from the 3' end of the antigenome. The leader TRS along with the leader transcript then base pairs with different anti-body TRS from the antigenome and continue transcription to produce sg mRNA synthesis. In the case of "discontinuous extension minus strand RNA synthesis" model (Fig. 1.5B)(Sawicki & Sawicki, 1995; 2005), there is discontinuous synthesis of minus strand with attenuation of RNA synthesis occurring at different body TRS. Then the TRS of partially synthesized RNA bind with leader TRS to form sub genomic length minus strand RNA. This again acts as template for sg mRNA synthesis (Pasternak *et al.*, 2006).

1.11 Virus assembly and budding

PRRSV assembly and budding occurs in the ER and Golgi. The four minor envelope proteins required to be present together for their transport from the ER to the Golgi complex (Wissink et al., 2005). GP5/M heterodimers also assemble in the ER and the Golgi complex (Mardassi *et al.*, 1996). Because of virus assembly in the ER and the Golgi complex, lower levels of structural proteins accumulate on the plasma membrane of the infected cells.

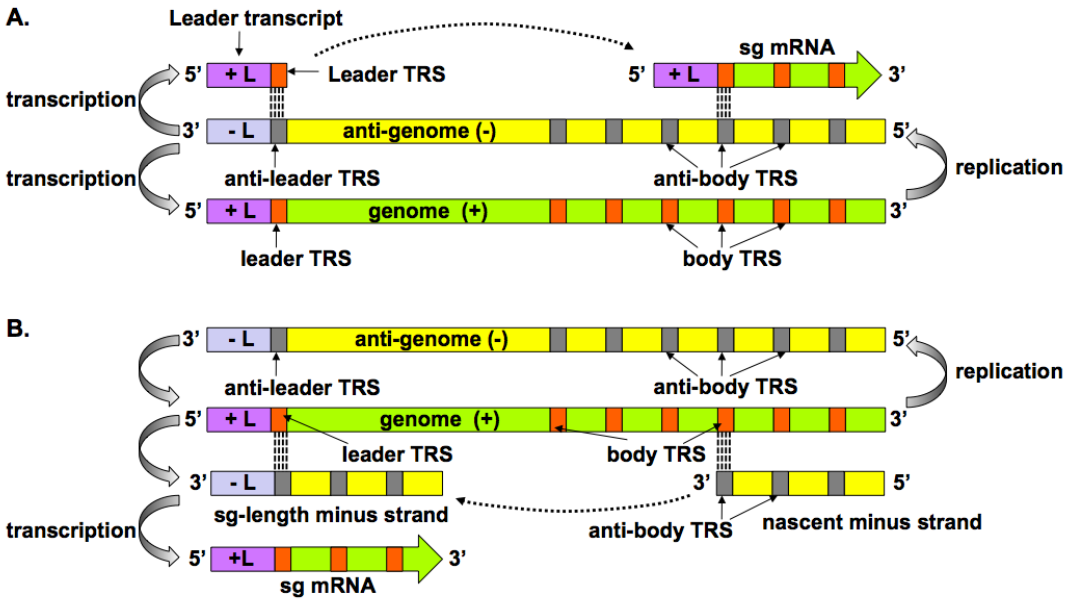

Figure 1.5 Models of transcription of PRRSV. (A) Leader primed transcription (discontinuous plus-strand RNA synthesis) model. This model proposes that the plus strand RNA synthesis is either continuous (producing genomic RNA) or discontinuous (producing sg mRNAs). Initially, the leader transcript (+L) is synthesized from the 3' end of the anti-genome. The leader TRS of the leader transcript further base pairs with anti-body TRS (of anti-genome) at the 5' end of the genomic RNA and facilitates synthesis of sg mRNA. (B) Discontinuous extension of minus strand RNA synthesis model. This model proposes that minus strand synthesis from the genomic RNA can be either continuous (producing anti-genomic RNA) or discontinuous (producing sg-length minus strands). During minus-strand RNA synthesis, the body TRSs (of genome) acts as attenuation signal and terminate the minus strand synthesis at different body TRS. The nascent minus strand RNAs with the anti-body TRS further transferred to the 5' end of the genomic RNA template, the anti-body TRS base pairs with the leader TRS (of genome), and anti-leader (-L) is added to form the sg-length minus strands. Then, the differentially terminated sg-length minus strands serves as templates for sg mRNA synthesis.

1.12 Immune response to PRRSV

It takes approximately 3 month to develop protective acquired immunity against PRRSV during natural infection. Because PRRSV has different strains, immunity developed against one strain is not sufficient for protection against another strains (Kimman et al., 2009) demonstrating a lack of heterologous protection.

1.12.1 Innate immunity against PRRSV infection

PRRSV infection of pigs fails to elicit any significant cytokine expression including type I interferon (IFN), interleukin (IL)-1, and TNF-α in the lungs (Thanawongnuwech et al., 2001; Van Reeth et al., 1999). IFN-α inhibits PRRSV replication (Albina *et al.*, 1998; Le Bon *et al.*, 2001) and downregulation of IFN-α expression is probably one of the key steps in virus pathogenesis. PRRSV infection downregulates of IFN-α production in alveolar macrophages by interfering dsRNA mediating signalling pathways (Beura et al., 2010). During PRRSV infection, the weak initial innate immune response probably leads to longer survival of the virus in the infected animals (Kimman et al., 2009). The virus suppresses immune response by altering cytokine production in the macrophages and dendritic cells. It also modifies antigen presentation (Kimman et al., 2009). This leads to delayed activation and mobilization of natural killer cells, which reduces neutralizing antibody responses, lymphoproliferative, and IFN-γ responses against PRRSV (Butler et al., 2008; Chang et al., 2008; Flores-Mendoza et al., 2008; Kimman et al., 2009). Besides weak innate immune responses, other factors that lead to viral persistence includes antibody mediated enhancement of infectivity and lack of incorporation of viral proteins in the plasma

membrane of infected cells (Kimman et al., 2009). The latter is due to the fact that PRRSV budding and assembly occurs in the ER and the Golgi complex compartments, which leads to accumulation of the nucleocapsid and other viral proteins at the site of budding. Hence, PRRSV specific antibodies fail to detect the virus (Costers *et al.*, 2006; Kimman *et al.*, 2009). Additionally, IFN-γ response was found to rise in serum immediately after PRRSV infection and this serum titer lasts for approximately 3 weeks (Wesley *et al.*, 2006). This rise may correlate with an increase in viral load (Loving et al., 2008) in the infected animals because both IFN-α and IFN-γ inhibit PRRSV replication in vitro (Bautista & Molitor, 1999; Gaudreault *et al.*, 2009).

1.12.2 Cell mediated (T cell) immunity

PRRSV T cell mediated immune response is characterized by type I cytokine expression which includes IFN-γ and IL-2 (Kimman et al., 2009). Although cell mediated immunity that includes IFN-γ level is inefficient in downregulating PRRSV infection (Batista *et al.*, 2004; Kimman *et al.*, 2009; Lowe *et al.*, 2005; Murtaugh *et al.*, 2002), a live attenuated vaccine against PRRSV inducing higher level of IFN-γ secreting cells was shown to be protective to pigs against viremia (Meier *et al.*, 2003). IFN-γ is known to reduce PRRSV titers in infected PAM cells in vitro (Gaudreault *et al.*, 2009). T cell response in PRRSV infected pigs is directed against GP2a, GP3, GP4, GP5, M, and N protein. Of all these proteins, the M protein is the most potent inducer of T cell proliferation (Bautista *et al.*, 1999; Jiang *et al.*, 2007a; Jiang *et al.*, 2007b; Kimman *et al.*, 2009; Wesley *et al.*, 1999). With regard to GP5, amino acid residues 117-131 and 149-

163 were identified to contain immunodominant T cell epitopes (Vashisht et al., 2008). T cell epitopes in other structural proteins have not been characterized yet.

PRRSV infection causes apoptosis of dendritic cells (Costers *et al.*, 2008; Kimman *et al.*, 2009; Lee & Kleiboeker, 2007). It further down regulates inflammatory cytokine production and T cell response. Also, virus infections interferes with major histocompatibility complex (MHC) I and MHC II antigen presentation leading to down regulation of antigen presentation by T cells (Chang *et al.*, 2008; Flores-Mendoza *et al.*, 2008; Kimman *et al.*, 2009; Loving *et al.*, 2007; Wang *et al.*, 2007).

1.12.3 Humoral (antibody mediated) immunity

Both neutralizing and non-neutralizing antibodies are produced during PRRSV infection in pigs. Antibodies directed against N protein of PRRSV are most abundant during viral infection, but they are non-neutralizing and hence do not confer protection against virus infection (Kimman et al., 2009). Non-neutralizing antibodies directed against M and N proteins of PRRSV can be detected as early as 5 days post infection. Lower titers of neutralizing antibodies appear between 2 and 4 weeks post infection (Kimman et al., 2009; Loemba et al., 1996; Plagemann, 2006). It blocks PRRSV by reducing the number of virus attachment and internalization (Delputte et al., 2004). The epitopes for neutralizing antibody production are present in GP3, GP4, GP5, and M protein of PRRSV (Ansari *et al.*, 2006; Cancel-Tirado *et al.*, 2004; Kim & Yoon, 2008; Kimman *et al.*, 2009; Plagemann, 2006; van Nieuwstadt *et al.*, 1996; Yang *et al.*, 2000). Out of all the above proteins, neutralizing antibodies produced against GP5 is most relevant for protection against PRRSV infection (Ansari *et al.*, 2006; Ostrowski *et al.*, 2002). The major neutralization epitopes of GP5 are located in the middle of the

ectodomain of the protein encompassing amino acids 36 to 52 (Ostrowski *et al.*, 2002; Plagemann *et al.*, 2002) and this region is flanked by N-glycosylation sites (Ansari et al., 2006).

1.13 Immune evasion of PRRSV

Upon virus infection of a host, neutralizing antibodies are produced against specific epitopes of the envelope proteins of the virus. They mostly bind to the epitopes to neutralize the virus. On the other hand, viruses evolve various mechanisms to evade host immune response. Like other viruses, PRRSV also uses different protective strategies for its successful replication inside host cells and evasion against the host immune response. Some of the key strategies are outlined below:

1.13.1 Introduction of random mutations and quasispecies variation

PRRSV mutates quickly in pigs (Horter et al., 2002; Rowland et al., 1999) and several multiple variants co-exist in experimentally infected pigs (Chang et al., 2002). Several PRRSV strains exist in the field as quasispecies of each genotypes of PRRSV (Goldberg et al., 2003). Heterogeneity of these strains is observed both antigenically and clinically but not distinct enough to be regarded as geographical subpopulation (Kapur et al., 1996; Meng et al., 1995; Stadejek et al., 2002). Previous studies for GP5 of PRRSV (Rowland et al., 1999) have shown that appearance of quasispecies by variability in the single nucleotide level of GP5 leads to positive and negative selection. Existence of quasispecies in PRRSV may result in the inability of traditional methods of vaccination to control the virus infection in a herd or in a region.

The random mutations elicited in the viral genome can be present both in the specific epitopes targeted for neutralization as well as other regions of the envelope

proteins. Once mutations are present in the neutralizing antibody targeted epitopes, it inhibits the binding of the neutralizing antibodies to the epitope (Mascola & Montefiori, 2003) and the virus escapes neutralization by the antibody.

1.13.2 Antibody mediated enhancement

Studies in murine models (Cancel-Tirado *et al.*, 2004; Kimman *et al.*, 2009) for PRRSV have shown that virus infection can be enhanced by certain enhancing antibodies. In this case, virus specific antibodies either maternal origin or due to previous vaccination can facilitate entry of the virus in to target cells. The antibody mediated enhancing epitopes were reported to be present N and GP5 proteins of PRRSV (Cancel-Tirado *et al.*, 2004).

1.13.3 "Decoy" epitopes

Presence of immunodominant "decoy" epitopes adjacent to neutralizing epitopes in GP5 evokes early and robust of non-protective (non-neutralizing) antibody response against PRRSV. This effect further masks the early recognition of crucial neutralizing epitopes leading to delay in neutralizing antibody production in the virus infected host (Fang et al., 2006; Ostrowski et al., 2002).

1.13.4 Glycan shielding of neutralizing epitopes

The viral envelope glycoproteins act as shield or cover for the neutralizing epitopes so that the neutralizing antibodies fail to bind to those epitopes. Also, by shielding the epitopes it prevents neutralizing antibody production against those epitopes. This mechanism was first proposed for Human Immunodeficiency Virus (HIV) and Simian Immunodeficiency Virus (SIV) (Reitter *et al.*, 1998; Scanlan *et al.*, 2007; Wei *et al.*, 2003) and latter discovered in many other viruses including PRRSV. The glycan

moities present on the GP5 of PRRSV are required for protection against neutralizing antibody response (Ansari et al., 2006). It is unknown whether glycan moities present in three other minor envelope glycoproteins (GP2a, GP3, and GP4) of PRRSV are also required for glycan shielding. I have examined the role of N-glycosylation of these three proteins of PRRSV in glycan shielding mechanism in this dissertation (chapter V).

1.14 N-glycosylation as a post-translational modification of the protein

N-glycosylation is one of the post-translational modifications of the proteins. The motif of N-glycosylation is N-X-S/T where X can be any amino acid other than proline. Oligosaccharyl transferase (OST) enzyme is required for glycosylation and is composed of seven to eight subunits (Kelleher & Gilmore, 2006). STT3 subunit of yeast has homolog (STT3A and STT3B) in mammals. STT3A and STT3B subunits of OST are essential for co-translational and post-translational glycosylation of a glycoprotein. Most of the glycoproteins are co-translationally glycosylated during their synthesis in the ER. But, recent studies have shown that some of the host glycoproteins are also post-translationally glycosylated (Bolt *et al.*, 2005; Ruiz-Canada *et al.*, 2009). Besides host proteins, the large envelope protein of hepatitis B virus is also post-translationally glycosylated (Lambert & Prange, 2007). Whether post-translational glycosylation occurs in PRRSV is not known and studies reported in this dissertation address this aspect.

1.15 Role of N-glycosylation of viral proteins

Viruses take advantage of N-glycosylation for their propagation in the host. There are several reports regarding the different roles played by N-glycosylation of viral proteins of Hantaan virus, hepatitis C virus, influenza virus, Dengue virus, West Nile virus, Bunyamwera virus, and prototype foamy virus for tissue tropism, receptor

interactions, viral entry, protein folding, targeting, secretion, assembly, exit, immune evasion, and morphogenesis etc (Beasley *et al.*, 2005; Daniels *et al.*, 2003; Fournillier *et al.*, 2001; Hanna *et al.*, 2005; Luftenegger *et al.*, 2005; Mondotte *et al.*, 2007; Shi *et al.*, 2005; Shi & Elliott, 2004; Vigerust & Shepherd, 2007). N-glycosylation of SIV, HIV and Bunyamwera virus, HCV, and Ebola virus not only promotes viral replication and infectivity, but also provides a glycan shield against host neutralizing antibodies and thereby facilitates virus spread (Lin *et al.*, 2003; Reitter *et al.*, 1998; Scanlan *et al.*, 2007; Shi *et al.*, 2005; Vigerust & Shepherd, 2007; Wei *et al.*, 2003).

1.16 Experimental plan

1.16.1 Overall objective

PRRSV has four N-glycosylated envelope proteins present on its surface. Although the OST enzyme is required for glycosylation, it is unknown whether the four glycoproteins of PRRSV are co-translationally and/or post-translationally glycosylated. There is not much information available regarding the intermolecular interactions of the four glycoproteins among themselves and with the receptor CD163 for PRRSV. Previous studies from our laboratory examined the role of glycosylation of GP5 in virus infectivity and neutralizing antibody response (Ansari et al., 2006). However, little is known about the role of glycosylation of the other minor envelope glycoproteins (GP2a, GP3, and GP4) on production of infectious PRRSV and neutralizing antibody response. The studies reported in this thesis were undertaken to decipher the molecular interactions of GP2a, GP3, GP4, and GP5 among themselves and with the receptor CD163. Additionally, the role of N-glycosylation of GP2a, GP3, and GP4 in virus infectivity, neutralizing antibody

response, and receptor interactions was examined. The following hypotheses were developed and experiments were conducted to examine each of these hypotheses.

1.16.2 Hypothesis I, objective, and experimental approach

I hypothesized that GP2a, GP3, GP4, and GP5 of PRRSV are co-translationally and/or post-translationally glycosylated. My objective was to determine which of the viral glycoproteins are co-translationally and/or post-translationally glycosylated.

The experimental approach for this objective was to clone the individual viral glycoproteins in various expression vectors and examine expression of the individual glycoproteins in transfected cells and compare to those synthesized in PRRSV-infected cells. Subsequently, the proteins were metabolically labelled in transfected cells by short pulse-labelling to allow synthesis of the proteins, chased for various lengths of time and examine how the synthesized proteins are glycosylated. These pulse-chase studies allowed me to determine if the glycoproteins are co-translationally and/or post-translationally glycosylated.

1.16.3 Hypothesis II, objective, and experimental approach

All four envelope glycoproteins are required for infectious PRRSV production. The proteins must be transported from the ER to the Golgi complex during virus assembly. I hypothesized that these proteins interact with each other for virus assembly and to facilitate entry by binding to cell receptors. The objective of this study was to determine the intermolecular interactions of these glycoproteins and identify which of the glycoproteins specifically interact with CD163.

In order to study the interactions among the glycoproteins of PRRSV, the glycoproteins were co-expressed in various combinations in BHK-21 cells and co-

immunoprecipitation (co-IP) assays performed. Similarly, the porcine CD163 molecule was cloned from porcine alveolar macrophage (PAM) cells and its specific interaction with the envelope glycoproteins examined. These studies allowed me to develop an interactome map of PRRSV GPs and CD163.

1.16.4 Hypothesis III, objective, and experimental approach

The N-glycosylation of GP5 of PRRSV was shown to be important for infectious virus production and protection against host neutralizing antibody response. Hypoglycosylation of GP5 was also shown to be important for induction of higher neutralizing antibody titers in infected animals. I hypothesized that glycosylation of GP2a, GP3, and GP4 may be required for infectious virus production, protection against host neutralizing antibody response in infected animals, and interaction with receptor CD163. Hypoglycosylation of these minor glycoproteins may also induce higher neutralizing antibody response. The objective of this study was to determine if glycosylation at certain sites in the glycoproteins was important for infectious virus production and whether deglycosylation affects neutralizing antibody response.

To study the importance of N-glycosylation in virus production, the asparagine (N) residues of each predicted glycosylation site were mutated to alanine (A) in the coding sequences of the glycoproteins. Expression and glycosylation of these proteins were compared to that seen in wild type proteins. Further, the mutant coding sequences were cloned in the FL12 infectious clone and the effect of glycosylation mutation on infectious virus production examined. Subsequently, neutralizing antibody response in mutant virus-infected pigs was examined.

Chapter II: MATERIALS AND METHODS

2.1 Cell culture and maintenance of cells

The Baby hamster kidney-21 (BHK-21) cells were maintained in minimal essential media (MEM) containing 5% FBS and 100 units of Penicillin, 20 units of Kanamycin and 20 units of Streptomycin (1X PKS) antibiotics per one milliliter of media. MARC-145 cells were maintained in low bicarbonate-low glucose Dulbecco's modified Eagle's medium (DMEM) with 10% FBS and 1X PKS (Ansari et al., 2006; Truong et al., 2004). HeLa cells were maintained in high glucose containing DMEM with 10% FBS and 1X PKS.

2.2 Preparation of recombinant vaccinia virus (vTF7-3) stocks

The vTF7-3 virus (Fuerst et al., 1986), a recombinant vaccinia virus that expresses the bacteriophage T7 RNA polymerase in the cytoplasm of infected cells, was grown and titrated in BHK-21 cells as described before (Ansari et al., 2006) and stored at -80^0C in small aliquots.

The frozen vTF7-3 virus was thawed and reconstituted in PBS containing 0.01% $CaCl_2$ and 0.01% $MgCl_2$. BHK-21 cells plated in 100 mm tissue culture dish were infected with 0.1 multiplicity of infection (MOI) of vTF7-3 virus and incubated in 37^{o}C with 5% CO_2 concentration for 45 min with intermittent rocking in each 10 min interval. Following incubation, the residual virus was aspirated and the cells were washed with DMEM twice. The BHK-21 cells were further incubated in 37^{o}C with 5% CO_2 concentration containing 8 ml of DMEM with 2% FBS and 1X PKS antibiotics per one milliliter of media. The cells were incubated for 42–48 h until the 90–95% of cells show extensive cytopathic effect (CPE). The supernatant was aspirated and the cells were

collected in 2ml of 10mM Tris-HCl pH 9.0 by scrapping with rubber polishman. The collected cells were centrifuged at 500 X g for 5 min and the supernatant was discarded. The cell pellet was frozen in -80^{o}C overnight. Then, the cell pellet was thawed and resuspended in 10mM Tris-HCl pH 9.0 and sonicated for 2 min. The freeze-thawing procedure was repeated twice and the collected supernatant from each step was pooled together and aliquoted in 40µl volume and stored in -80^{o}C. The titer of the prepared vTF7-3 virus stock was determined by plaque assay in BHK-21 cells.

2.3 Preparation of PRRSV stocks

The infectious clone derived FL12 virus was grown in MARC-145 cells as described before (Ansari et al., 2006; Truong et al., 2004). The MARC-145 cells were plated in 100 mm tissue culture dish. Two days after cell splitting, the cell monolayers with 90% confluency were washed with 1X phosphate buffered saline (PBS) twice. Previously stored FL12 or mutant FL12 virus was used to infect fresh MARC-145 cells with 0.1 MOI. The virus was diluted in low bicarbonate-low glucose DMEM with 10% FBS and 1X PKS media. The cell monolayer in 100 mm tissue culture dish was treated with 1ml of the diluted virus and incubated at 37^{o}C for 45 min with intermittent rocking at 10 min intervals. After virus adsorption, the residual virus was aspirated and 8ml of media containing low bicarbonate-low glucose DMEM with 10% FBS and 1X PKS was added to the culture dish. The culture dish was incubated at 37^{o}C and 5% CO_2 concentration for 4–5 days or until 95% of the cells in the monolayer exhibited significant CPE. The media containing virus and cell debris were collected in a tube and kept in -80^{o}C. After overnight storage, the supernatant was freeze-thawed 2-3 times and centrifuged at 500 X g for 5 min to pellet the cell debris. The supernatant containing the

virus was aliquoted in 500 µl volume and stored in -80^{o}C. The viral titer in plaque forming unit (PFU)/ml was determined by plaque assay in MARC-145 cells.

2.4 Virus concentration by ultracentrifugation

The thawed FL12 virus stock was centrifuged at 3000 X g for 30 min (or 6000 x g for 10 min) to clarify the supernatant. 5ml of 10% (w/v) sucrose solution in NTE (50mM NaCl, 10mM Tris-HCl pH 7.5, and 1mM EDTA) was loaded in polyallomer ultracentrifuge tube (Beckman, Palo Alto, CA) and the clarified virus stock was slowly added on top of this sucrose cushion. One ml of low bicarbonate-low glucose DMEM was added slowly on top of the loaded virus stock. The virus was pelleted by centrifugation at 100,000 X g for 3 h at 4^{o}C in SW41 rotor (Beckman, Palo Alto, CA). Following centrifugation, the supernatant was aspirated and the virus pellet was resuspended in 100 µl of PBS. The titer of the concentrated virus stock was measured by plaque assay and the virus was stored in -80^{o}C.

2.5 RNA electroporation and virus recovery

RNA electroporation was performed as described before (Ansari et al., 2006; Truong et al., 2004). MARC-145 cells were plated in 100 mm dish two days before electroporation. The cells were trypsinized, washed with 1X PBS and resuspended in E buffer (DMEM containing 1.25% dimethyl sulfoxide [DMSO]) with a final concentration of 5 x 10^6 cells per milliliter. Approximately 2µg each of MARC-145 cell RNA and FL12 (wild type or its mutant form) RNA was mixed in a microfuge tube and further transferred to a 4mm cuvette (BioRad laboratories, CA) containing 2 X 10^6 MARC-145 cells per 400µl of E buffer. The RNA-MARC-145 cell suspension was subjected to

electroporation using Gene Pulser Xcell electroporator (BioRad, CA) at 225 volts and 925 μF capacitance. The electroporated cells were transferred to a 35mm dish containing 2 ml of recovery media (media for MARC-145 cells as described earlier). Roughly 10% of the electroporated cells were separately plated in a 24 well plate for indirect immunofluorescence to check for the biological activity of the transfected RNA as described latter. The media from the plates were replaced with fresh media 12 h after electroporation and incubated for desired length of time.

2.6 Multi step growth kinetics assay

Multi step growth kinetics was performed by infecting MARC-145 cells seeded in a six well plate with 0.1 MOI of FL12 and N-glycosylation defective mutant viruses. Due to significantly lower titer of some of the recovered GP3 N-glycosylation defective mutant viruses, 0.001 MOI was used for performing multi step growth kinetics. The appropriately diluted virus with the low bicarbonate-low glucose DMEM was added on top of the 90% confluent MARC-145 cells and incubated at 37^{o}C and 5% CO_2 concentration for 45 min with intermittent rocking. After adsorption, the residual virus was aspirated; the cell monolayer was washed with 1X PBS, and 2ml of low bicarbonate-low glucose DMEM containing 10% FBS and 1X PKS was added on the cell monolayer. The cells were further incubated at 37^{o}C for up to 5 days. The supernatant was collected at 12 h intervals up to 120 h post infection. Approximately 300μl of supernatant was collected at each time point and equal volume of fresh media was added after each collection.

2.7 Plaque assay

Previously collected virus supernatant was used for plaque assay. Each virus was diluted with 10-fold dilution. After 45 min post infection of MARC-145 cells with either FL12 or mutant viruses, the cells were washed with cold PBS twice followed by an overlay of 4 ml of DMEM containing 1.2% low melting point (LMP) agar, 2% FBS, and IX PKS as described before (Ansari et al., 2006). After polymerization of agar, the cells were incubated at 37^{o}C for 4-5 days as per the requirement (till the plaques appear). Following incubation, the cell monolayer was fixed by addition of 2% glutaraldehyde for 2 h. The agar plugs were removed and the cells stained with 0.01% crystal violet and 30% methanol solution for 30 min followed by washing off the excess stain by water. The plaques were counted manually.

2.8 Antibodies

The porcine anti-CD163 monoclonal antibody was purchased from AbD Serotec USA (Raleigh, NC). The monoclonal antibody (SDOW17) against the PRRSV N protein (Nelson et al., 1993) was purchased from National Veterinary Services Laboratories (Ames, Iowa). The anti-HA polyclonal antibody was purchased from Santa Cruz biotechnology, Inc (Santa Cruz, CA). The anti-FLAG monoclonal antibody, anti-FLAG polyclonal antibody, and anti-cMyc monoclonal antibody were purchased from Sigma Aldrich (St. Louis, MO). The anti-GP5 rabbit polyclonal antibody was kindly provided by Dr. Carl Gagnon (University of Quebec, Montreal, Canada). Alexa Fluor-488 and 594 goat anti-rabbit and anti-mouse IgG antibodies were purchased from Molecular Probes and used as secondary antibody for fluorescence microscopy. Monospecific antibodies against GP2a, GP3, and GP4 were generated by co-immunization of rabbits with two

highly immunogenic peptides for each protein as described (de Lima et al., 2009). The details of production and characterization of the GP3 monospecific antibody were reported earlier (de Lima et al., 2009). The selection of peptides, their synthesis, and production of anti-GP2a and anti-GP4 monospecific polyclonal antibodies were followed similarly as reported previously (de Lima et al., 2009; de Lima et al., 2006). The amino acid residues of the selected peptides for GP2a are CEMVSRRMYRTMEKA and CKAGQAAWKQVVSEAT. The amino acid residues of the selected peptides for GP4 are CLFYASEMSEKGFK and CFTSYVQHVKEFTQR. The peptides were synthesized and conjugated to a carrier protein (keyhole limpet hemocyanin [KLH]) either by adding a cysteine residue at the amino terminus (underlined) or via activated 1-ethyl-3-(3-dimethylaminopropyl)carbodiimide hydrochloride (EDC) chemistry to its N-terminal region. The antibodies were produced by Sigma and were characterized in our laboratory. Sera collected at day 77 post-immunization were used in all experiments.

2.9 Preparation of chemically competent bacterial cells

For preparation of the competent cells, DH5α cells were used. Two buffers were prepared prior to the preparation of competent cells: (1) 0.5 M PIPES (piperazine-1,2-bis[2-ethanesulfonic acid]) and (2) Inoue transformation buffer – The buffer contains 55 mM $MnCl_2 (H_2O)_4$, 15 mM $CaCl_2(H_2O)_2$, 250 mM KCl, and 10 mM PIPES (pH 6.7). Both the solutions were filter sterilized and stored at -20^oC.

The *Escherichia coli* (*E.coli*) strain DH5α cells were streaked on LB agar plate (without any antibiotics) and incubated at 37^oC incubator for overnight. Starter culture was prepared by inoculating a single bacterial colony in 25 ml of LB media and incubating at 37^oC incubator with a shaking speed of 300 rpm for 6-8 h. Approximately 8

ml of starter culture was further inoculated in to 250 ml of LB media and incubated in an incubator with constant shaking speed of 250 rpm at 18-20^{o}C. The bacterial growth was checked periodically with a spectrophotometer and once the OD_{600} reading of 0.5 was achieved, the culture was removed from the incubator and kept on ice cold water bath for 10 min. The bacteria were pelleted by centrifuging at 2500 X g for 10 min at 4^{o}C. After aspiration of the supernatant, the bacterial pellet was resuspended in 80 ml of ice cold Inoue transformation buffer by gentle swirling. The resuspended bacterial pellet was again centrifuged as described above and the bacterial pellet was finally resuspended in 20 ml of Inoue transformation buffer containing 1.5 ml of DMSO. The cell suspension was mixed gently by swirling and kept on ice cold water bath for 10 min. The competent bacterial cells were then aliquoted as 100µl volume in 0.5 ml tubes and snap-frozen in liquid nitrogen. The competent cells were further stored in -80^{o}C for future use.

2.10 DNA Ligation

The restriction endonuclease enzymes were purchased from New England Biolabs (Ipswich, MA). Restriction digestion of the plasmid and PCR product was performed by restriction endonuclease enzyme as per manufacturer's instruction. The enzymes and buffers were stored in -20^{o}C. The digested plasmid (or PCR product) was resolved in 0.8% LMP agarose gel and purified by either phenol-chloroform extraction method or glass silica extraction method. The DNA was resuspended in water. The concentration of the insert and vector was checked by examining small aliquots of DNA in agarose gel. T4 DNA ligase (Invitrogen) was used for DNA ligation reaction as per manufacturer's instructions. Generally, for ligation reaction, the vector-insert ratio was kept as 1:3. The

ligation reaction was either incubated at room temperature for 2-3 h or at 16^{o}C for overnight.

2.11 Bacterial transformation

Transformation of bacteria was performed as described in 'Molecular Cloning: A laboratory Manual' (Russell, 2001) with modifications. About 5µl of the ligation mixture was incubated with 50µl of competent DH5α bacterial cells for 30 min on ice. Following incubation, the bacterial cells were heat shocked at 42^{o}C for 90 seconds. After the heat shock, the cells were incubated on ice for 5 min, 950µl of LB was added and the cells were incubated at 37^{o}C for 1 h with gentle shaking (160 rpm). Cells were concentrated and reconstituted in 100µl of LB and plated in dry and warm LB agar plates containing 100 µg/ml of ampicillin (Shelton Scientific, Shelton, CT) as 10µl and 90µl fraction volumes. The plates were incubated at 37^{o}C in inverted posture for overnight for the growth of bacterial colonies.

2.12 Plasmid preparation

Miniprep and midiprep was performed for small scale and large scale plasmid preparation, respectively. For miniprep plasmid preparation method, individual bacterial colonies were inoculated in 1.5 ml of LB containing 100µg/ml of ampicillin in either 5 ml or 14 ml tubes and incubated at 37^{o}C overnight with a rotor speed of 280-300 rpm. The grown bacterial culture was transferred to microfuge tube. The cells were pelleted by centrifugation at 10,000 X g and the supernatant was aspirated leaving 40-50 µl of media on top of the pellet. The bacterial pellet was resuspended by vortexing and the cells lysed by adding 300 µl of TENS buffer (10 mM Tris-HCl, pH 8.0, 1 mM EDTA, 0.1 M NaOH,

0.5% SDS).The suspension was neutralized by addition of 150 µl of 3M sodium acetate, pH 5.2. Cellular debris was pelleted by centrifugation at 16,000 X g for 5 min. The supernatant was transferred to fresh microfuge tubes and the plasmid DNA was recovered by addition of 900µl of ice cold absolute ethanol followed by centrifugation at 16,000 X g for 5 min. The precipitated plasmid DNA was washed with ice cold 70% ethanol and dried. The dried plasmid DNA was resuspended in 40 µl of tris-ethylenediaminetetraacetic acid [EDTA] (TE) buffer containing 100 µg/ml of RNaseA. The size of the plasmid was analyzed by agarose gel electrophoresis.

For large scale plasmid preparation, midiprep was performed. About 100µl of previously grown bacterial culture was transferred to 100 ml of LB containing 100µg/ml of ampicillin and incubated at 37^{o}C shaker overnight. The plasmid DNA was prepared by gravity flow column purification method using Qiagen's midiprep method (Qiagen tip-100) as per manufacturer's instructions. The buffers used for midiprep are: (1) Buffer P1 resuspension buffer) - It contains 50 mM Tris-Cl (pH 8.0), 10 mM EDTA, and 100 µg/ml RNase A; (2) Buffer P2 (lysis buffer) - It contains 200 mM NaOH and 1% sodium dodecyl sulfate (SDS) (w/v); (3) Buffer P3 (neutralization buffer) - It contains 3.0 M potassium acetate (pH 5.5); (4) Buffer QBT (equilibration buffer) - It contains 750 mM NaCl, 50 mM MOPS (pH 7.0), 15% isopropanol (v/v), and 0.15% Triton X-100 (v/v); (5) Buffer QC (wash buffer) - it contains 1.0 M NaCl, 50 mM MOPS (pH 7.0), and 15% isopropanol (v/v); and (6) Buffer QF (elution buffer) - It contains 1.25 M NaCl, 50 mM Tris-Cl (pH 8.5), and 15% isopropanol (w/v). The plasmid DNA concentration and purity

was determined using Eppendorf's biophotometer (Hauppauge, NY) and also quantitated by agarose gel electrophoresis using known amounts of DNA.

2.13 Plasmid construction

The coding regions of the minor GPs were cloned from the infectious clone FL12 of PRRSV (Truong et al., 2004). The genes for the individual minor GPs were amplified by PCR using gene-specific primers (Table 2.1) and cloned in pGEM3 vector (Promega Biotech, Madison, WI) under the control of T7 RNA polymerase promoter or in pcDNA3.1 (+) vector (Invitrogen) under the control of CMV promoter and T7 RNA polymerase promoter.

2.13.1 Subcloning of genes of structural proteins of PRRSV

The FL12 genome of PRRSV was previously cloned in pBR322 vector (Truong et al., 2004). The FL12 clone was digested with EcoRV and BstZ17I restriction enzymes to release ~ 4.9 kilo base pair (kbp) fragment containing majority of ORF2 and rest of the ORFs for structural proteins of PRRSV. The 4.9 kbp fragment was cloned in pBR322 vector (Ansari et al., 2006). This intermediate vector (EP vector) was used for subcloning of mutants of GP2a, GP3, GP4, and GP5 ORFs in to FL12 infectious clone.

2.13.2 Construction of GP2a, GP3, GP4, and GP5 plasmids

The coding regions of individual structural proteins were amplified by polymerase chain reaction (PCR) and cloned in pGEM3 vector (Promega Biotech, Madison, WI) under the control of T7 RNA polymerase promoter. The FLAG-tag (DYKDDDDK) was fused at the carboxy-terminus of GP2a by PCR using primers GP2a-FLAG-EcoRI-Rev and GP2a-NheI-For (Table 2.1) and cloned in pGEM3 vector that was modified to contain CMV promoter in addition to the T7 RNA polymerase promoter. The ORF for

Table 2.1 Primers used for cloning of ORF of GP2a, GP3, GP4, GP5, and CD163 proteins

Primer name	Primer nucleotide sequence
GP2a-EcoRI-For	ATATATGAATTCGCCACCATGAAATGGGGTCCATGC
GP2a-SphI-Rev	ATATATGCATGCTCACCGTGAGTTCGAAGG
GP2a-NheI-For	ATATGCTAGCGCCGCCACCATGAAATGGGGTCCATGC
GP2a-FLAG-EcoRI-Rev	ATATGAATTCTCACTCGAGCTTGTCATCGTCGTCCTTGT AGTCCATCCGTGAGTTCGAAGGAAAAATTGC
GP2a-N178A For	CATGACAGGGTCA**GCT**GTAACCATAG
GP2a-N184A For	GTAACCATAGTGTAT**GCT**AGTACTTTG
GP2a-N178/184A For	CATGACAGGGTCA**GCT**GTAACCATAGTGTAT**GCT**AGT ACTTTGAATC
GP3-EcoRI-For	ATATAGAATTCGCCACCATGGCTAATAGCTGTGC
GP3-BamHI-Rev	TATATGGATCCCTATCGCCGCGCGGC
GP3-N29A-Rev	CAGTACGTAGT**AGC**GGAATCCGC
GP3-N42A-Rev	GAGTTCGAAGGAAAAA**AGC**GCCCCTAAC
GP3-N50A-For	TCCTTCGAACTCACGGTG**GCT**TACACGGTG
GP3-N131A-For	GGGATAGGG**GCT**GTGAGTCAAG
GP3-N152A-For	CGACGGGGAG**GCC**GCCACCTTGCC
GP3-N160A-For	CGTCATGAC**GCT**ATTTCAGCCG
GP3-N195A-For	GTTGGTTTTA**GCT**GTTTCTTGG
GP4-EcoRI-For	ATATAGAATTCGCCACCATGGCTGCGCCCCTTC
GP4-BamHI-Rev	TATATGGATCCTCAAATTGCCAGTAAGATG
GP4-FLAG-BamHI-Rev	TATATGGATCCTCACTTGTCATCGTCGTCCTTGTAGTCA ATTGCCAGTAAGATGGCAAAAAAACAGGC
GP4-N37A-Rev	CGGTAGT**GGC**GGTTTTGATGTC
GP4-N84A-For	CCCGTGTACATCACTGTCACAGCC**GCT**GTCACAGATG
GP4-N120A-Rev	GATGCCTGACAC**AGC**GCCAAATATC
GP4-N130A-Rev	CGTAGCTGGTAAA**GGC**GACACAC
GP5-EcoRI-For	GCCGGAATTCGGAGCCGCCGCCACCATGTTGGGGAGA TGCTTGAC
GP5-HindIII-XhoI-Rev	ATCACTCGAGAAGCTTCTAAAGACGACCCCATTGTTC
GP5-Myc-XhoI-Rev	ATATATCTCGAGTTACAGATCTTCTTCAGAAATAAGTT TTTGTTCAAGACGACCCCATTGTTC
pBR131-For	CTGGATGCTGTAGGCATAGGCTTG
FL12-12816-For	GGGGCAATTTTTCCTTCGAACTCA CGG
FL12-13177-For	CTACCAACATCAGGTCGATGGCGG
FL12-13465-Rev	CTGTGATGGTGATATACACGGGTG
FL12-14473-Rev	GTCGGCCGCGACTTACCTTTAGAG
CD163-HindIII-For	ATATAAGCTTATGGACAAACTCAGAATGGTGCTAC
CD163-XhoI-Rev	ATATCTCGAGTCATTGTACTTCAGAGTGGTCTCCTG

Primer sequences are in the 5' to 3' direction. Restriction enzymes are underlined. The nucleotides for N to A mutation are shown in bold.

GP3 and GP4 was PCR amplified and cloned in pGEM3 vector by EcoRI and BamHI restriction sites. A FLAG tag was fused at the carboxy-terminus of GP4 by PCR using GP4-EcoRI-For and GP4-FLAG-BamHI-Rev primers (Table 2.1) and cloned in the pGEM3 vector. Additionally, an HA tag (YPYDVPDYAL) was fused at carboxy-terminus of GP4 by PCR using the primers GP4-HA-XhoI-Rev and GP4-EcoRI-For (Table 2.1) and cloned in pcDNA3.1(+) vector at EcoRI and XhoI restriction sites. The GP5 ORF was cloned in pGEM3 by EcoRI and HindIII restriction sites. A c-Myc tag (EQKLISEEDL) was fused at the carboxy terminus of GP5 by PCR using primers GP5-EcoRI-For and GP5-myc-XhoI-Rev (Table 2.1) and cloned in pcDNA3.1 (+) vector by EcoRI and XhoI restriction sites. Nucleotide sequence of the plasmids encoding various GPs was determined to ensure that correct clones were used in the studies.

2.13.3 Construction of plasmids encoding N-glycosylation mutants of GP2a, GP3, and GP4

EP-GP2a-N178A construct was generated by megarprimer based PCR (Sarkar & Sommer, 1990) by use of GP2a-N178A-For, GP2a-SphI-Rev and pBR131-For primers and cloned in EP vector by BstBI and EcoRV restriction digestion. EP-GP2a-N184A and EP-GP2a-N178/184A constructs were generated similarly as described for EP-GP2a-N178A construct but by use of GP2a-N184A-For and GP2a-N178/184A-For primers respectively. The coding region of GP2a harbouring appropriate mutation was further transferred from EP vector to FL12 viral genome by EcoRV and PacI restriction enzyme digestion (FL-GP2a-N178A, FL-GP2a-N184A, and FL-GP2a-N178/184A). The cloning of the carboxy terminal FLAG tagged GP2a protein was described earlier. The ORF of GP2a-FLAG containing N to A mutation was further PCR amplified by GP2a-NheI-For

and GP2a-FLAG-NheI-Rev primers and cloned in pGEM3 vector which in addition to T7 RNA polymerase promoter also contain cytomegalovirus (CMV) promoter from pCDNA3.1(+) to produce GP2a-FLAG-N178A, GP2a-FLAG-N184A, and GP2a-FLAG N178/184 mutant constructs.

The FL-GP3-N29A plasmid was generated by PCR using GP3-N29A-Rev and pBR131-For primers and cloned in FL12 viral genome by SnaBI and EcoRV restriction enzyme digestion. The FL-GP3-N42A plasmid was generated by PCR using GP3-N42A-Rev and pBR131-For primers and cloned in FL12 genome by BstBI and EcoRV restriction enzyme digestion. EP-GP3-N50A was generated by PCR using GP3-N50A-For and GP4-N120A-Rev primers (Table 2.1) and cloned in EP vector by BstBI and BsrGI restriction enzyme digestion. EP-GP3-N131A, EP-GP3-N152A, EP-GP3-N160A, and EP-GP3-195A plasmids were generated megaprimer PCR using respective forward primers, GP4-N120A-Rev, and FL12-12816-For primers (Table 2.1) and cloned in EP vector by BstBI and BsrGI restriction enzyme digestion. The FL-GP3-N50A, FL-GP3-N131A, FL-GP3-152A, and FL-GP3-N160A plasmids were generated by transferring the coding sequences from respective EP vectors to FL12 genome by EcoRV and PacI restriction enzyme digestion. The FL-GP3-N29/152A, FL-GP3-N29/160A plasmids were generated by fragment exchange between FL-GP3-N29A, FL-GP3-N152A, and FL-GP3-N160A respectively. EP-GP3-N152/160A plasmid was generated by megaprimer PCR using EP-GP3-N160A as template plasmid, GP4-N120A-Rev, GP3-N152A-For, and FL12-12816-For primers (Table 2.1) and cloned in EP vector by BstBI and BsrGI restriction enzyme digestion. The FL-GP3-N152/160A plasmids were generated by transferring appropriate coding sequences from EP-GP3-N152/160A to FL12 genome by

EcoRV and PacI restriction enzyme digestion. The FL-GP3-N29/152/160A plasmid was generated by fragment exchange between FL-GP3-N152/160A and FL-GP3-N29/152A plasmids by BstBI and PacI restriction enzyme digestion. The ORF of GP3 containing specific N to A mutation was amplified by GP3-ECoRI-For and GP3-BamHI-Rev and cloned in pGEM3 vector under T7 RNA polymerase promoter.

Megaprimer PCR was performed by using GP4-N37A-Rev, FL12-1286-For and FL12-14473-Rev primers (Table 2.1) and the PCR product was cloned in EP vector by BstBI and BstEII restriction enzyme digestion to generate EP-GP4-N37A plasmid. EP-GP4-N84A plasmid was generated by PCR mutagenesis using GP4-N84A-For and FL12-14473-Rev primers (Table 2.1) and cloned in EP vector by BsrGI and BstEII restriction enzyme digestion. EP-GP4-N120A construct was generated by megaprimer PCR using FL12-13177-For, GP4-N120-Rev, and FL12-14473-Rev primers (Table 2.1) and cloned in EP vector by BsrGI and BstEII restriction enzyme digestion. EP-GP4-N130A construct was generated similarly as described for EP-GP4-N120A but using GP4-N130A-Rev primer instead of GP4-N120A-Rev primer (Table 2.1). The FL-GP4-N37A, FL-GP4-N84A, FL-GP4-N120A, and FL-GP4-N130A plasmids were generated by transferring specific coding sequences from EP vector to FL12 genome by EcoRV and PacI restriction enzyme digestion. The EP-GP4-N37/84A, EP-GP4-N37/120A, and EP-GP4-N37/130A plasmids were generated by restriction digestion and fragment exchange between EP-GP4-N37A, EP-GP4-N84A, and EP-GP4-N130A plasmids with BstBI and BsrGI enzymes. The EP-GP4-N84/120A plasmid was generated by megaprimer PCR using EP-GP4-N84A template plasmid, GP4-N120A-Rev, FL12-13177-For, and FL12-14473 Rev primers (Table 2.1) and cloned in EP vector by BsrGI and BstEII restriction

enzyme digestion. The EP-GP4-N84/130A plasmid was generated by megaprimer PCR using EP-GP3-N84A template plasmid, GP4-N130A-Rev, FL12-13177-For, and FL12-14473-Rev primers (Table 2.1) and cloned in EP vector by BsrGI and BstEII restriction enzyme digestion. The EP-GP4-N120/130A plasmid was generated by megaprimer PCR using EP-GP4-N130A template, GP4-N120A-Rev, FL12-13177-For, and FL12-14473-Rev primers (Table 2.1) and cloned in EP vector by BsrGI and BstEII restriction enzyme digestion. The FL-GP4-N37/84A, FL-GP4-N37/120A, FL-GP4-N37/130A, FL-GP4-N84/120A, FL-GP4-N84/130A, and FL-GP4-N120/130A constructs were generated by transferring coding sequences from their respective EP vectors to FL12 genomes by EcoRV and PacI restriction enzyme digestion. The ORF of GP4 containing N to A mutation was amplified by GP4-EcoRI-For and GP4-BamHI-Rev primers (Table 2.1) and cloned in pGEM3 vector under T7 RNA polymerase promoter.

2.13.4 Construction of GP5 N-glycosylation defective plasmids

Previously GP5-I_E-M construct was generated by cloning GP5, internal ribosome entry sites (IRES) element of encephalo myocarditis virus (EMCV), and M in pGEM3 vector (Ansari et al., 2006). Also GP5-N34A, GP5-N44A, GP5-N51A, GP5-N34/44A, GP5-N44/51A, GP5-N34/51A, and GP5-N34/44/51A constructs were generated introducing corresponding mutations in the GP5 protein in GP5-I_E-M plasmid (Ansari et al., 2006). I further released GP5 containing the above mentioned mutations from GP5-I_E-M plasmid by restriction digestion with EcoRI restriction enzyme and cloned the fragments in pGME3 vector. The GP5 mutant clones obtained are pGEME3-GP5-N34A, pGEME3-GP5-N44A, pGEME3-GP5-N51A, pGEME3-GP5-N34/44A, pGEME3-GP5-N44/51A, pGEME3-GP5-N34/51A, and pGEME3-GP5-N34/44/51A. The correct

orientation of the clones was checked by SacI and SacII restriction enzyme digestion. The presence of appropriate mutations was confirmed by nucleotide sequencing.

2.13.5 Construction of GP2a and GP4 deletion mutant plasmids

Seven deletion constructs were generated for GP2a protein by sequentially deleting 35-40 amino acids from amino terminus to carboxy terminus of the protein by PCR based mutagenesis. The FLAG tag was fused at the carboxy terminus of the GP2a (described earlier). The PCR product was purified and cloned in pGEME3 vector by ECoRI and BamHI restriction enzyme digestion. GP2a-FLAG Δ2-38 construct was generated by PCR using GP2a Δ2-38 EcoRI-For and GP2a-FLAG-SphI-Rev primers (Table 2.2). GP2a-FLAG Δ39-75 construct was generated by megaprimer based PCR using GP2a-EcoRI-For, GP2a Δ39-75-Rev, GP2a Δ39-75-For and GP2a-FLAG-SphI-Rev primers (Table 2.2). GP2a-FLAG Δ 76-112, GP2a-FLAG Δ113-149, GP2a-FLAG Δ150-181, GP2a-FLAG Δ182-218, and GP2a-FLAG Δ219-256 constructs were generated using appropriate primer pairs (Table 2.2).

Five deletion constructs were generated for GP4 by sequentially deleting ~ 35 amino acids from amino terminus to carboxy terminus of the protein. A FLAG tag fused at the carboxy terminus of GP4 (GP4-FLAG) and its deletion constructs by PCR mutagenesis. The PCR product was digested with EcoRI and BamHI restriction enzyme and cloned in pGEM3 expression vector. GP4-FLAG Δ2-35 construct was generated by PCR using GP4 Δ2-35-EcoRI-for and GP4-FLAG-BamHI-Rev primers (Table 2.2). Other GP4 deletion mutant constructs were generated similarly using appropriate primer pairs (Table 2.2).

Table 2.2 Primers used for GP2a and GP4 deletion mutant construction

Primer name	Primer nucleotide sequence	Constructs generated
GP2a-FLAG-SphI Rev	TATATGCATGCTCACTTGTCATCG TCGTCCTTGTAGTCCCGTGAGTTC GAAGGAAAAATTGCCCC	
GP2a Δ2-38 EcoRI For	ATATATGAATTCGCCACCATGTTG GCTTTACCATCGCTG	GP2a-FLAG Δ2-38
GP2a Δ39-75 For	CATATTTTTGGCCATTTTGTGAGGC CTTTCTTTCTCAG	GP2a-FLAG Δ39-75
GP2a Δ39-75 Rev	CTGAGAAAGAAAGGCCTCACAAA ATGGCCAAAAATATG	
GP2a Δ76-112 For	GCAATTACAGAAGATCCTATCGTC GGATGTACCGCACC	GP2a-FLAG Δ76-112
GP2a Δ76-112 Rev	GGTGCGGTACATCCGACGATAGG ATCTTCTGTAATTGC	
GP2a Δ113-149 For	GATTGATGAAATGGTGTCGCATCT TGCCGCCATTGAAG	GP2a-FLAG Δ113-149
GP2a Δ113-149 Rev	CTTCAATGGCGGCAAGATGCGACA CCATTTCATCAATC	
GP2a Δ150-181 For	GATGTGGTGGCTCATTTTCAGGTG TATAATAGTACTTTGAATCAGG	GP2a-FLAG Δ150-181
GP2a Δ150-181 Rev	CCTGATTCAAAGTACTATTATACA CCTGAAAATGAGCCACCACATC	
GP2a Δ182-218 For	GGGTCAAATGTAACCATATCCTCC GTTGCGGCTTCTTG	GP2a-FLAG Δ182-218
GP2a Δ182-218 Rev	CAAGAAGCCGCAACGGAGGATAT GGTTACATTTGACCC	
GP2a-FLAG Δ219-256 - SphI-Rev	TATATGCATGCTCACTTGTCATCG TCGTCCTTGTAGTCAAATATGGAG GAGTGCACAGCTATTAG	GP2a-FLAG Δ219-256
GP4 Δ2-35 EcoRI For	ATATAGAATTCGCCACCATGACCA ACACTACCGCAGCATC	GP4-FLAG Δ2-35
GP4 Δ36-70 For	CAAGTCTTTCGGACATCAAAGCGG CGATAGGGACGCCC	GP4-FLAG Δ36-70
GP4 Δ36-70 Rev	GGGCGTCCCTATCGCCGCTTTGAT GTCCGAAAGACTTG	
GP4 Δ71-105 For	CAAAAGCTCTCAGTGCCGCGCTTC TGAGATGAGTGAAAAG	GP4-FLAG Δ71-105
GP4 Δ71-105 Rev	CTTTTCACTCATCTCAGAAGCGCG GCACTGAGAGCTTTTG	
GP4 Δ106-140-For	CTTTCTTCTTGCCTTTTCTATTTTAC CCAACGCTCCTTG	GP4-FLAG Δ106-140
GP4 Δ106-140-Rev	CAAGGAGCGTTGGGTAAAATAGA AAAGGCAAGAAGAAAG	
GP4-FLAG Δ141-178-BamHI-Rev	TATATGGATCCTCACTTGTCATCG TCGTCCTTGTAGTCCTCCTTGACAT GTTGGACGTAG	GP4-FLAG Δ141-178

Primer sequences are in the 5' to 3' direction. Restriction enzyme sites are underlined.

2.13.6 Subcloning of receptor porcine-CD163

The ORF of porcine CD163 receptor was amplified from the total RNA isolated from PAM cells by reverse transcription and PCR using specific primers, CD163-HindIII-For and CD163-XhoI-Rev (Table 2.1) and cloned in pGEM-T vector (Promega Corporation). Four clones of the CD163 receptor with correct size inserts were further transferred from the pGEM-T vector by restriction enzyme digestion with HindIII and XhoI and cloned by blunt-end ligation in pcDNA3.1 (+) vector.

2.14 RNA extraction and reverse transcription PCR (RT-PCR)

The RNA from the MARC-145 cells was obtained by Trizol LS reagent (Invitrogen) treatment as per the manufacturer's instruction. The RNA was dissolved in 20µl of nuclease free water and quantitated. Approximately 2µg of RNA was denatured by heating at 95^{o}C for 5 min followed by cooling on ice. RT-PCR reaction was set using superscript III kit (Invitrogen) as per the manufacturer's instructions. To the chilled RNA solution, 5X first strand buffer (50 mM Tris-HCl pH 8.3, 75 mM KCl, 3 mM $MgCl_2$), 0.1 M DTT, 5 mM dNTPs, 40 units RNasin (RNase inhibitor), and 200 units Superscript III enzyme, and appropriate reverse primer were added to make the final reaction volume of 10 µl. The reaction mixture was incubated at 55^{o}C for 1 h to synthesize cDNA. Following cDNA synthesis, the target DNA was PCR amplified using either Taq polymerase or PFU turbo polymerase as per the manufacturer's protocol.

2.15 Generation of in vitro transcript

The capped in vitro transcripts for either FL12 virus or mutant FL12 virus was generated by using mMEESAGE mMACHINE T7 Ultra (Ambion, Austin, TX) as per the manufacturer's instructions. The pBR322-FL12 (or mutant FL12) plasmids were digested

with AclI restriction enzyme and treated with mungbean nuclease (or DNase I) enzyme (NEB) to digest the DNA template and remove single stranded DNA overhangs respectively. The restriction enzyme digested DNA was purified by phenol-chloroform extraction and the DNA was resuspended in 3-4 μl of nuclease free water. The concentration of the DNA was checked by agarose gel electrophoresis. For in vitro transcription reaction, 1 μg of linearized template DNA was incubated with 1 X T7 NTP / anti-reverse cap analog (ARCA) (7.5 mM ATP, 7.5 mM CTP, 7.5 mM UTP, 1.5 mM GTP, 6 mM ARCA), 4.5 mM GTP, 1X T7 reaction buffer, and T7 RNA polymerase in a final reaction volume of 10 μl at 37^{o}C for 2 h. Then, 1μl (2 units) of DNase I was added to the reaction mixture to remove the template DNA and further incubated at 37^{o}C for 15 min. The in vitro transcription reaction was stopped by addition of 40μl of ammonium acetate stop solution (5M ammonium acetate and 100mM EDTA) and 1μl of glycogen was added to serve as a carrier during RNA extraction and precipitation. The in vitro transcript was recovered by phenol chloroform extraction and precipitation by addition of equal volume of isopropanol and centrifugation at 16,000 X g for 30 min. The RNA pellet was washed with 75% cold ethanol. The dried RNA pellet was resuspended in 20μl of nuclease free water. The purity, concentration, and size of the in vitro transcript were checked by spectrophotometer and glyoxal-agarose gel electrophoresis.

2.16 Plasmid transfection

Plasmids were transfected into cells using Lipofectamine2000 (Invitrogen) as described earlier (Ansari et al., 2006). Briefly, BHK-21 cells were plated in 6-well culture plates 24 h before transfection. The cells were first infected with vTF7-3 (Fuerst

et al., 1986) at a MOI of 5. The DNA-Lipofectamine2000 complexes prepared according to the manufacturer's recommendations were added to the infected and washed BHK-21 cells and incubated at 37^{o}C for 4 h. Following incubation, the cells were washed and incubated in media containing Dulbecco's modified Eagle's media (DMEM) containing 2% FBS and antibiotics as described before (Ansari et al., 2006). The transfected cells were processed for radiolabeling or immunofluorescent staining as described below.

2.17 Metabolic labeling of proteins

The plasmid transfected cells at 16-18 h post-transfection were washed twice in PBS and incubated with cysteine-methionine-free DMEM for 1 h prior to radiolabeling with 33 μCi of Expre^{35}S^{35}S protein labeling mix (Perkin Elmer) per ml of methionine-cysteine free DMEM without serum for 4 h.

2.18 Immunoprecipitation, co-immunoprecipitation, and analysis of proteins

Following radiolabeling, the cells were washed with cold PBS and the cell lysate was prepared in radioimmunoprecipitation (RIPA) buffer as described before (Ansari et al., 2006) or co-IP buffer (1% NP40, 0.5% Triton X-100, 50mM Tris-HCl pH 7.6 , 500 mM NaCl, 2mM EDTA and 1X protease inhibitor cocktail) as described before (Das & Pattnaik, 2005). The cell lysate was clarified by centrifugation at 16,000 X g for 5 min. The supernatant was used for immunoprecipitation with appropriate antibody at 4^{0}C for 8-10 h. A slurry of approximately 3.0 mg of protein A sepharose (GE Health care Bioscience AB) washed and resuspended in 100 ml RIPA or co-IP buffer was added and incubated further for 2 h at 4^{0}C. The protein A sepharose beads with bound immune complexes were washed in RIPA or co-IP buffer three times, resuspended in sodium dodecyl sulfate-polyacrylamide gel electrophoresis (SDS-PAGE) sample buffer (50 mM

Tris-HCl, pH 6.8, 100 mM dithiothreitol, 2% SDS, 0.1% bromophenol blue, and 10% glycerol) and boiled for 5 min. After centrifugation at 16,000xg for 1 min, the proteins in the clarified supernatant were resolved by SDS-10% or 12% polyacrylamide gel electrophoresis (PAGE). Following electrophoresis, the gels were processed for fluorography as described previously (Ansari et al., 2006).

2.19 Endo H and PNGase F treatment of glycoproteins

The endoglycosidase H (endo H) and the peptide N-glycosidase F (PNGase F) was purchased from New England Biolabs. For Endo H treatment, RIPA buffer was removed from the immunoprecipitated complexes and 50 µl of 1X denaturing buffer (0.5% SDS, 1.0% β-mercaptoethanol) was added to it. The resuspended immunoprecipitated complex was boiled for 10 min. The supernatant was collected and split in to two tubes. The reaction mixture was then adjusted to 1X G5 buffer (0.05 M sodium citrate, pH 5.5) and 100 units of Endo H was added to one of the two tubes while an equal volume of 1X G5 buffer was added to the other tube. Both the samples were incubated at 37^0C for 16 h (Ansari et al., 2006; Truong et al., 2004). Following endo H digestion, the sample was mixed with an equal volume of 2X SDS-PAGE sample buffer, boiled for 5 min and resolved by SDS-10% PAGE under denaturing conditions along with protein marker (Bio-Rad, Hercules, CA).

For PNGase F digestion, the reactions were carried out as described for endo H digestion, except that 1X G7 buffer (0.05 M sodium phosphate, pH 7.5), 1.0% NP-40, and 2 units of PNGase F was added. Following PNGase F digestion, the sample was mixed with an equal volume of 2X SDS-PAGE sample buffer, boiled for 5 min and resolved by SDS-10% PAGE under denaturing conditions.

2.20 Tunicamycin treatment

Tunicamycin was purchased from Sigma Aldrich. After 16 h of transfection, the cells were washed and treated with 2.0 μg of tunicamycin per ml of cysteine-methionine-free DMEM for 1 h prior to radiolabeling with by 33 μCi of Expre^{35}S^{35}S protein labeling mix (Perkin Elmer) per ml of methionine-cysteine free DMEM without serum. The radiolabeling was performed in the presence of the tunicamycin for 4 h (Ansari et al., 2006).

2.21 Pulse-chase assay

We performed pulse-chase assay to study co-translational and post-translational glycosylation of envelope glycoproteins of PRRSV. The individual envelope proteins were expressed in BHK-21 cells by plasmid transfection in 35mm cell culture dish. The transfected cells were washed with PBS after 16 h of transfection and incubated with cysteine-methionine-free DMEM for 1 h prior to radiolabeling with by 55 μCi of Expre^{35}S^{35}S protein labeling mix per 100μl of methionine-cysteine free DMEM without serum for 1 min at 37^{o}C. After incubation, the radiolabeling mix was promptly removed from the cell culture dish and the cells were washed with DMEM containing 2% FBS and 1X PKS twice. DMEM containing 2% FBS, 1X PKS, and 100μl of cycloheximide per ml was added on the cells and the cells were further incubated in 37^{o}C. The chase times were 0 min, 10 min, 30 min, and 60 min post radiolabeling. The cells were processed for immunoprecipitation as described earlier.

2.22 Fluorescence microscopy

The transfected cells were either fixed with 4% paraformaldehyde for 30 min at room temperature (for surface staining) or with methanol-acetone solution (1:1) for 30

min at -20^{0}C (for cytoplasmic staining). The cells were blocked with 5% BSA in PBS containing 0.05% Tween20 for 30 min at room temperature. Immunofluorescence staining was performed (Das et al., 2006) with appropriate primary and secondary antibodies and visualized under Olympus FV500/IX81 inverted laser scanning confocal microscope (Center for Biotechnology, University of Nebraska-Lincoln). The images were captured with a charge-coupled-device camera.

2.23 Animal experiment

Recently weaned 21 days mixed breed piglets were purchased from a PRRSV free farm (University of Nebraska-Lincoln swine unit, NE). The pigs were free from any clinical signs of disease and were serologically negative for any detectable antibodies against PRRSV. Four animals were grouped in one room. The animals were bled at time 0 (pre-inoculation time) to obtain a sample of pre-inoculum serum. Subsequently, the animals were inoculated on the same day with PRRSV (wild type and mutant viruses). Viral supernatants collected on 2nd passage post electroporation were used for inoculation of the animals. The animals were maintained in biosafety level 2 (BSL-2) with strict biosecurity to prevent cross contamination between strains. The biosecurity measures included changing lab coats, boots, mask, and gloves in each room per strain. One empty room was maintained between two groups of animals to further prevent cross contamination. One group was used as negative control, in which all the pigs were injected intramuscularly with 2ml of low bicarbonate-low glucose DMEM with 10% FBS and 1X PKS. The other group was kept as positive control, in which case the pigs were intramuscularly injected with FL12 virus with a viral load of 5 x 10^4 PFU/animal (10^5 $TCID_{50}$/animal). The mutant strains of PRRSV used for animal studies are FL-GP2a-

N178A, FL-GP3-N29/152A, FL-GP3-N29/152/160A, FL-GP4-N37A, FL-GP4-N84A, FL-GP4-N120A, and FL-GP4-N130A. The serum was collected on 0, 7, 14, 21, 35, and 46 days post inoculation. The animals were killed and incinerated at the animal research facility in the university. Serum samples of 7, 14, and 21 days were used to test infectivity on MARC-145 cells. RT-PCR was performed from 21st day collected serum to check the stability of the mutation and to test glycosylation phenotype of the virus recovered from the cell culture. All the serum samples collected on different time points were used to check neutralizing antibody titer by serum neutralization assay.

2.24 Serum neutralization assay

This assay was performed in 96 well cell culture plates. Serum from each animal was diluted by two-fold serial dilution. First, 50µl of medium (low bicarbonate-low glucose DMEM with 10% FBS and 1X PKS) was mixed with 50µl of serum from each specific animal from each group. Subsequent two-fold dilution of sera was prepared similarly. To the serum-media mixture, equal volume (100µl) of virus stock with a titer of 100 $TCID_{50}$ was added (final reaction volume- 200µl) and incubated at 37^{o}C for 1hr. After incubation, 100µl of serum-virus mix was transferred to the MARC-145 cells plated in 96 well cell culture plates two days earlier. The cells were further incubated for 36 h at 37^{o}C in cell culture incubator. The infected cells were fixed with 50% methanol-50% acetone solution and stained for N protein of PRRSV by SDOW-17 primary antibody (Nelson et al., 1993). Alexa Fluor-488 goat anti-mouse IgG antibody was used as secondary antibody. For positive control for serum neutralization assay, MARC-145 cells (in one well of the same 96 well plate) were infected with 100 $TCID_{50}$ titer of FL12

virus. For homologous serum neutralization assay, serum and virus was from the same mutant strain. For heterologous serum neutralization assay, serum from mutant virus infected pigs was titrated against wild type (FL12) PRRSV.

The above protocol for animal studies was approved by institutional animal care and use committee (IACUC) at University of Nebraska-Lincoln.

2.25 Bioinformatics analysis

The putative N-glycosylation sites of envelope glycoproteins of PRRSV were determined by use of NetNGly 1.0 server (http://www.cbs.dtu.dk/services/NetNGlyc/). Multiple nucleotide sequence alignment was performed using Clustal W server (http://www.ebi.ac.uk/Tools/clustalw/). NEB cutter V 2.0 server (http://tools.neb.com/NEBcutter2/) and reverse complement server (http://www.bioinformatics.org/sms/rev_comp.html) was used during primer design. NCBI server (http://www.ncbi.nlm.nih.gov/) and ExPASy server (http://ca.expasy.org/) was used for general nucleotide and protein sequence analysis.

CHAPTER III

EXPRESSION OF ENVELOPE GLYCOPROTEINS OF PRRSV AND EXAMINATION OF CO-TRANSLATIONAL AND POST-TRANSLATIONAL GLYCOSYLATION

Part of the work described in this chapter was published in Journal of Virology, 2010.

Das, P.B., Dinh, P.X., Ansari, I. H., de Lima, M., Osorio, F.A., and A. K. Pattnaik. 2010. The minor envelope glycoproteins GP2a and GP4 of Porcine Reproductive and Respiratory Syndrome Virus interact with the receptor CD163. J. Virol. 84: 1731-1740

The envelope glycoproteins GP2a, GP3, GP4, and GP5 of PRRSV are 256 amino acids (aa), 254 aa, 178 aa, and 200 aa long, respectively. The unglycosylated forms of these proteins have the predicted sizes of approximately 29 kDa, 29 kDa, 20 kDa, 18 kDa respectively, whereas that of the unglycosylated FLAG-tagged GP2a used in latter studies is approximately 30 kDa. Each of these proteins also has several predicted N-linked glycosylation sites as well as amino-terminal signal sequences (Fig. 1.3).

3.1 Expression of PRRSV glycoproteins in BHK-21 and HeLa cells

We had previously shown that the major glycoprotein GP5, when expressed ectopically in transfected cells remained in the endoplasmic reticulum or in the cis-Golgi region (Ansari et al., 2006). To examine expression of the minor glycoproteins in transfected cells, plasmids encoding these glycoproteins under the control of T7 RNA polymerase promoter were transfected into BHK-21 cells that had been infected with vTF7-3 that expresses the T7 RNA polymerase. Expression of these proteins could be readily detected (Fig. 3.1) by radiolabeling and immunoprecipitation with monospecific polyclonal antibodies prepared against peptides containing immunodominant epitopes (de Lima et al., 2006) from each of these glycoproteins. The molecular masses of the fully mature glycoproteins (identified by white dots on the left side of the lanes in the panels) were estimated to be approximately 32 kDa, 42 kDa, and 29 kDa, respectively, for GP2a, GP3, and GP4 proteins. Although the major species of GP3 and GP4 corresponded to the fully glycosylated and mature forms of the proteins (white dots in lanes 4 and 6), the fully glycosylated GP2a (white dot in lane 2) represented only a small fraction, while a smaller GP2a was detected as the major protein species (top black dot in lane 2). The electrophoretic mobility of this protein appeared to be consistent with GP2a lacking

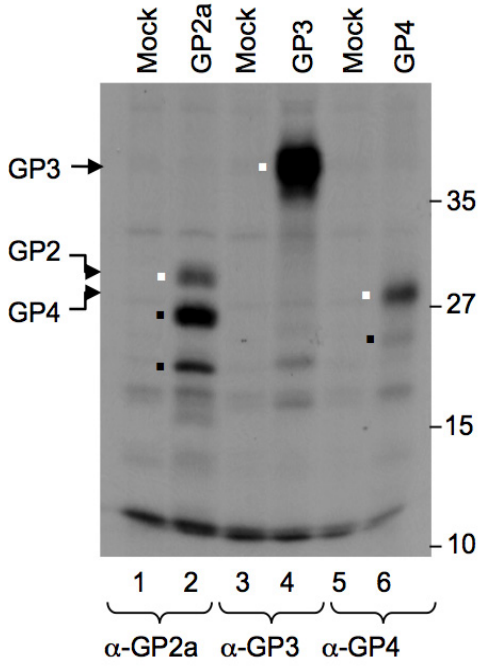

Figure 3.1 Expression of the GPs in BHK-21 cells. The BHK-21 cells were infected with vTF7-3 and subsequently mock-transfected (mock) or transfected with plasmids encoding individual envelope glycoproteins as shown on top of the lanes. The cells were radiolabeled with ^{35}S protein labeling mix as described in the materials and methods, cell extracts were prepared and immunoprecipitated with monospecific polyclonal antibodies as shown on the bottom of the lanes and the proteins were detected by SDS-10%PAGE and fluorography. The fully-glycosylated proteins are identified by white dots whereas the partially glycosylated forms of the proteins are identified by black dots on the left side of the lanes. Relative mobilities of molecular mass markers in kDa are shown on the right.

glycans at one of the sites and may represent a partially glycosylated form of the protein. In addition, it should be noted that these proteins contain signal sequences at the amino terminus, which appear to be cleaved off to generate the mature proteins and therefore may be smaller than the expected length non-glycosylated proteins. Furthermore, based on the predicted size, it appears that these proteins possess anomalous mobilities in the gels.

I also transiently expressed four envelope glycoproteins of PRRSV in HeLa cells (Fig. 3.2). Like BHK-21 cells, HeLa cells can also express these four proteins and apart from the fully glycosylated version of each protein, I can detect partially glycosylated forms of the proteins in my system (Fig. 3.2, white dots in lanes 2, 4, 6, and 8).

3.2 Expression of glycoproteins in MARC-145 cells

Since the predominant protein species in cells transfected with GP2a expression plasmid was smaller than the fully-glycosylated mature GP2a protein, I examined if incompletely glycosylated forms of GP2a and possibly other minor glycoproteins were also synthesized in MARC-145 cells that are normally used for propagation of PRRSV. Additionally, since the major species of GP2a possessed electrophoretic mobility similar to GP4 (Fig. 3.3, lanes 2 and 6), I also examined the expression of a carboxy-terminal FLAG-tagged GP2a protein (GP2a-FLAG) for use in latter studies as GP2a-FLAG fusion protein is expected to have a different electrophoretic mobility compared to GP4. My results revealed that the predominant protein in MARC-145 cells transfected with GP2a-Fl encoding plasmid also corresponded to the partially glycosylated form of the protein (Fig. 3.3) as observed earlier in BHK-21 and HeLa cells. Furthermore, the GP2a-FLAG-

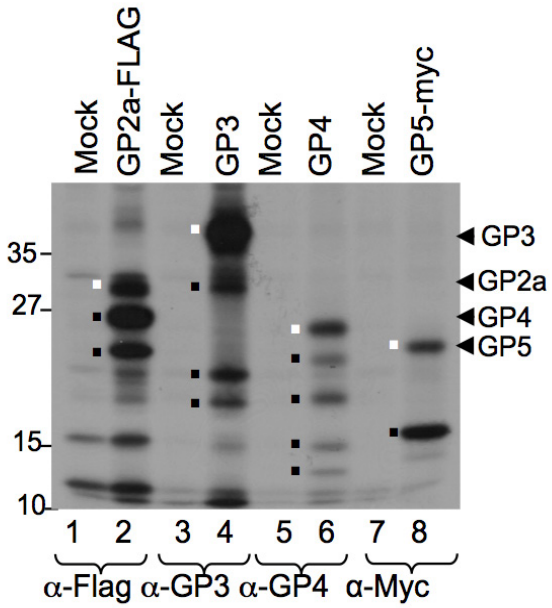

Figure 3.2 Expression of the GPs in HeLa cells. HeLa cells were infected with vTF7-3 virus and transfected with specific plasmids encoding for GP2a, GP3, GP4, and GP5 proteins as described in materials and methods. The transfected cells were radiolabeled with ^{35}S and immunoprecipitated with specific antibodies as denoted in the bottom of the representative fluorogram. The proteins were resolved in SDS-10% PAGE. The mature glycoproteins (fully glycosylated) are denoted as white dots and labeled on the right side of the fluorogram. The partially glycosylated proteins are denoted as black dots. The relative mobilities of the molecular mass markers in kDa are shown on the left.

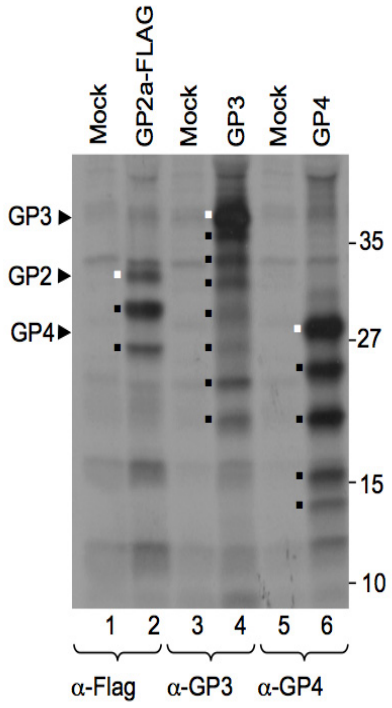

Figure 3.3 Expression of the GPs in MARC-145 cells. The MARC-145 cells were infected with vTF7-3 and subsequently mock-transfected or transfected with plasmids encoding individual envelope glycoproteins as shown on top of the lanes. The cells were radiolabeled with ^{35}S protein labeling mix as described in the materials and methods, cell extracts were prepared and immunoprecipitated with monospecific polyclonal antibodies as shown on the bottom of the lanes and the proteins were detected by SDS-10%PAGE and fluorography. The plasmid encoding GP2a with FLAG-tag was used in place of GP2a and the fusion protein was detected with anti-FLAG antibody. The full-length mature GPs are identified with white dots in lanes 2, 4, and 6 whereas the partially glycosylated forms of the proteins are identified by black dots in the lanes. Relative mobilities of molecular mass markers in kDa are shown on the right.

tagged protein could be readily distinguished from the GP4 protein based on the mobility in the gel, a property that I have used in my protein-interaction studies reported later. Interestingly, in MARC-145 cells, these three proteins produced ladder-like pattern (Fig. 3.3, lanes 2, 4, and 6), indicating that the proteins were also incompletely glycosylated in these cells. However, the fully mature glycoproteins (identified by white dots in Fig. 3.3, lanes 2, 4, and 6) with mobilities similar to that observed in BHK-21 cells were readily detected in each case. Ladder-like pattern of the glycoproteins were also seen in MARC-145 cells infected with PRRSV FL-12 (data not shown). It is possible that the ladder-like pattern of the viral glycoproteins may represent various degraded forms of the proteins. However, my observation that single and multiple N-linked glycosylation mutant proteins co-migrate with the protein bands seen in the ladder-like pattern (data to be reported elsewhere) and the fact that endo-H digestion (Fig. 3.4) has resulted in detection of single species of these proteins (except for GP2a for which the signal-cleaved form of the protein is also detected), argue against the possibility that the ladder-like pattern represent degraded proteins.

3.3 Intracellular localization of glcoproteins of PRRSV

The intracellular localization of the minor glycoproteins in BHK-21 cells was further studied by examining their sensitivity to Endo H digestion and also by confocal microscopy. All of the fully and partially glycosylated proteins in BHK-21 cells were found to contain only high-mannose type glycans as they were sensitive to digestion by Endo H, yielding species that corresponded to the protein backbones only (Fig. 3.4). It should be noted that a smaller protein species (identified by asterisk on the right of lane 3) was also detected. This protein is most likely the signal-cleaved GP2a without glycans.

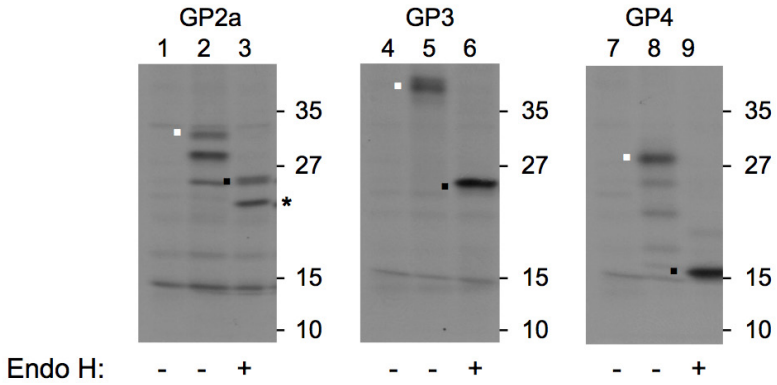

Figure 3.4 Endo H sensitivity of the GPs. The proteins expressed in BHK-21 cells and radiolabeled as described above were recovered by immunoprecipitation, treated without (-) or with (+) Endo H and detected by electrophoresis as above. Mock-transfected cells immunoprecipitated with the antibodies and treated without Endo H are shown in lanes 1, 4, and 7. White dots show the fully glycosylated proteins, black dots show the protein species generated by the enzyme treatment. The protein band identified by asterisk (*) is most likely the signal-cleaved deglycosylated form of GP2a. Relative mobilities of molecular mass markers in kDa are shown on the right.

Sensitivity of the glycoprotein to digestion by endo H suggests that these glycoproteins are localized in the ER. Immunofluorescent staining of cells expressing the individual glycoproteins with monospecific antibodies showed that most of the minor glycoproteins were localized in the cytoplasm in association with the ER (Fig. 3.5). Similar results were also obtained in MARC-145 cells. Overall, my results show that the minor glycoproteins (GP2a, GP3, and GP4) synthesized in transfected cells are localized in the ER, similar to that previously described for the major envelope protein GP5 (Ansari et al., 2006; Wissink et al., 2005).

3.4 Comparison of envelope glycoprotein expression pattern of FL12 PRRSV infected cells and transiently transfected cells

I compared the protein expression pattern of GP2a, GP3, GP4, and GP5 in MARC-145 cells infected with FL12 virus and BHK-21 cells transiently expressing individual envelope glycoproteins (Fig. 3.6A to D). In FL12 virus infected MARC-145 cells, one of the two N-glycosylation sites of GP2a protein is favourably glycosylated in comparison to other sites (Fig 3.6A, lanes 2 and 4). I did not observe any significant difference between protein expression pattern of GP3 (Fig 3.6B), GP4 (Fig 3.6C), and GP5 (Fig 3.6D) proteins in FL12 infected cells and in transiently expressed BHK-21 cells. The slight difference of mobilities of transiently expressed proteins in contrast to virus-infected cells may be attributed to interactions of these proteins among themselves as has been described later.

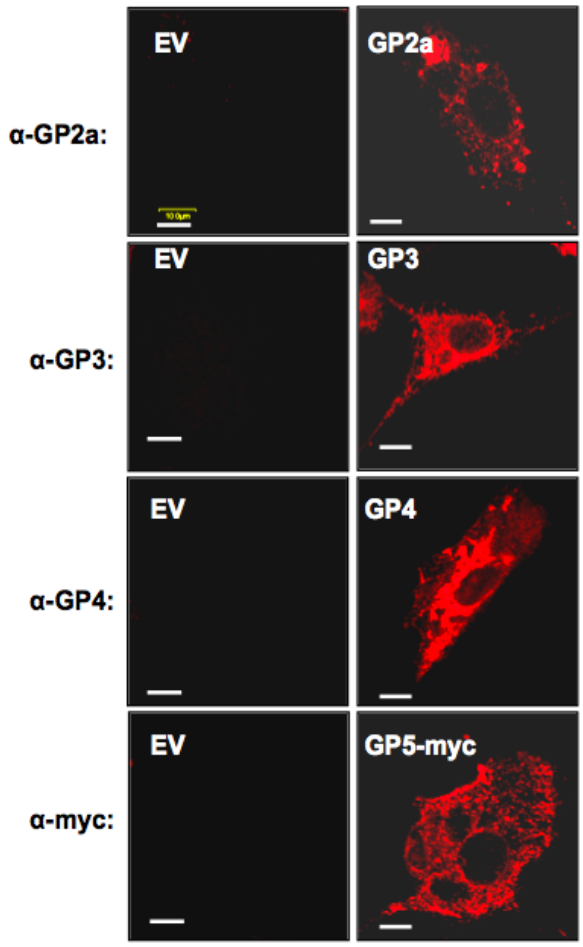

Figure 3.5 Intracellular localization of PRRSV GPs. The BHK-21 cells were infected with vTF7-3 and subsequently transfected with empty vector control (EV), plasmids for GP2a, GP3, GP4, and GP5-myc. The cells were fixed with 50% methanol-acetone solution after 16 h posttransfection. The cytoplasmic staining was performed using specific GP specific antibodies (as mentioned on the left side of each panel) and Alexa-594 conjugated secondary antibody.

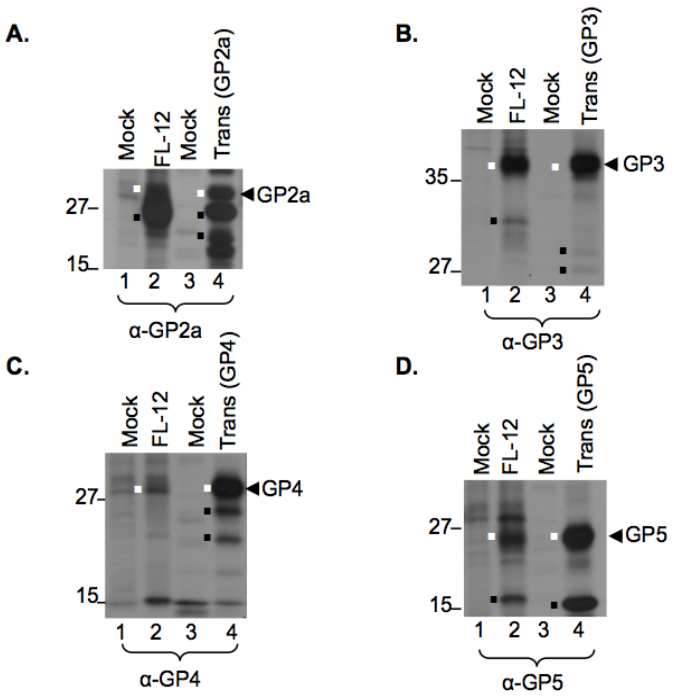

Figure 3.6 Comparison of protein expression in FL12 infected MARC-145 cells and transiently expressed BHK-21 cells. MARC-145 cells were infected with FL12 virus and BHK-21 cells were transfected with individual plasmids encoding specific envelope glycoproteins as described in materials and methods. The infected (lanes 1 and 2) and transfected (lanes 3 and 4) cells were radiolabeled with ^{35}S, lysed and incubated with specific antibodies. The immunoprecipitated proteins were resolved in SDS-10%PAGE and representative fluorograph are shown. The antibodies against specific proteins are shown at the bottom of each fluorograph. The relative mobilities of the molecular mass markers in kDa are shown on the left. The relative mobilities of the molecular mass markers in kDa are shown on the left.

3.5 Co-translational and post-translational glycosylation of PRRSV glycoproteins

The glycoproteins after their synthesis in the ER are post-translationally glycosylated. Based on the position of N resides in the newly synthesized protein, the various putative glycosylation sites in the protein can be either co-translationally or post-translationally glycosylated (Ruiz-Canada *et al.*, 2009). The predicted glycosylation sites for envelope glycoproteins of PRRSV are shown in Fig. 1.3. To study the glycosylation pattern of envelope proteins of PRRSV, I transiently expressed individual glycoproteins in HeLa cells and studied their glycosylation kinetics by pulse-chase assay (Fig. 3.7, 3.8, 3.9, and 3.10). Previously it was reported that the rate of amino acid synthesis in the ER is 6 residues/second. I pulsed the individual envelope proteins for 1 min which would allow synthesis of full-length proteins and then followed by chase for up to 1 h in presence of cycloheximide. The samples were collected at 0, 10, 30, and 60 min post-pulse period. A previous report has shown that treatment of HeLa cells with 10 μg/ml of cycloheximide can prevent 98% protein synthesis (Loh *et al.*, 1970). To prevent complete protein synthesis during chase period, I used a ten times higher concentration than that reported before. Following chase, cell extracts were prepared and the proteins were immunoprecipitated with antibodies against the specific proteins. My results show that both the predicted glycosylation sites of GP2a are co-translationally glycosylated to different extents. But, latter in the chase period one site is preferentially glycosylated (Fig. 3.7, lanes 3 and 6). In contrast, the glycosylation sites in GP3 were all used for glycosylation in a co-translational mechanism (Fig. 3.8), immediately after the pulse, indicating that glycan addition is very efficient. Glycan addition at various sites in GP4 also followed the co-translational mechanism but with slower kinetics (Fig. 3.9). Overall,

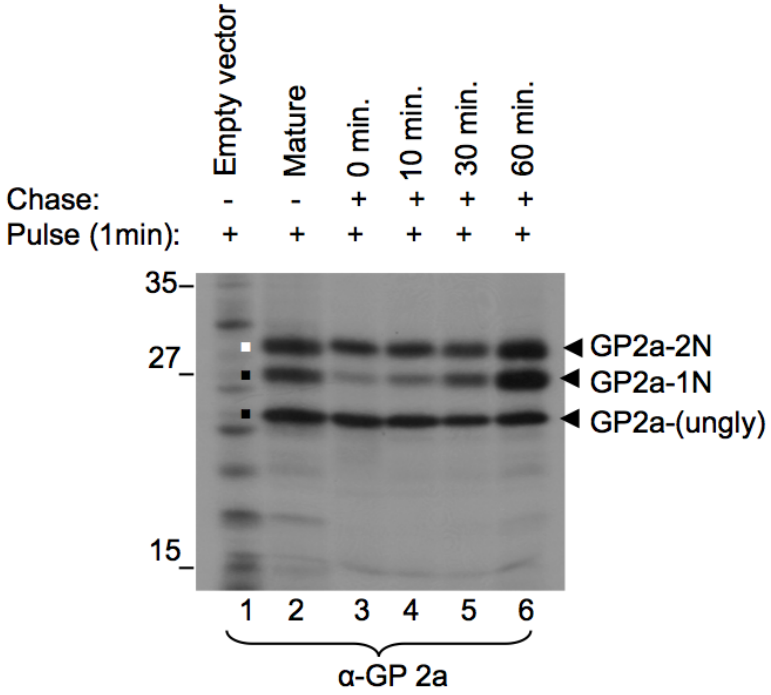

Figure 3.7 Examination of co- or post-translational glycosylation of GP2a protein. Plasmids encoding GP2a protein was transfected in vTF7-3 infected HeLa cells as described in materials and methods. The cells were pulsed with ^{35}S for 1 minute followed by chase 0, 10, 30, and 60 min as indicated (lanes 3 to 6). The empty vector transfected cells are indicated above (lane 1). The GP2a protein immunoprecipitated from cells radiolabeled with ^{35}S are indicated as 'mature' (lane 2). The specific antibody for immunoprecipitation is shown at the bottom. The proteins were resolved by SDS-10%PAGE and detected by fluorography. The bands corresponding to number of glycosylation sites are shown at the right. The relative mobilities of the molecular mass markers in kDa are shown on the left.

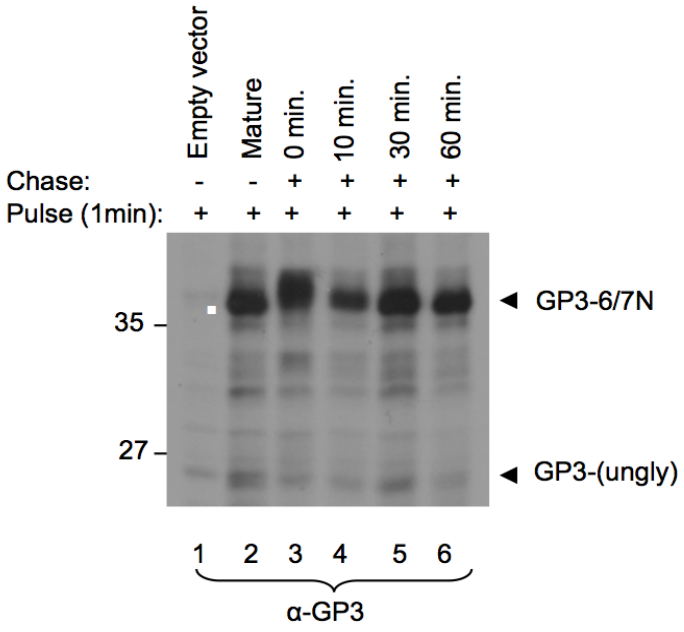

Figure 3.8 Examination of co- and post-translational glycosylation of GP3 protein. Plasmids encoding GP3 protein was transfected in vTF7-3 infected HeLa cells as described in materials and methods. The cells were pulsed with ^{35}S for 1 minute followed by chase 0, 10, 30, and 60 min as indicated (lanes 3 to 6). The empty vector transfected cells are indicated above (lane 1). The GP3 protein immunoprecipitated from cells radiolabeled with ^{35}S are indicated as 'mature' (lane 2). The specific antibody for immunoprecipitation is shown at the bottom. The proteins were resolved by SDS-10%PAGE and detected by fluorography. The bands corresponding to number of glycosylation sites are shown at the right. The relative mobilities of the molecular mass markers in kDa are shown on the left.

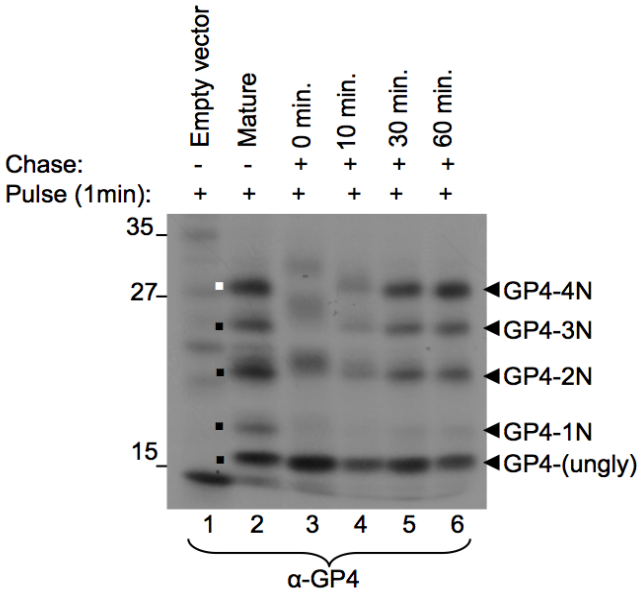

Figure 3.9 Examination of co- and post-translational glycosylation of GP4 protein. Plasmids encoding GP4 protein was transfected in vTF7-3 infected HeLa cells as described in materials and methods. The cells were pulsed with ^{35}S for 1 minute followed by chase 0, 10, 30, and 60 min as indicated (lanes 3 to 6). The empty vector transfected cells are indicated above (lane 1). The GP4 protein immunoprecipitated from cells radiolabeled with ^{35}S are indicated as 'mature' (lane 2). The specific antibody for immunoprecipitation is shown at the bottom. The proteins were resolved by SDS-10%PAGE and detected by fluorography. The bands corresponding to number of glycosylation sites are shown at the right. The relative mobilities of the molecular mass markers in kDa are shown on the left.

these studies suggest that GP2a, GP3, and GP4 proteins are glycosylated co-translationally. However, immediately after pulse, GP5 is only synthesized as a full-length, unglycosylated protein (Fig. 3.10, lane 3). At this time, fully or partially glycosylated forms of the protein were not detectable. Following various times of chase, the fully glycosylated mature form of the protein could be detected (Fig. 3.10, lanes 4-6), indicating that the glycosylated GP5 was generated after synthesis of the unglycosylated GP5. These results suggest that GP5 is post-translationally glycosylated.

3.6 Discussion

The four glycoproteins of PRRSV GP2a, GP3, GP4, and GP5 are present on the envelope and are highly glycosylated. My studies have revealed that (i) recombinant vaccinia virus based transient expression of envelope proteins of PRRSV mimic the protein expression pattern in virus infected cells; (ii) GP2a, GP3, and GP4 are co-translationally glycosylated; and (iii) GP5 is post-translationally glycosylated.

Expression of the individual minor glycoproteins in transfected cells resulted in detection of these proteins by the corresponding monospecific antibodies. Several partially glycosylated forms of the proteins could be readily detected by the antibodies. Particularly striking was the detection of ladder-like pattern of GP3 in MARC-145 cells (Fig. 3.3), which most likely correspond to the partially glycosylated forms of the protein. Partially glycosylated forms were also observed for GP2a and GP4 proteins in BHK-21, HeLa and MARC-145 cells. For GP2a, the size of the major species of the protein corresponds to the one lacking one glycan moiety. GP2a contains two N-glycosylation sites at residues 178 and 184 (Fig. 1.3). The reason(s) for the synthesis of predominantly a GP2a molecule with one glycan moiety is not clear at this time. But, it is possible that

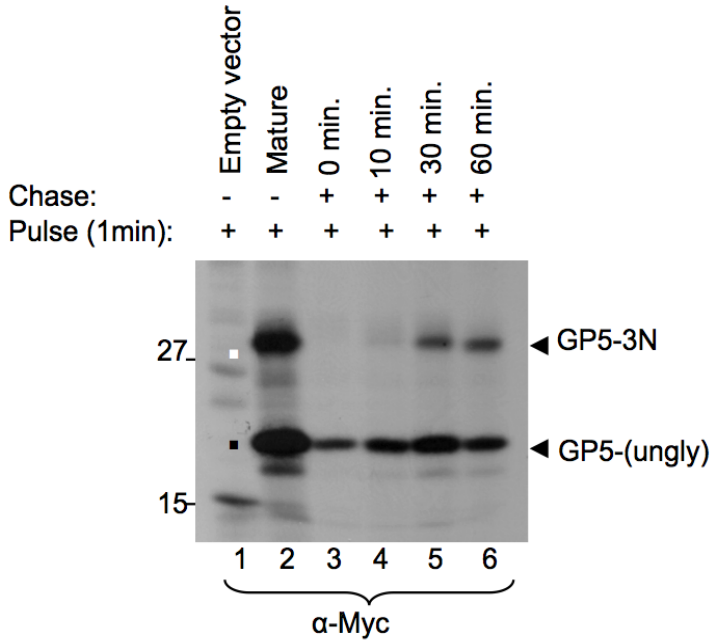

Figure 3.10 Examination of co- and post-translational glycosylation of GP5-myc protein. Plasmids encoding GP5-myc protein was transfected in vTF7-3 infected HeLa cells as described in materials and methods. The cells were pulsed with ^{35}S for 1 minute followed by chase 0, 10, 30, and 60 min as indicated (lanes 3 to 6). The empty vector transfected cells are indicated above (lane 1). The GP5-myc protein immunoprecipitated from cells radiolabeled with ^{35}S are indicated as 'mature' (lane 2). The specific antibody for immunoprecipitation is shown at the bottom. The proteins were resolved by SDS-10%PAGE and detected by fluorography. The bands corresponding to number of glycosylation sites are shown at the right. The relative mobilities of the molecular mass markers in kDa are shown on the left.

one of the N-glycosylation sites is glycosylated inefficiently or with reduced frequency resulting in a predominantly monoglycosylated GP2a. It has been suggested that N-glycosylation sites are less likely to be used if they have not passed through the OST active site prior to translation termination (Gavel & von Heijne, 1990). The estimated distance between the peptidyl transferase site of a ribosome attached to the translocation pore on the ER membrane and the active site of OST complex roughly corresponds to 75 amino acid residues (Ben-Dor *et al.*, 2004; Gavel & von Heijne, 1990; Glabe *et al.*, 1980; Whitley *et al.*, 1996). Since co-translational and post-translational glycosylation on a single protein has been demonstrated (Bolt *et al.*, 2005) and that such modifications occur by distinct mammalian OST isoforms (Ruiz-Canada *et al.*, 2009), I speculate that the glycosylation site at residue 184 in GP2a is most likely modified inefficiently and/or modified by post-translational glycosylation. It is possible that glycan addition at the sites in GP3 and GP4 proteins is also inefficient and may be occurring through co- and post-translational mechanisms resulting in ladder-like patterns of these proteins as seen in Fig.3.1, 3.2, and 3.3.

Comparison of protein expression pattern of envelope glycoproteins in FL12 infected cells and plasmid transfected cells lead us to conclude that there is no significant difference observed between these two systems of protein expression used in my study. GP2a expression pattern observed in virus infected cells and plasmid transfected cells indicate that one of the two N-glycosylation sites is preferentially glycosylated in the virion. But, when I mutated each of the two glycosylation sites and expressed the two mutant proteins in BHK-21 cells, I did not observe any difference in protein expression pattern of the two mutant proteins (described in chapter V). As observed for N-glycans of

rabies virus G protein (Wojczyk et al., 2005), it is plausible that glycosylation at one sequon of GP2a of PRRSV probably regulates glycosylation of the second sequon in the protein. It is also possible that because both of these sequons of GP2a are present in the carboxy terminus of the protein, one of the two sites passes out from the translocon complex (sec 61) without being actually glycosylated as the difference between the last sequon of the protein and termination codon of the protein is less than 75 resides in length (Fig. 1.3) (Ruiz-Canada *et al.*, 2009). Further studies would be needed to confirm this conclusion.

Though N-glycosylation of a protein is mostly co-translational, post-translational modification of some of the host protein including human coagulation factor VII (Bolt *et al.*, 2005) is observed. It is not known whether the phenomenon that dictates co- and post-translational glycosylation of a host protein (Ruiz-Canada *et al.*, 2009) also regulate viral protein glycosylation. Not much information is available regarding glycosylation pattern of different envelope viruses. As per my knowledge, one report suggests existence of post-translational glycosylation in case of hepatitis B virus large (L) protein (Lambert & Prange, 2007). My study shows for the first time the existence of post-translational glycosylation for PRRSV GP5 protein. Even if all the three minor envelope proteins of PRRSV are co-translationally glycosylated, one of the two sequons of GP2a is also post-translationally glycosylated. As STT3A and STT3B subunits of OST complex regulate co- and post-translational glycosylation of the proteins (Ruiz-Canada *et al.*, 2009), further study is required to find which of these two subunits of OST preferentially controls the glycosylation pattern of the four PRRSV envelope proteins. I performed co- and post-translational glycosylation studies in HeLa cells transiently expressing the individual

glycoproteins. Considering the fact that I did not observe any significant difference in protein expression pattern in FL12 infected cells and BHK-21 cells expressing the individual proteins, I speculate co- and post-translational glycosylation pattern as observed in HeLa cells expressing individual proteins may also reflect the actual pattern in the virus infected cells. But, I also do not rule out the possibility of effect of glycosylation of one of the four envelope protein on the other proteins in virus infected cell. Further studies are warranted to clarify this issue in future.

CHAPTER IV

INTERACTION OF ENVELOPE GLYCOPROTEINS OF PRRSV AMONG THEMSELVES AND WITH THE PRRSV RECEPTOR, CD163

Part of the work described in this chapter was published in Journal of Virology, 2010.

Das, P.B., Dinh, P.X., Ansari, I. H., de Lima, M., Osorio, F.A., and A. K. Pattnaik. 2010. The minor envelope glycoproteins GP2a and GP4 of Porcine Reproductive and Respiratory Syndrome Virus interact with the receptor CD163. J. Virol. 84: 1731-1740

4.1 Interaction of envelope glycoproteins of PRRSV amongst each other

4.1.1 Interaction of GP2a with other glycoproteins of PRRSV

To examine if the envelope glycoproteins interact with each other, I co-transfected BHK-21 cells with plasmids encoding GP2a-FLAG along with GP3, GP4, or GP5 encoding plasmids. Approximately 16 h after transfection, the cells were radiolabeled with ^{35}S methionine and the cell extracts were examined for protein interactions by co-IP assays using monospecific antibody against one of the proteins. Results (Fig. 4.1) show that the GP2a polyclonal antibody was able to co-immunoprecipitate GP3 (lane 6) or GP4 (lane 7) protein when expressed together. Since the GP2a antibody did not immunoprecipitate GP3 (lane 3), GP4 (lane 4), or GP5 (lane 5) proteins when these proteins were expressed alone in transfected cells, co-IP of GP3 or GP4 by GP2a antibody in co-transfected cells indicates that GP2a interacts with both of these proteins. On the other hand, GP5 protein could not be immunoprecipitated from co-transfected cells by GP2a antibody indicating that no detectable level of interaction was observed between GP2a and GP5 (lane 8).

4.1.2 Interaction of GP3 with other glycoproteins of PRRSV

BHK-21 cells were co-transfected with the plasmid encoding GP3 along with plasmids encoding GP2a-FLAG, GP4, or GP5. Approximately 16 h after transfection, cells were radiolabeled and the cell extracts were examined for protein interactions by co-IP assays. By the use of anti-GP3 polyclonal antibody, GP2a (Fig. 4.2, lane 9) and GP4 (lane 10) proteins could be co-immunoprecipitated with GP3 in co-transfected cells, suggesting that GP3 interacts with GP2a and GP4. Interaction between GP3 and GP5 was not observed (lane 11) under these conditions.

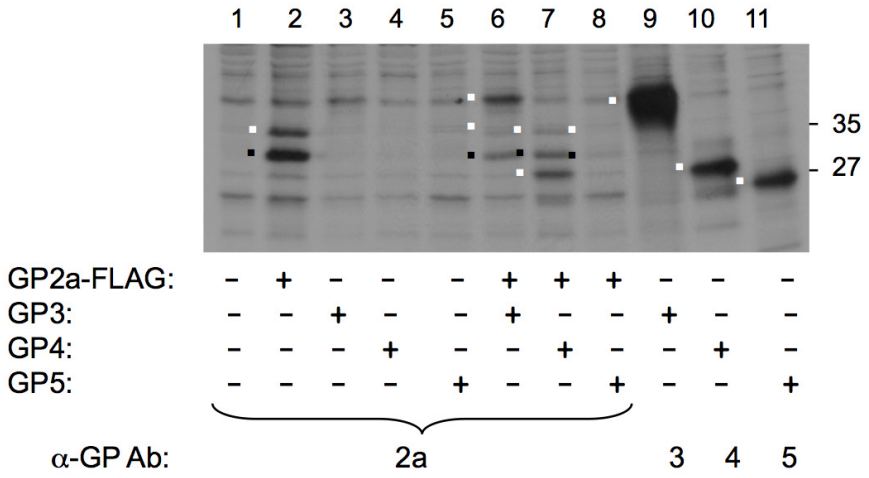

Figure 4.1 Examination of GP interactions using GP2a antibody. BHK-21 cells were infected with vTF7-3 virus and mock-transfected (lane 1) or transfected with plasmids encoding the GPs as shown in the bottom of the panel. – and + indicate without or with the plasmid shown on the left. At 16 h post-transfection, the cells were radiolabeled with ^{35}S protein labeling mix as described in the materials and methods, cell extracts were prepared and immunoprecipitated with monospecific polyclonal antibodies as shown on the bottom of the lanes and the proteins were detected by SDS-12%PAGE and fluorography. The full-length mature GPs are identified with white dots whereas the partially glycosylated forms of the proteins are identified by black dots on the left side of the lanes. Relative mobilities of molecular mass markers in kDa are shown on the right.

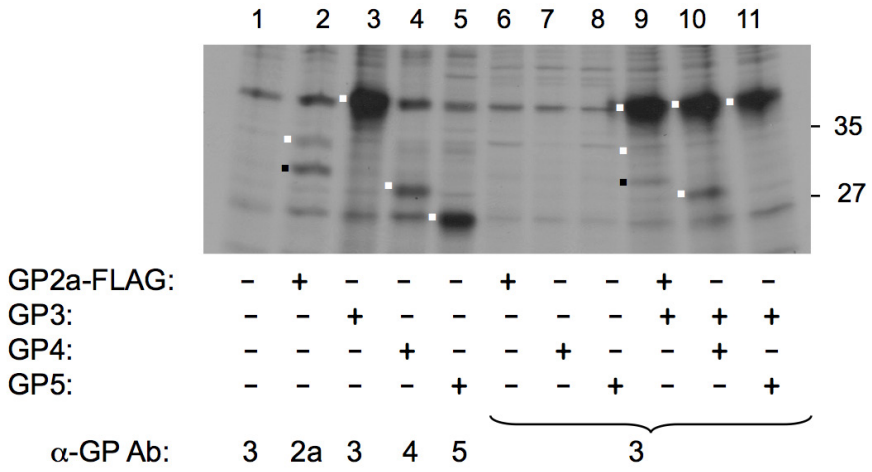

Figure 4.2 Examination of GP interactions using anti-GP3 antibody. BHK-21 cells were infected with vTF7-3 virus and mock-transfected (lane 1) or transfected with plasmids encoding the GPs as shown in the bottom of the panel. – and + indicate without or with the plasmid shown on the left. At 16 h post-transfection, the cells were radiolabeled with ^{35}S protein labeling mix as described in the materials and methods, cell extracts were prepared and immunoprecipitated with monospecific polyclonal antibodies as shown on the bottom of the lanes and the proteins were detected by SDS-12%PAGE and fluorography. The full-length mature GPs are identified with white dots whereas the partially glycosylated forms of the proteins are identified by black dots on the left side of the lanes. Relative mobilities of molecular mass markers in kDa are shown on the right.

4.1.3 Interaction of GP4 with other glycoproteins of PRRSV

BHK-21 cells were co-transfected with the plasmids encoding GP4 along with GP2a-FLAG, GP3, or GP5. Approximately 16 h after transfection, the cells were radiolabeled and the cell extracts were examined for GP4 protein interactions with other glycoproteins by co-IP assays using monospecific antibody against GP4 protein. The anti-GP4 polyclonal antibody immunoprecipitated GP2a, GP3, and GP5 proteins indicating interaction of GP4 with the other three glycoproteins (Fig. 4.3, lanes 9, 10, and 11, respectively).

4.1.4 Interaction of GP5 with other glycoproteins

Similarly, BHK-21 cells were co-transfected with plasmids encoding GP5 along with GP2a-FLAG, GP3, or GP4. Approximately 16 h after transfection, the cells were radiolabeled and the cell extracts were examined for GP5 protein interactions with other glycoproteins by co-IP assays. By the use of monospecific anti-GP5 antibody, GP4 protein could be efficiently immunoprecipitated from cells co-transfected with plasmids encoding the GP4 and GP5 proteins (Fig. 4.4, lane 11), indicating strong interaction between these two proteins. GP2a protein could be consistently detected at low levels when co-expressed with GP5 and immunoprecipitated with anti-GP5 antibody (lane 9). However, undetectable to very low levels of GP3 protein could be seen in some but not all experiments when GP3 is co-expressed with GP5 and immunoprecipitated with anti-GP5 antibody (lane 10).

To further confirm GP4-GP5 interaction, I used confocal immunofluorescent microscopy. GP4-HA and GP5-myc tagged proteins were co-expressed in cells co-

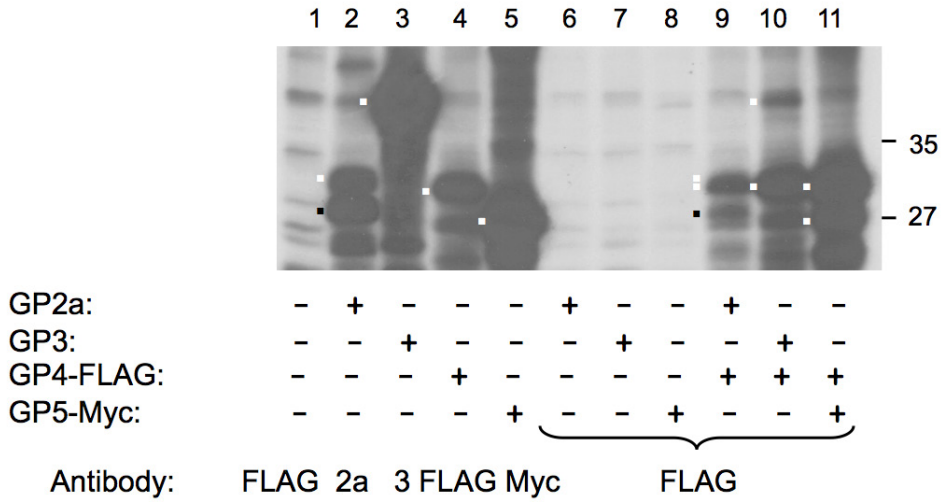

Figure 4.3 Examination of GP interactions using anti-FLAG antibody. BHK-21 cells were infected with vTF7-3 virus and mock-transfected (lane 1) or transfected with plasmids encoding the GPs as shown in the bottom of the panel. – and + indicate without or with the plasmid shown on the left. At 16 h post-transfection, the cells were radiolabeled with ^{35}S protein labeling mix as described in the materials and methods, cell extracts were prepared and immunoprecipitated with monospecific antibodies as shown on the bottom of the lanes and the proteins were detected by SDS-12%PAGE and fluorography. The full-length mature GPs are identified with white dots whereas the partially glycosylated forms of the proteins are identified by black dots on the left side of the lanes. Relative mobilities of molecular mass markers in kDa are shown on the right.

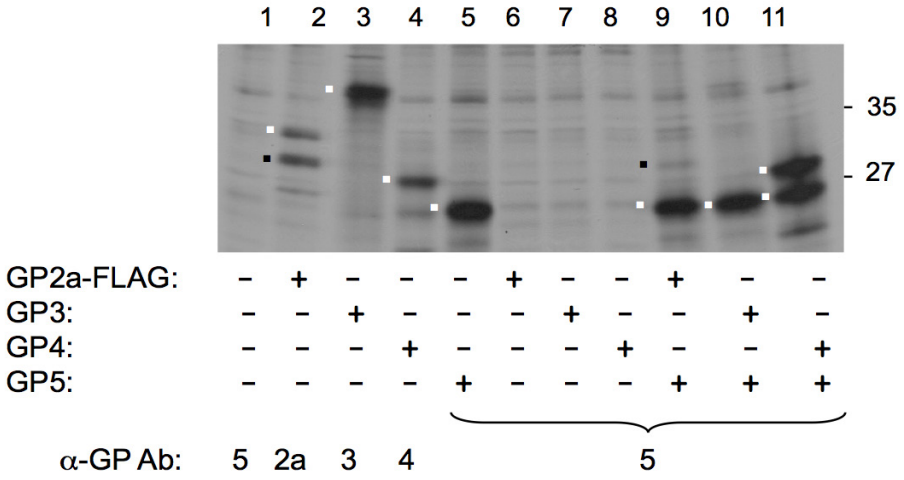

Figure 4.4 Examination of GP interactions using anti-GP5 antibody. BHK-21 cells were infected with vTF7-3 virus and mock-transfected (lane 1) or transfected with plasmids encoding the GPs as shown in the bottom of the panel. – and + indicate without or with the plasmid shown on the left. At 16 h post-transfection, the cells were radiolabeled with ^{35}S protein labeling mix as described in the materials and methods, cell extracts were prepared and immunoprecipitated with monospecific polyclonal antibodies as shown on the bottom of the lanes and the proteins were detected by SDS-12%PAGE and fluorography. The full-length mature GPs are identified with white dots whereas the partially glycosylated forms of the proteins are identified by black dots on the left side of the lanes. Relative mobilities of molecular mass markers in kDa are shown on the right.

transfected with the two plasmids and after 16 h of transfection, the cells were subjected to immunofluorescent microscopy using the primary antibodies against the two tags followed by the use of two secondary antibodies conjugated to two different fluorophores. The GP4-HA and GP5-myc proteins were found to be co-localized in co-expressed cells (Fig. 4.5) as judged by the overlapping of the two fluorescent signals. From this result and those from the co-IP studies, I conclude that GP5 protein interacts strongly with GP4 protein and that both the proteins are co-localized in the cytoplasm of the cell.

Overall, the results from these co-IP studies suggest that GP2a protein interacts with GP3, GP4 and GP5 proteins, GP3 interacts with GP2a and GP4 but not with GP5, GP4 also interacts with all the three glycoproteins, whereas GP5 interacts with GP4 and GP2a proteins (Table 4.1). Although the extent of interaction between the GPs is difficult to estimate from the co-IP studies, it is clear that the interaction of GP4 with GP5 appears to be much stronger than the interactions between the other GPs.

4.2 GP4 mediates interactions resulting in detection of multiprotein complex

To further examine if multiprotein glycoprotein complexes can be detected by co-IP assay, I transiently expressed multiple glycoproteins of PRRSV in BHK-21 cells and attempted to pull down all the interacting glycoproteins using one monospecific antibody by co-IP. I chose to use GP3 antibody in this study, as the use of this antibody in BHK-21 cell extracts resulted in less background bands (Fig. 4.2). I observed that the GP3 antibody was not able to pull down GP5 protein when both of these proteins were co-expressed (Fig. 4.6, lane 6), confirming the results obtained previously. Furthermore, this antibody was able to pull down small amounts of GP2a protein, but not GP5 protein

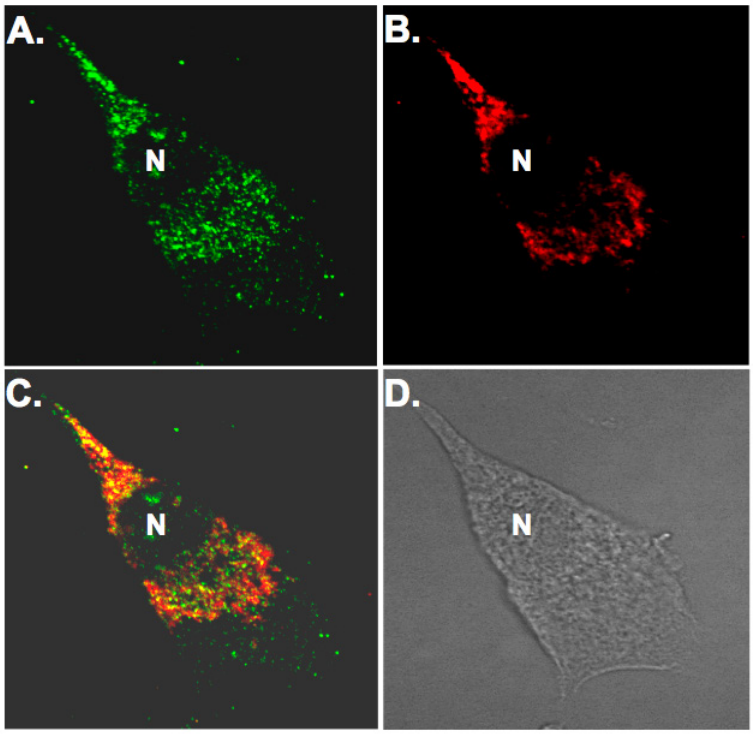

Figure 4.5 Co-localization of GP4 protein and GP5 protein in transfected cells. BHK-21 cells plated on glass coverslips were infected with vTF7-3 and transfected with plasmids encoding HA-tagged GP4 (GP4-HA) and myc-tagged GP5 (GP5-myc) proteins. At 16 h after transfection, the cells were fixed, permeabilized, and processed for immunofluorescent microscopy as described in the materials and methods. The GP4 protein was detected using rabbit anti-HA polyclonal antibody and Alexa-488 conjugated goat anti-rabbit IgG as secondary antibody whereas the GP5 protein was detected with and anti-myc monoclonal antibody and Alexa-594 conjugated anti-mouse IgG as secondary antibody. Images were captured using 100X aperture. Intracellular expression of GP4 (A) GP5 (B) in the same cell is shown. (C) Merged image showing co-localization of the two proteins. (D) DIC image of the cell. N, nucleus.

Table 4.1 Complete map of interaction pattern of envelope glycoproteins.

	GP2a	**GP3**	**GP4**	**GP5**
GP2a		++++	++++	-/+
GP3	+++		+++	-/+
GP4	+++	+++		++++
GP5	-/+	-/+	++++	

The strength of interaction between two glycoproteins is denoted by different numbers of plus or minus signs. A non-significant to weaker interaction between two glycoproteins is denoted as -/+ sign whereas, the strongest interaction between two glycoproteins is denoted as ++++ sign. The interaction pattern between homologous proteins was not studied and hence the space is left as blank.

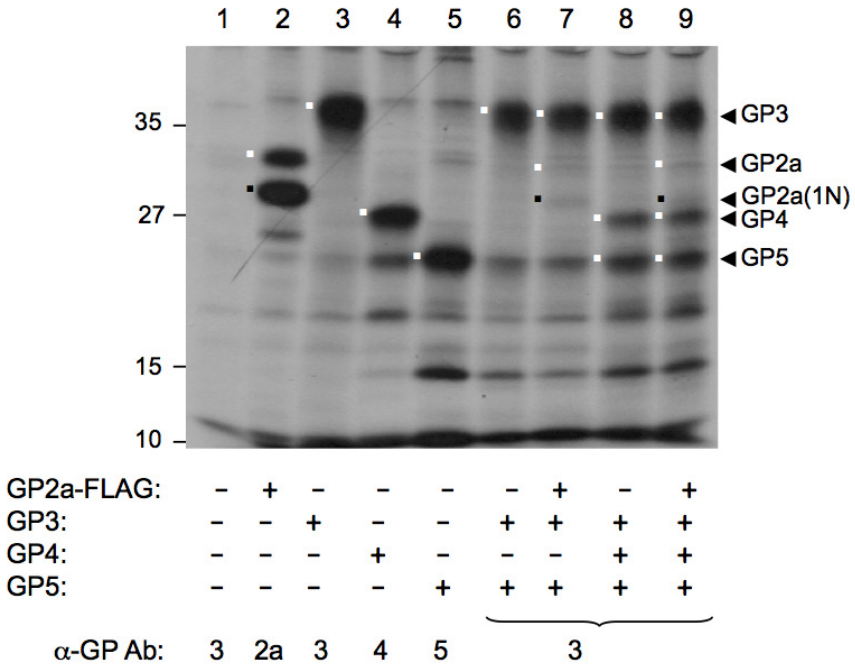

Figure 4.6 Interaction of GP5 with GP4 is necessary for multiprotein complex formation. BHK-21 cells were infected with vTF7-3 and subsequently mock-transfected (lane 1) or transfected with individual or combinations of plasmids encoding various GPs as shown in the bottom of each lane. Cells were radiolabeled as described in the materials and methods and immunoprecipitated with antibodies shown below the lanes. The proteins were detected by SDS-12%PAGE and fluorography. Various GPs are identified on the right. The fully glycosylated GPs are identified with white dots on the left side of the lanes. GP2a (1N), the monoglycosylated form of GP2a, is identified with a black dot on the left side of the lanes. Relative mobilities of molecular mass markers in kDa are shown on the left.

when these three proteins were co-expressed (lane 7), indicating that GP3 interaction with GP2a is not sufficient to pull down GP5 protein in co-IP assay. However, when GP3, GP4, and GP5 proteins were co-expressed, all three proteins could be specifically immunoprecipitated with anti-GP3 antibody (lane 8), indicating that GP4 protein was important for generation of this tripartite glycoprotein complex. Additionally, when all the four glycoproteins were co-expressed and immunoprecipitation was carried out with GP3 antibody, all the four proteins could be detected (lane 9). The results suggest that the GP4 most likely mediates the interactions among PRRSV glycoproteins to generate the multiprotein glycoprotein complex.

4.3 Role of N-glycosylation of GP5 on its interaction with GP4 protein

GP5 of North American strain of PRRSV has three N-glycosylation sites with N at positions 34, 44, and 51. Previously the role of these three glycosylation sites in infectious virus production and evasion of neutralizing antibody response was reported (Ansari et al., 2006). I further studied the role of glycosylation of GP5 in its interaction with GP4 proteins. Seven mutant constructs were generated having N to A mutation in different combination. Three single N mutant clones were GP5-N34A, GP5-N44A, and GP5-N51A. Three double mutant constructs generated were GP5-N34/44A, GP5-N34/51A, and GP5-N44/51A. The triple glycosylation mutant construct GP5-N34/44/51A construct was generated by mutating all the three glycosylation sites of GP5. Stable protein expression for all the seven GP5 constructs were observed by expression of these proteins in BHK-21 cells. The anti-GP5 polyclonal antibody was able to immunoprecipitate both completely glycosylated as well as partially glycosylated form of GP5 (Fig. 4.7). Faster electrophoretic mobility of GP5 N-glycosylation defective proteins

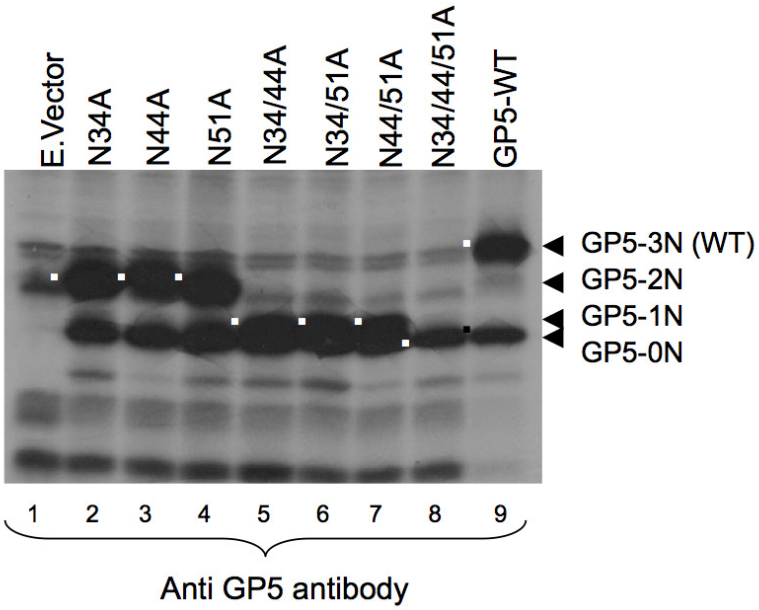

Figure 4.7 Expression of GP5 N-glycosylation defective mutants. BHK-21 cells were infected with vTF7-3 and transfected with pGEM3 (E. Vector, lane 1) or GP5 and its N-glycosylation defective mutant clones. Cells were radiolabeled for 4 h at 16 h post-transfection, and the radiolabeled proteins were analyzed by immunoprecipitation with anti-GP5 polyclonal antibody, resolved in SDS-15%PAGE and detected by fluorography. The fully glycosylated proteins are identified by white dots, whereas the partially glycosylated forms of the proteins are identified by black dots, on the left side of the lanes. Mobilities of completely glycosylated GP5 and partially glycosylated form GP5 are shown on the right.

was observed that correlated with the loss of glycosylation sites by mutation of N to A residues. Overall, these results showed that various N-glycosylation mutant GP5 proteins are stable and can be readily detected in transfected cells.

To further study the role of N-glycosylation of GP5 in its interaction with GP4 protein, I co-expressed GP4 with various GP5 constructs in BHK-21 cells. After 16 h of transfection, the cells were radiolabeled with ^{35}S and co-IP assay was performed. The proteins complexes were immunoprecipitated by anti-GP5 polyclonal antibody. Results show that single N-glycosylation sites mutants of GP5 interact with GP4 since GP4 protein could be readily immunoprecipitated with GP5 antibody (Fig. 4.8, lanes 7 to 9). Further, the double and triple glycosylation mutant GP5 proteins also have been shown to interact with GP4 (Fig. 4.8, lanes 10 to 13). These results indicate that N-glycosylation of GP5 is dispensable for its interaction with GP4.

4.4 Cloning, expression, and functionality of porcine CD163, the cellular receptor for PRRSV

4.4.1 Cloning of porcine CD163

It was previously reported that the expression of porcine CD163 in non-permissive cells confers susceptibility to the PRRSV infection (Calvert et al., 2007). A recent study (Van Gorp et al., 2008) suggested that CD163 acts internally to uncoat the virus genome and that expression of both CD163 and sialoadhesin are simultaneously required for efficient infection by PRRSV. However, in the same study (Van Gorp et al., 2008), it was also shown that expression of CD163 alone in BHK-21 cells that are

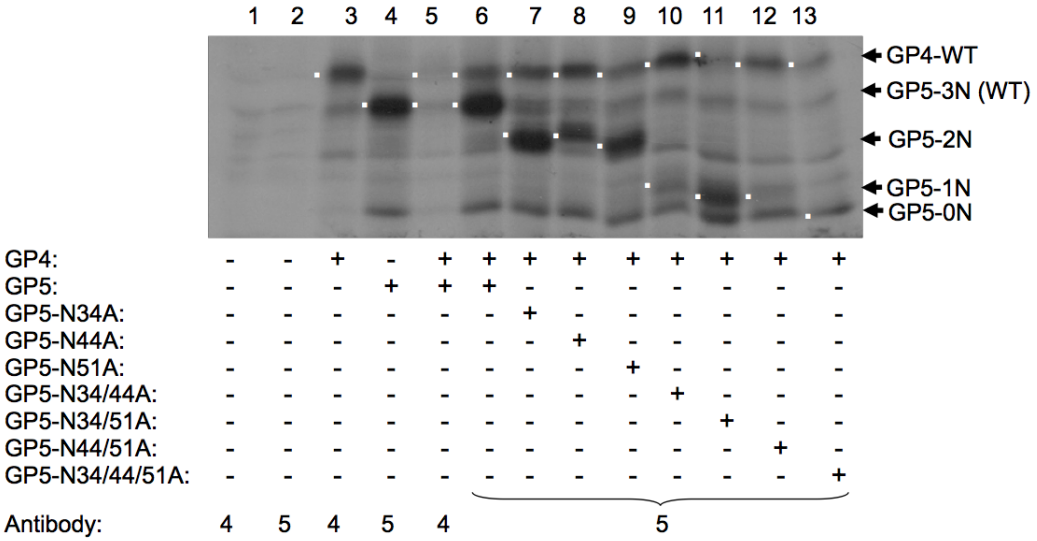

Figure 4.8 Examination of GP4 interaction with GP5 N-glycosylation defective mutants using anti-GP5 antibody. BHK-21 cells were infected with vTF7-3 virus and mock-transfected (lane 1) or transfected with plasmids encoding the GPs as shown in the bottom of the panel. – and + indicate without or with the plasmid shown on the left. At 16 h post-transfection, the cells were radiolabeled with ^{35}S protein labeling mix as described in the materials and methods, cell extracts were prepared and immunoprecipitated with monospecific polyclonal antibodies as shown on the bottom of the lanes and the proteins were detected by SDS-12%PAGE and fluorography.

otherwise non-permissive to PRRSV infection, led to productive infection, indicating that CD163 alone is sufficient to establish a productive replicative cycle of the virus. Therefore, PRRSV must bind to cells expressing CD163 to initiate the viral replication process. To determine which of the PRRSV envelope glycoproteins interact with CD163, I first cloned in pcDNA3.1 (+) vector, the full-length cDNA of CD163 from porcine alveolar macrophage (PAM) cells by RT-PCR amplification of total RNA from the cells using CD163 specific primers (Table 2.1).

4.4.2 Expression of receptor CD163

Four clones were used to examine the expression of the encoded protein by transfection, radiolabeling, and immunoprecipitation with porcine anti-CD163 antibody. I observed that three of the clones expressed proteins (Fig. 4.9B, lanes 3-5) that could be specifically immunoprecipitated with anti-CD163 antibody and possessed electrophoretic mobility (~130 kDa) corresponding to the full-length CD163 (Calvert et al., 2007). A smaller protein product of ~100 kDa encoded in another the clone was also detected by the CD163 antibody (Fig. 4.9B, lane 2). Sequence analysis of the clones showed that CD163 in the clone that produced the smaller protein contained a premature termination codon at aa position 893, resulting in a truncated protein of 892 aa corresponding to the observed molecular mass. This truncated protein lacks the carboxy-terminal cytoplasmic domain, the transmembrane (TM) domain as well as the ninth repeat unit of the scavenger receptor cysteine-rich (SRCR) protein domain (Fig. 4.9A) (Madsen et al., 2004). I have termed this truncated protein as CD163ΔTM. The CD163 cDNAs in the other clones contained full-length sequences of 1115 amino acids with greater than 99%

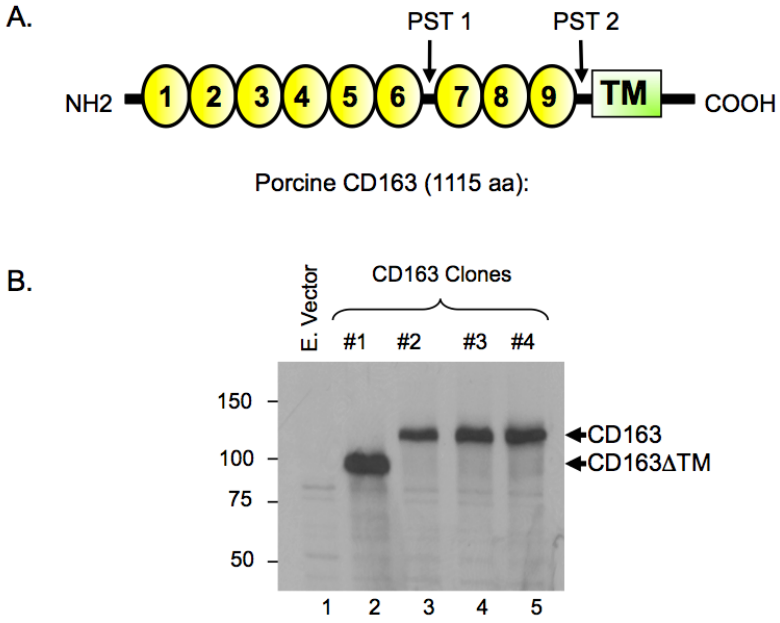

Figure 4.9 Porcine CD163. (A) The structure of porcine CD163, the cellular receptor for PRRSV. The extracellular amino terminus (NH_2), transmembrane (TM) and cytoplasmic (COOH) domains at the carboxy-terminus of the molecule are shown. The main backbone of the protein contains nine scavenger receptor cysteine-rich (SRCR) domains. Two proline-serine-threonine (PST) rich interdomains (PST1 and PST2) are shown.

(B) Expression of CD163 in transfected cells. BHK-21 cells were infected with vTF7-3 and transfected with pcDNA3.1 (E. Vector, lane 1) or CD163 cDNA containing clones (# 1, 2, 3, and 4, lanes 2-5, respectively). Cells were radiolabeled for 4 h at 16 h posttransfection, the radiolabeled proteins were analyzed by immunoprecipitation with porcine anti-CD163 monoclonal antibody, resolved in SDS-10%PAGE and detected by fluorography. Mobilities of full-length (CD163) and the truncated form (CD163ΔTM) of CD163 are shown on the right. Relative mobilities of molecular mass markers in kDa are shown on the left.

sequence identity with the reported sequence of the porcine CD163 (Calvert et al., 2007; Sanchez-Torres et al., 2003).

4.4.3 Functionality of receptor CD163

To determine if the cloned CD163 confers susceptibility to PRRSV infection, I transfected the plasmids into BHK-21 cells that are non-permissive to PRRSV infection. Subsequently, the cells at about 48 h post-transfection were infected with PRRSV. Synthesis of N protein, indicative of PRRSV entry, transcription, and replication was examined in these cells by immunofluorescent staining of the cells at 48 h post-infection with anti-N monoclonal antibody, SDOW17 (Nelson et al., 1993). Synthesis of the N protein was readily detected in the cells transfected with clones encoding the full-length CD163 (Fig. 4.10), indicating that the CD163 encoded in these clones conferred susceptibility to PRRSV infection. The N protein was not detected in cells transfected with the clone encoding CD163ΔTM, suggesting that this truncated protein is non-functional in conferring PRRSV susceptibility to the cells. The inability of CD163ΔTM to confer PRRSV susceptibility to the cells is not due to low levels of expression of the protein since under similar transfection conditions, CD163ΔTM is detected at least at levels similar to or greater than that of the full-length protein (Fig. 4.9B). The results indicate that the carboxy-terminal 223 amino acids of CD163 are required for the function of the protein in conferring PRRSV susceptibility. It is possible that the CD163ΔTM may have defective cellular localization or improper folding leading to loss of its function.

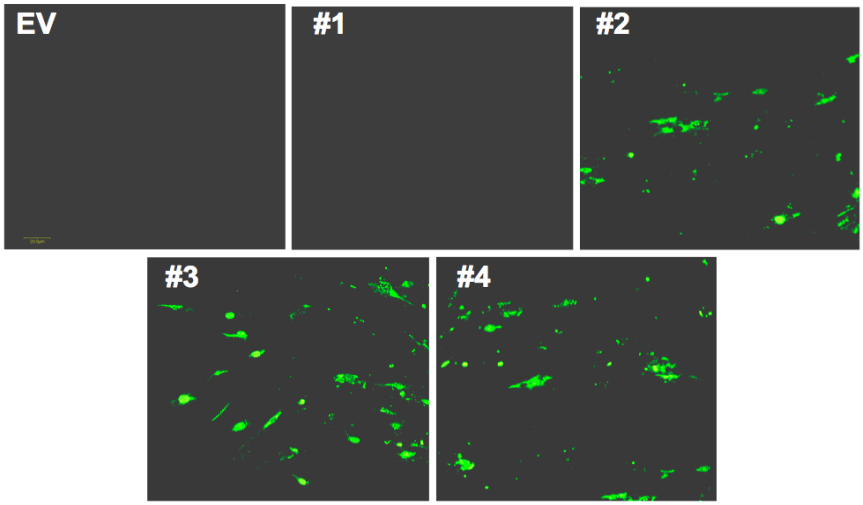

Figure 4.10 Susceptibility of BHK-21 cells expressing CD163 encoded in the clones to PRRSV infection. Cells were transfected with the plasmid clones as shown (EV, empty vector control) and expression of CD163 was driven by CMV promoter in pcDNA3.1 vector. Forty-eight hours after transfection, cells were infected with PRRSV and expression of N protein was examined using the monoclonal antibody SDOW17 and secondary antibody conjugated to Alexa-488.

Immunofluorescence microscopic examination of cells transfected with one of the full-length CD163 clone showed that CD163 protein was seen localized on the plasma membrane (Fig. 4.11, panel c) as well as in the cytoplasm (Fig. 4.11, panel d). Cells transfected with the clone encoding CD163ΔTM showed no surface expression of the protein (Fig. 4.11, panel e), although the protein was expressed in the cytoplasm (Fig. 4.11, panel f), indicating that CD163ΔTM is defective in plasma membrane localization. Empty vector transfected cells did not exhibit any immunofluorescent staining on the plasma membrane or in the cytoplasm (Fig. 4.11, panels a and b).

4.5 Interaction of receptor CD163 with the envelope proteins of PRRSV

I next wanted to examine which of the PRRSV envelope glycoprotein(s) interact with the receptor CD163. To perform the studies, the CD163 along with each of the four envelope glycoproteins were co-expressed in transfected cells and interactions were examined by co-IP with porcine CD163 monoclonal antibody. This antibody did not immunoprecipitate the individual glycoproteins when these glycoproteins were expressed alone (Fig. 4.12, lanes 7-10), demonstrating that the antibody does not immunoprecipitate the proteins non-specifically. However, when the individual glycoproteins were co-expressed with CD163, GP2a and GP4 proteins could be specifically immunoprecipitated with anti-CD163 antibody (lanes 11 and 13) in multiple repeat experiments. Interestingly, both the mature GP2a and partially glycosylated GP2a proteins (identified by white and black dots, respectively, in lane 11) could be immunoprecipitated with the CD163 antibody (lane 11), indicating that both forms of GP2a interact with CD163. The use of GP-specific antibodies also showed that CD163 protein could be immunoprecipitated with anti-GP2a or anti-GP4 antibodies (data not shown). The GP3 and GP5 proteins

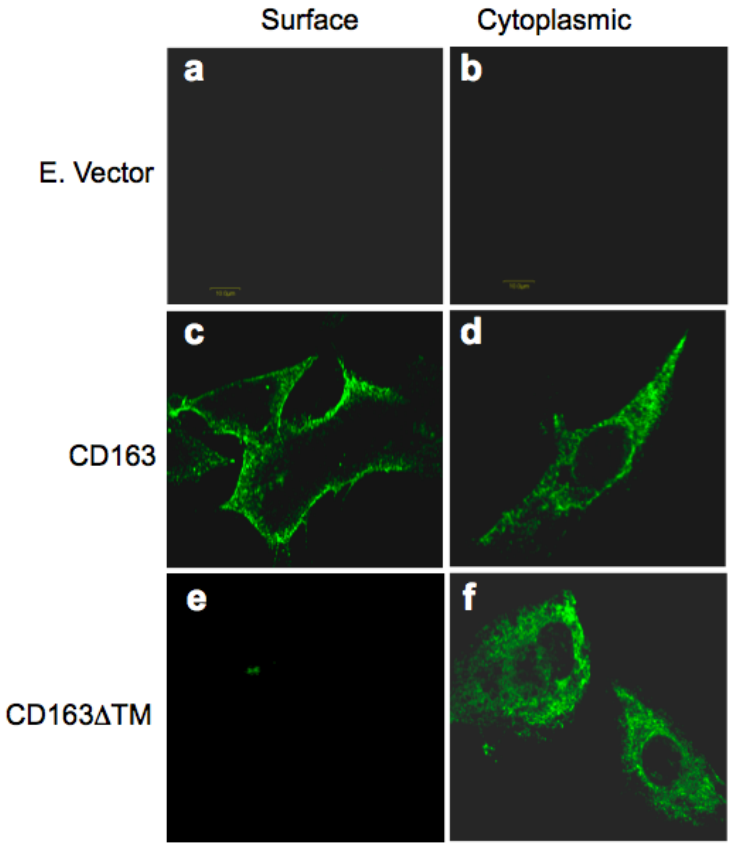

Figure 4.11 Intracellular distribution of CD163. Immunofluorescent staining of BHK-21 cell transfected with empty vector (panels a and b), full-length CD163 receptor encoding clone # 2 (panels c and d), or CD163ΔTM encoding clone (panels e and f). Cell surface or cytoplasmic staining was performed with CD163 monoclonal antibody and Alexa-488 conjugated secondary antibody.

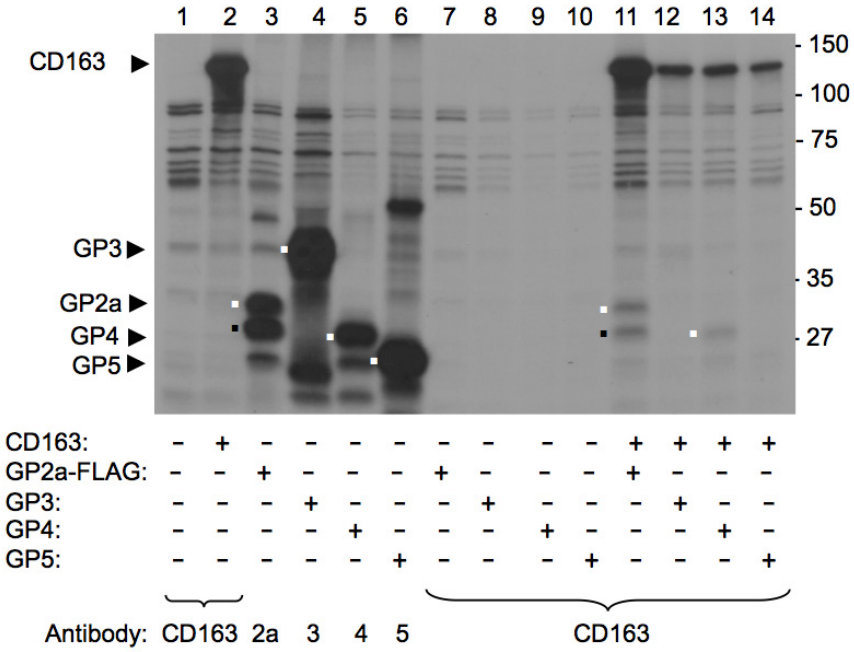

Figure 4.12 Interaction of CD163 with PRRSV GPs. BHK-21 cells were infected with vTF7-3 and transfected with various GPs alone or in combination with CD163 (clone #2). The cells were radiolabeled and the proteins were immunoprecipitated with antibodies as shown below the lanes. Immunoprecipitated proteins were detected by SDS-10%PAGE and fluorography. Mobilities of molecular mass marker proteins in kDa are shown on the right. CD163 and the fully glycosylated viral GPs are identified on the left. Fully glycosylated GPs are identified with white dots in the fluorograms on the left side of each lane. The monoglycosylated GP2a is identified with black dots on the left side in lanes 3 and 11.

could not be detected by immunoprecipitation with anti-CD163 antibody (lanes 12 and 14) from co-transfected cells. These results suggest the GP3 and GP5 proteins do not interact with the CD163 or that their interactions can not be detected under conditions in which interactions with GP2a and GP4 could be readily detected.

To further address whether CD163 co-localizes with either with GP2a or GP4, I co-expressed CD163 with GP2a, GP3, and GP4 proteins (Fig. 4.13). By confocal microscopic studies, I found that strong co-localization of CD163 with both GP2a and GP4 (Fig. 4.13, panels C and I) observed whereas GP3 did not co-localize with CD163 (Fig. 4.13, panel F). This result confirmed the previous observation from co-IP studies that CD163 specifically interacts with both GP2a and GP4 proteins.

4.6 Interaction of CD163ΔTM with envelope proteins of PRRSV

Further, I performed a co-IP assay in which the CD163ΔTM was co-expressed with the viral GPs (Fig. 4.14). By using the CD163 monoclonal antibody, I was able to pull down GP2a or GP4 protein, indicating that the 223 amino acids from the carboxy terminus of CD163 that are missing in CD163ΔTM, are not required for its interaction with GP2a or GP4 proteins.

4.7 Mapping of the domains of GP2a that interact with CD163

To map the amino acid residues of GP2a that are required for its interaction with receptor CD163, I generated a series of deletion mutant proteins of GP2a by sequentially deleting ~ 35-40 amino acids from amino-terminus to carboxy-terminus of the protein and cloned them in pGEM3 expression vector. To avoid the problem of losing possible anti-GP2a antibody binding epitope by deletion of amino acids, a FLAG tag was fused in frame at the carboxy-terminus of the GP2a (GP2a-FLAG) and its deletion

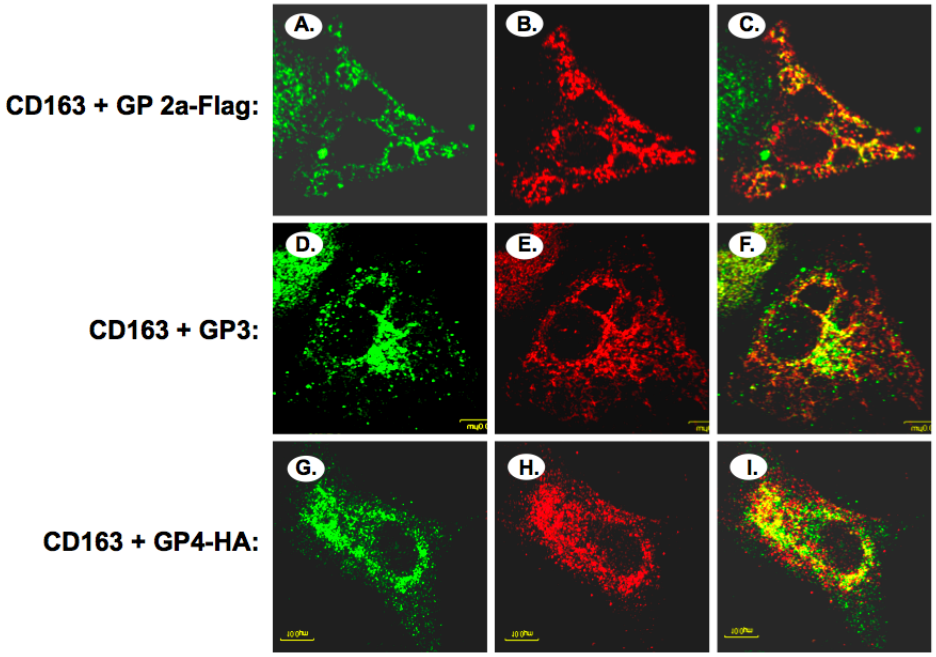

Figure 4.13 Co-localization of CD163 with GP2a and GP4. BHK-21 cells plated on glass coverslips were infected with vTF7-3 and transfected with plasmids encoding CD163 and FLAG tagged GP2a (GP2a-FLAG), GP3 and HA tagged GP4 (GP4-HA) proteins. At 16 h post transfection, the cells were fixed, permeabilized, and processed for immunofluorescent microscopy as described in the materials and methods. The CD163 protein (green) was detected using mouse anti CD163 monoclonal antibody and Alexa-488 conjugated goat anti-mouse IgG as secondary antibody whereas the GP2 protein (red) was detected with and anti-FLAG polyclonal antibody and Alexa-594 conjugated anti-mouse IgG as secondary antibody. The GP3 (red) was detected with anti-GP3 polyclonal antibody and Alexa-594 conjugated anti-rabbit IgG as secondary antibody. The GP4-HA (red) protein was detected with anti-HA polyclonal antibody and Alexa-594 conjugated anti-rabbit IgG as secondary antibody. Images were captured using 100X aperture. Intracellular expression of CD163 (A, D, and G), GP2 (B), GP3 (E), and GP4 (H) in the same cell is shown. (C, F, and I) Merged image showing co-localization of the two proteins.

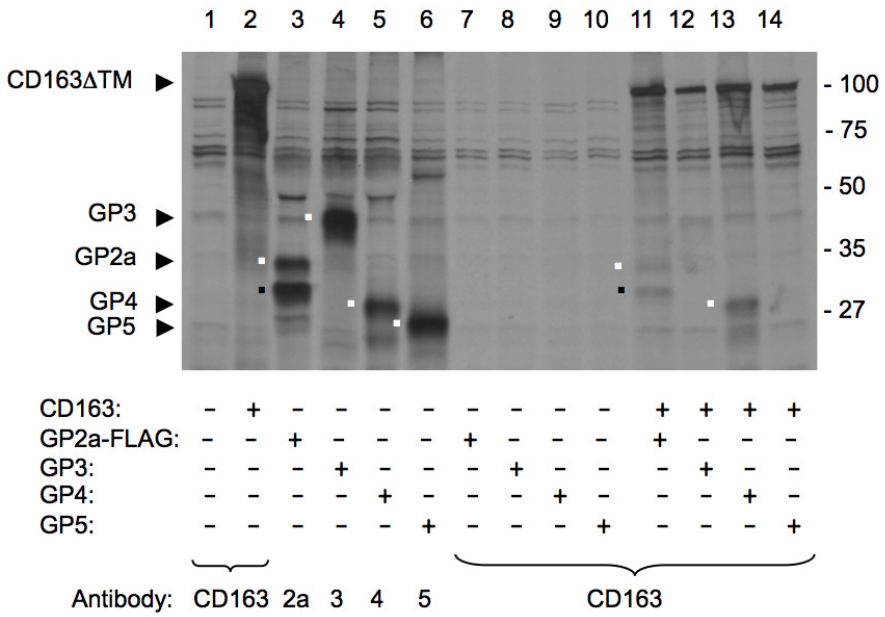

Figure 4.14 Interactions of GP2a and GP4 with CD163ΔTM. BHK-21 cells were infected with vTF7-3 and transfected with various GPs alone or in combination with CD163ΔTM protein. The cells were radiolabeled and the proteins were immunoprecipitated with antibodies as shown below the lanes. Immunoprecipitated proteins were detected by SDS-10%PAGE and fluorography. CD163ΔTM and the fully glycosylated viral GPs are identified on the left. Fully glycosylated GPs are identified with white dots in the fluorograms on the left side of each lane. The monoglycosylated GP2a is identified with black dots on the left side in lanes 3 and 11. Mobilities of molecular mass marker proteins in kDa are shown on the right.

mutant constructs. In this process, seven GP2a deletion mutant protein were constructed as schematically shown in Fig. 4.15A and named as GP2a-FLAG Δ2-38, GP2a-FLAG Δ39-75, GP2a-FLAG Δ76-112, GP2a-FLAG Δ113-149, GP2a-FLAG Δ150-181, GP2a-FLAG Δ182-218, and GP2a-FLAG Δ219-256. The GP2a and its deletion constructs were expressed in BHK-21 cells and all these constructs showed stable protein expression (Fig. 4.16A). The GP2a-FLAG protein possesses an electrophoretic mobility of 33 kDa (Fig. 4.16A, lane 2) whereas the GP2a-FLAG Δ2-38 protein has a molecular mass of ~ 20kDa (Fig. 4.16A, lane 3). This construct lacks the signal cleavage sequence (cleavage between amino acids 40 and 41 of GP2a) and probably does not get glycosylated. The molecular mass of fully mature form of GP2a-FLAG Δ39-75, GP2a-FLAG Δ76-112, GP2a-FLAG Δ113-149, GP2a-FLAG Δ150-181, GP2a-FLAG Δ182-218, and GP2a-FLAG Δ219-256 were estimated to be approximately 29 kDa, 26 kDa, 29 kDa, 26 kDa, 22 kDa, and 32 kDa, respectively (Fig. 4.16A, lanes 4-9). The anti-FLAG polyclonal antibody was also able to immunoprecipitate partially glycosylated form the GP2a-FLAG and its deletion constructs.

The deletion constructs of GP2a was co-expressed with CD163 molecule and co-IP study was performed by use of anti-CD163 monoclonal antibody. The results show that CD163 antibody immunoprecipitated all the deletion mutants of GP2a proteins except GP2a-FLAG Δ2-38 and GP2a-FLAG Δ76-112 proteins (Fig. 4.16B, lanes 4 and 6, respectively). The signal cleavage sequence of GP2a is present between amino acids 40 and 41. Even if, I observed loss of interaction of GP2a with CD163 by deletion of 2-38 amino acid sequences, this region may not be actually responsible for the interaction.

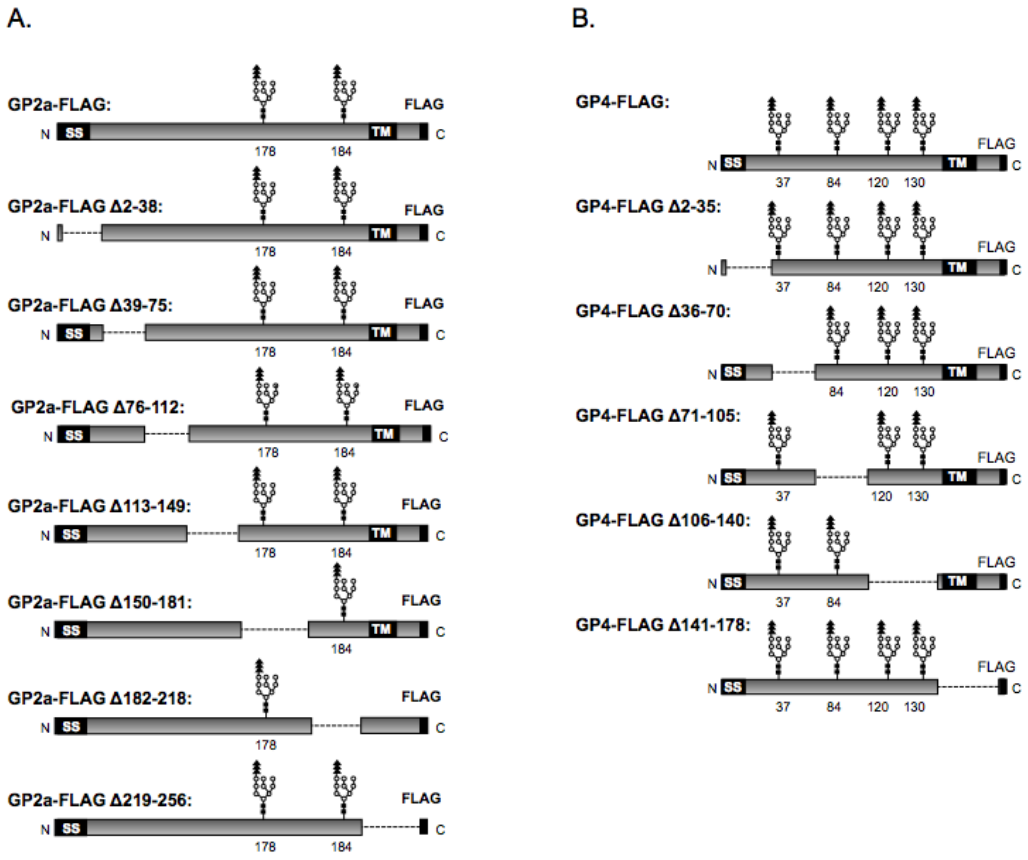

Figure 4.15 Schematics of GP2a (A) and GP4 (B) deletion mutants constructed. The name of each of the mutant construct is shown on the left. The predicted N-glycosylation sites in amino acids numbers for GP2 and GP4 are shown. The signal cleavage sites (SS), transmembrane (TM) domains, and FLAG tag positions are indicated. The deleted amino acids are shown as dotted lines.

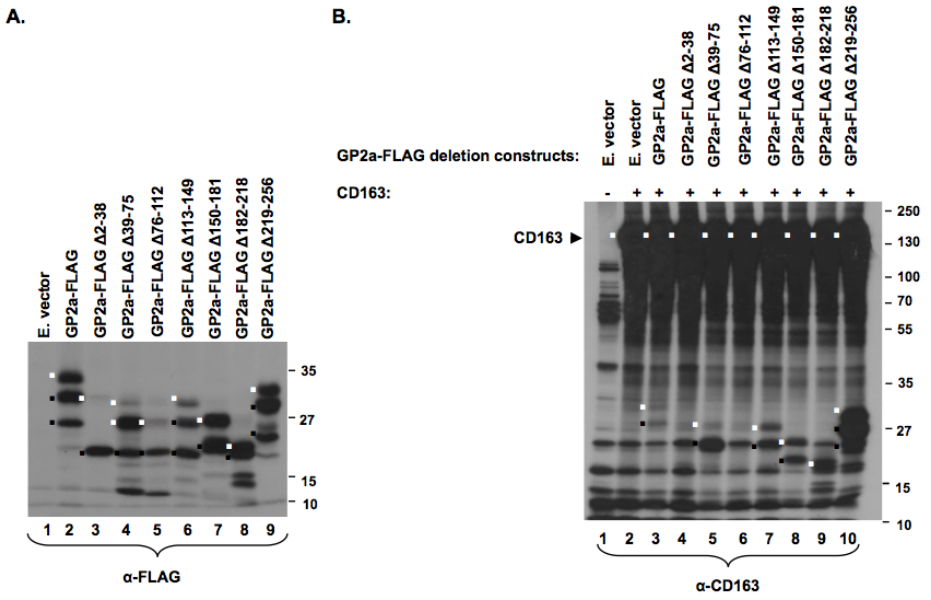

Figure 4.16 Mapping of the amino acids of GP2a required for its interaction with CD163. (A) Expression of GP2a deletion constructs. BHK-21 cells were infected with vTF7-3 virus and transfected with pGEM3 (E. vector, lane 1), or GP2a-FLAG (lane 2) and its deletion mutant clones (lane 3-9). Cells were radiolabeled with ^{35}S for 4h at 16h post-transfection, and radiolabeled proteins were analyzed by immunoprecipitation with anti-FLAG polyclonal antibody, resolved in SDS-10% PAGE, and detected by fluorography. The fully mature from of GP2a and its deletion constructs are identified with white dots in the fluorogram on the left side of each lane where as the partially glycosylated form of GP2a are shown as black dots. (B) Interaction of GP2a deletion constructs with CD163. BHK-21 cells were infected with vTF7-3 and transfected with pGEM3 vector alone (E. vector, lane 1), CD163 along with pGEM3 (lane2) or GP2a-FLAG (lane 3) and its deletion constructs (lane 4-10) as indicated at the top of panel. Cells were radiolabeled for 4h at 16h post-transfection, the proteins were immunoprecipitated with anti-CD163 monoclonal antibody, resolved in SDS-10% PAGE, and detected by fluorography. Mobility of CD163, fully mature form of GP2a deletion proteins are shown as white dots and immature forms are shown as black dots in the left side of each lane. The CD63 is identified. Relative mobilities of molecular mass markers in kDa are shown on the right.

Overall, these results indicate that amino acids 76-112 of GP2a are required for its interaction with CD163.

4.8 Mapping of the domains of GP4 that interact with CD163

To map the amino acid regions of GP4 that are required for its interaction with CD163, I generated deletion mutants of GP4 by sequentially deleting ~ 35 amino acid residues of GP4 from its amino-terminus to carboxy-terminus. To avoid the problem of potentially losing the GP4 antibody binding epitopes by deletion, I fused FLAG tag on the carboxy-terminus of GP4 to generate GP4-FLAG construct and cloned it in pGEM3 vector. Similarly all the five GP4 deletion constructs were generated with the FLAG tag fused in their carboxy terminus and cloned in pGEM3 vector. The GP4 deletion constructs are GP4-FLAG Δ2-35, GP4-FLAG Δ36-70, GP4-FLAG Δ71-105, GP4-FLAG Δ106-140, and GP4-FLAG Δ141-177 (Fig. 4.15B). All the deletion constructs of GP4 were found to be stable when expressed in BHK-21 cells (Fig. 4.17A). The GP4-FLAG migrated with an electrophoretic mobility of 30 kDa (Fig. 4.17A, lane 2). The GP4-FLAG Δ2-35 construct lacks the signal cleavage sequence (between amino acids 22 and 23) of GP4 and migrated with an electrophoretic mobility of 25 kDa (Fig. 4.17A, lane 3). The GP4-FLAG Δ36-70, GP4-FLAG Δ71-105, GP4-FLAG Δ106-140, and GP4-FLAG Δ141-177 protein has molecular mass of 21 kDa, 21 kDa, 18 kDa, and 23 kDa, respectively (Fig. 4.17A, lanes 4-7).

Either GP4-FLAG or its deletion constructs were co-expressed in BHK-21 cells and co-IP study was performed to check the effect of deletion of amino acids of GP4 with its interaction with receptor CD163 molecule by anti-CD163 monoclonal antibody

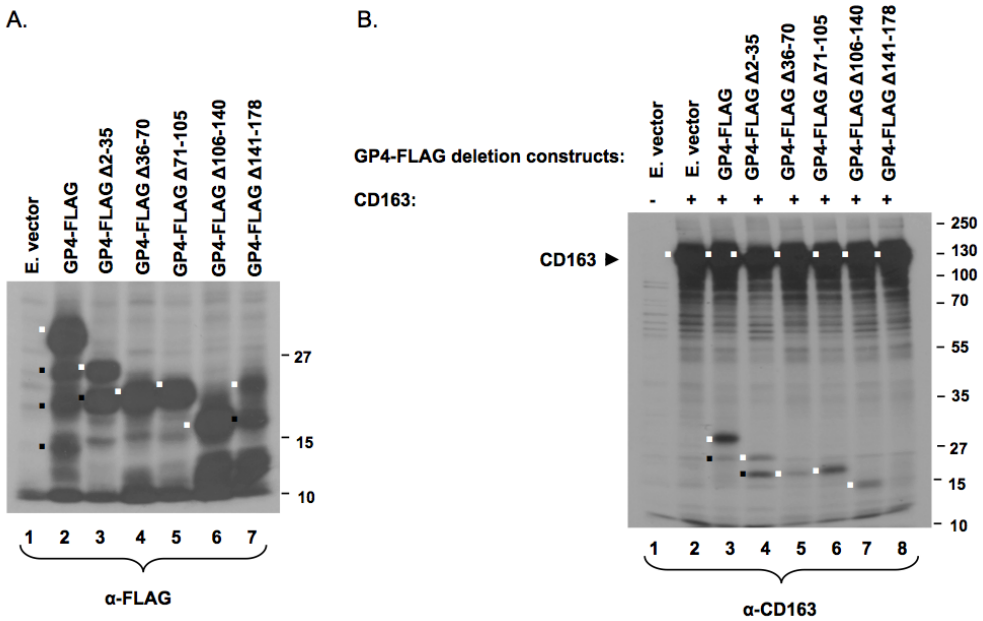

Figure 4.17 Mapping of the amino acids of GP4 required for its interaction with CD163. (A) Expression of GP4 deletion constructs. BHK-21 cells were infected with vTF7-3 virus and transfected with pGEM3 (E. vector, lane 1), or GP4-FLAG (lane 2) and its deletion mutant clones (lane 3-7). Cells were radiolabeled for 4h at 16h post-transfection, and the proteins were analyzed by immunoprecipitation with anti-FLAG polyclonal antibody, resolved in SDS-10% PAGE, and detected by fluorography. The fully mature from of GP4 and its deletion constructs are identified with white dots in the fluorogram on the left side of each lane where as the partially glycosylated form of GP4 are shown as black dots. (B) Interaction of GP4 deletion constructs with CD163. BHK-21 cells were infected with vTF7-3 and transfected with pGEM3 vector alone (E. vector, lane 1), CD163 along with pGEM3 (lane2) or GP4-FLAG (lane 3) and its deletion constructs (lane 4-8) as indicated at the top of panel. Cells were radiolabeled for 4h at 16h post-transfection, the proteins were immunoprecipitated with anti-CD163 monoclonal antibody, resolved in SDS-10% PAGE, and detected by fluorography. Mobility of CD163 is shown on the left whereas the mobilities of GP4 deletion proteins are shown as white dots in the left side of each lane. Relative mobilities of molecular mass markers in kDa are shown on the right.

(Fig. 4.17B). The results show that the CD163 antibody immunoprecipitated all the deletion mutants of GP4 protein except GP4-FLAG Δ141-178 protein (Fig. 4.17B, lane 8), indicating that the amino acids 141-178 of GP4 are required for its interaction with CD163.

4.9 Discussion

PRRSV contains one major glycoprotein (GP5) and three minor glycoproteins (GP2a, GP3, and GP4) on the virion envelope. All of these glycoproteins are required for generation of infectious virions, indicating that they play critical roles in virion assembly and/or interactions with the cell surface receptor for virus entry and/or uncoating. Previous studies have reported that GP2a, GP3, GP4, and the unglycosylated envelope protein 2b form a multiprotein complex in cells expressing these proteins (Wissink et al., 2005). In this report, I have examined the interactions of the envelope glycoproteins among themselves as well as the interactions of these proteins with the cell surface receptor, CD163. Overall, my studies lead me to conclude that (i) the GP4 and GP2a proteins interact with the other GPs; (ii) GP4 mediates the formation of the multiprotein complex between the minor GPs and the major envelope GP, the GP5; and (iii) the GP4 along with GP2a interact with CD163. These studies for the first time show that the GP4 protein is the key glycoprotein of PRRSV that is responsible for formation of the multiprotein complex and along with GP2a, may serve as the viral attachment protein, allowing virus binding to the cell surface receptor during infection.

It has been previously reported for the genotype II Lelystad virus that the minor envelope glycoproteins and 2b (or E) protein together form a heterotetrameric complex and that this complex formation is crucial for intracellular targeting of these proteins

from the ER through the Golgi complex to the plasma membrane (Wissink et al., 2005). My studies not only confirm these observations but also show that the major envelope glycoprotein GP5 interacts with GP4 strongly (Table 4.1). Although direct interaction between GP3 and GP5 could not be demonstrated, a multiprotein complex comprising of all the four envelope glycoproteins could be readily detected by immunoprecipitation with anti-GP3 antibody (Fig. 4.6). The studies reported here suggest that the GP4 mediates the formation of the large multiprotein complex between the minor and the major envelope proteins of PRRSV. In cells expressing the GP5 alone or in the presence of M protein, GP5 does not acquire endo-H resistance even after 4 h of synthesis (Ansari et al., 2006), but in virus-infected cells or in the extracellular virions, the GP5 becomes Endo H resistant (Ansari et al., 2006). These results indicate that the multiprotein complex generated by the interactions of the envelope proteins may be critical for the transport of these proteins from the ER to the Golgi complex and finally to the plasma membrane for incorporation into virus particles, consistent with previous findings that the minor envelope glycoproteins of Lelystad virus form a multimeric complex for their transport to the plasma membrane (Wissink et al., 2005).

Although multiprotein complexes can be detected in transfected cells, the molar ratio of the proteins in such complexes is unknown. Since GP5 and M proteins are the major envelope proteins, they are likely distributed uniformly throughout the virion envelope. Recent cryoelectron tomographic studies (Spilman et al., 2009) reveal that PRRSV particles mostly display smooth envelope outlines, for which the authors suggest that the small ectodomains of GP5 and M proteins are possibly not large enough to be detected as visible spikes on the virion envelope. On the other hand, the authors also

detected few features protruding from the virion envelope, which most likely correspond to the large multimeric complexes made from the bulkier but less abundant minor envelope glycoproteins such as GP2a (Spilman et al., 2009). I reason that the protruding features seen on PRRSV virion envelope (Spilman et al., 2009) represent the multimeric complexes of the minor envelope glycoproteins with or without the GP5 and M proteins and these are likely to be directly involved in interactions with the cell surface receptor during PRRSV infection.

The data presented here support the contention that the multimeric complexes of the minor glycoproteins with or without the M and GP5 proteins are involved in direct interaction with the cell surface receptor. Since GP5 and M proteins are present in abundant amounts on the virion envelope, these two proteins were considered to play a major role in receptor interaction. However, this contention was challenged by the results from the studies using chimeric viruses (Dobbe et al., 2001; Verheije et al., 2002), which suggested that the GP5 and M proteins do not play a role in receptor interaction. My studies show that only the GP2a and GP4 proteins interact with CD163. It appears that the GP4 is a critical viral envelope protein that not only mediates interactions with other GPs on the virion envelope, but also along with GP2a, mediates interactions with the CD163 for virus entry. Since the minor envelope proteins are not required for particle formation (Wissink et al., 2005) and there are only few large multimeric glycoprotein complexes present on the virion envelope (Spilman et al., 2009), I suggest that the major function of the minor glycoprotein complex on the virion envelope is to interact specifically with the cell surface receptor for virus entry. On the other hand, the GP5 and M heterodimeric complexes, which are present in large amount and are uniformly

distributed throughout the virion envelope (Spilman et al., 2009), play major roles in virion assembly. The GP5-M complexes on the virion envelope may also play additional roles in nonspecific interactions with heparin-like receptors on PAM cells since M protein has been shown to bind to such molecules (Delputte et al., 2002). The nonspecific interaction would allow initial virus binding to the cell surface followed by specific interaction with the receptor through GP2a and GP4 proteins for receptor-mediated entry of the virion.

It is possible then that GP2a and GP4, by containing viral receptor-interacting domains, would potentially be involved in the establishment of protective immunity against PRRSV infection. Viral receptor-interacting proteins and domains are known to induce highly neutralizing antibodies and contribute important targets for vaccine and therapeutic development (Delrue *et al.*, 2009). While a single report so far suggests that GP4 contains at least one neutralizing epitope (Meulenberg et al., 1997), the full potential of GP4 and GP2a to induce PRRSV-neutralizing antibodies and T-cell immunity should be further investigated. This becomes particularly important in the light of recent studies indicating that viral receptor-interacting domains may be directly involved in the induction of broadly reacting neutralizing antibodies, as shown for hepatitis C virus (Tarr et al., 2006), SARS coronavirus (Du et al., 2009), influenza virus (Lim et al., 2008), paramyxovirus (Hashiguchi et al., 2007) etc. These broadly reactive, cross-neutralizing and possibly cross-protective antibodies may be of central importance for protection against highly variable viruses such as PRRSV (Lopez & Osorio, 2004).

Based on the results presented in this chapter, I propose a tentative model for the multiprotein complex on PRRSV envelope and its interaction with the cell surface

receptor CD163 (Fig. 4.18). Although the involvement of proteins 2b and M in the formation of this complex or interaction with CD163 has not been examined in the current study, several of these interactions have already been confirmed. Further studies are being conducted to test this preliminary model of GP-CD163 interaction. Although preliminary data on mapping of the regions of GP2a and GP4 that interact with CD163 have been generated, addition mutational and biochemical studies would be required to confirm the preliminary findings.

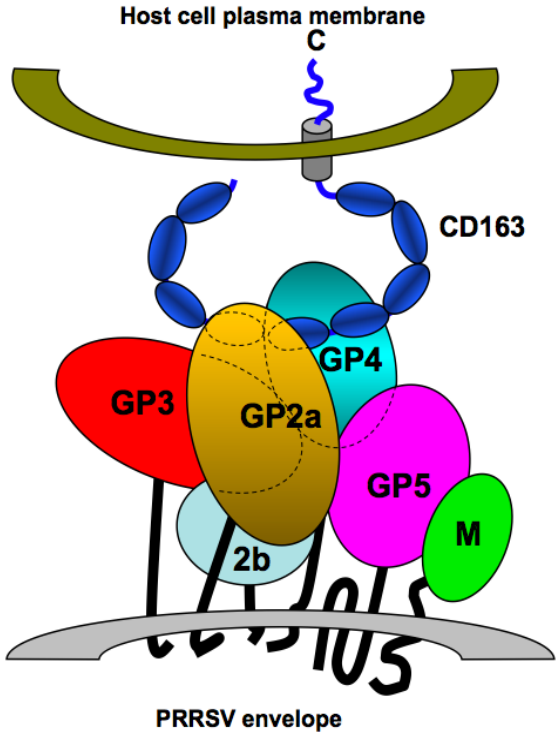

Figure 4.18 A preliminary model of PRRSV envelope protein complex and its interaction with CD163 on the host cell plasma membrane. For the sake of simplicity and convenience, the GPs are depicted as globular structures with lines spanning the viral envelope. CD163 is shown as a structure with extracellular region having repeating units (corresponding to the nine SRCR domains) projecting from the plasma membrane of a host cell. The carboxy-terminal cytoplasmic domain and the transmembrane domains are also shown. The dotted lines in the schematic represent the regions of the proteins that are masked by GP2a.

CHAPTER V

ROLE OF N-GLYCOSYLATION OF GP2A AND GP4 PROTEINS OF PRRSV IN INFECTIOUS VIRUS PRODUCTION, NEUTRALIZING ANTIBODY RESPONSE, AND INTERACTION WITH RECEPTOR CD163

Previous studies from our laboratory had shown that N-glycosylation of GP5 protein of PRRSV was required for protection against host neutralizing antibody response by glycan shielding mechanism (Ansari et al., 2006). Out of three predicted N-glycosylation sites in GP5 of North American strain of PRRSV, glycan addition on N44 was shown to be absolutely required for viral particle formation and infectious virus production. Whereas, glycosylation at N34 and N51 residues were important for the virus to escape from neutralization by the antibody (Ansari et al., 2006). Similar to North American strain, N46 of Lelystad virus was shown to be important for infectious virus production (Wissink et al., 2004). The same study also showed that both the N-glycosylation sites of GP2a protein of Lelystad virus were dispensable for infectious virus production (Wissink et al., 2004). But, these studies did not address the role of glycosylation of the viral GPs on virus neutralization or induction of neutralizing antibody response.

5.1 Role of N-glycosylation of GP2a and GP4 of PRRSV on infectious virus production

5.1.1 N184 of GP2a protein is important for virus recovery

The N-glycosylation of GP2a was shown to be dispensable for infectious virus production for Lelystad virus (Wissink et al., 2004). The GP2a of North American strain (FL12 virus) has two predicted glycosylation sites at positions 178 and 184 (Fig. 5.1). The N at these positions was mutated to A which abolished the ability of glycan moieties to be added at these positions. I used GP2a-FLAG encoding construct to generate glycosylation site mutants. Three mutant clones were generated for GP2a protein by mutating glycosylation sites for this protein. N178A and N184A denotes the mutation of

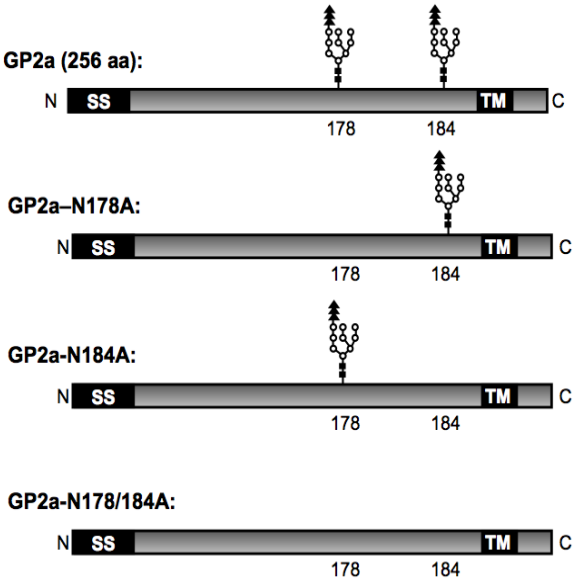

Figure 5.1 Schematic representation of GP2a protein showing positions of the two glycosylation sites. The signal sequence (SS) present of the amino-terminus and transmembrane (TM) domain at the carboxy terminus is denoted. The size of the protein in amino acids is shown on the left. The name of each of the mutant construct is shown on the left. Potential N-glycosylation sites with residue number on bottom of the rectangular boxes are shown. The N to A mutation sites are left blank without any glycan moiety.

individual glycosylation sites where as N178/184A denotes mutation of both the glycosylation sites of GP2a protein. The proteins were expressed in vitro by transfection of plasmid constructs into BHK-21 cells (Fig. 5.2). Both the wild type and mutant proteins were expressed at similar levels. The GP2a-FLAG protein has a molecular weight of 33 kDa. While the N178A-FLAG and N184A-FLAG proteins migrated with a molecular weight of 30.5 kDa (Fig. 5.2, lanes 3 and 4), the N178/184A-FLAG protein migrated with a molecular mass of 28 kDa (Fig. 5.2, lane 5). These results showed that mutation of glycosylation sites resulted in synthesis of the proteins with faster electrophoretic mobility that correlated with loss of glycan addition.

The N to A mutations was further introduced in the GP2a of FL12 genome and a virus recovery experiment was performed by electroporation of in vitro transcribed RNA in case of MARC-145 cells. The N protein expression was observed after 48 h post electroporation (Fig. 5.3). It indicated that the electroporated RNA was able to replicate inside the cells and produce N protein. Five days after electroporation, CPE was observed for FL-GP2a-N178A whereas, no CPE was observed for either FL-GP2a-N184A or FL-GP2a-N178/184A mutant clones. The presence of the correct mutation in FL-N178A recovered virus was confirmed by sequencing. In cells infected with the mutant virus, the GP2a-N178A protein migrated with a mobility that correlated with loss of one glycosylation site (Fig. 5.4A, lane 2). Further, the introduced mutation was found to be stable upon passage of the virus in cell culture as the cells infected with the passage 10 mutant virus still synthesized GP2a-N178A protein (Fig. 5.4A, lane 3) that co-migrated with GP2a-N178A protein synthesized in passage 1 mutant virus-infected cells. The GP2a proteins synthesized in these mutant virus-infected cells clearly migrated

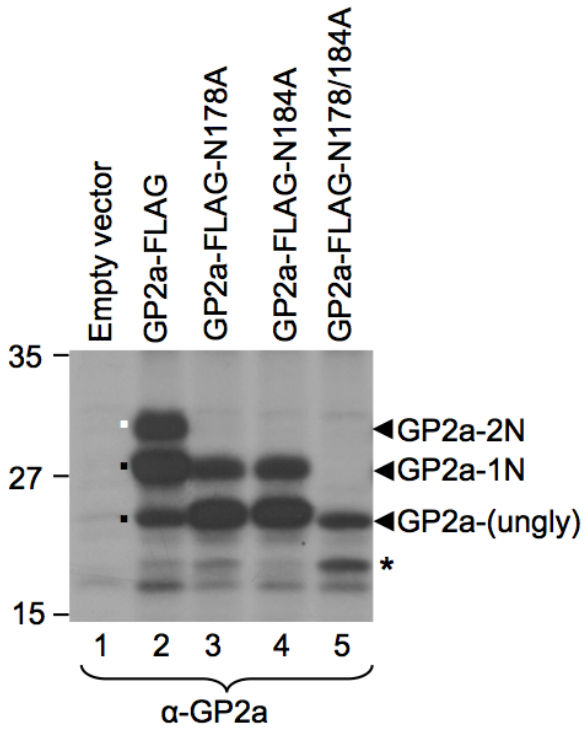

Figure 5.2 Protein expression of GP2a and its N-glycosylation mutant proteins. BHK-21 cells were infected with vTF7-3 and transfected with pGEM3 (Empty vector, lane 1) or GP2a and its N-glycosylation defective mutants (lanes 2-5). Cells were radiolabeled for 4 h at 16 h post-transfection, and the radiolabeled proteins were analyzed by immunoprecipitation with anti-GP2a antibody, resolved in SDS-12%PAGE and detected by fluorography. The completely glycosylated protein is indicated as white dot whereas, the partially glycosylated or unglycosylated forms are indicated as black dots. The protein band identified by an asterisk is most likely the signal-cleaved deglycosylated form of GP2a. The different glycosylated forms of GP2a proteins are shown on the right side of the fluorogram. Relative mobilities of molecular mass markers in kDa are shown on the left.

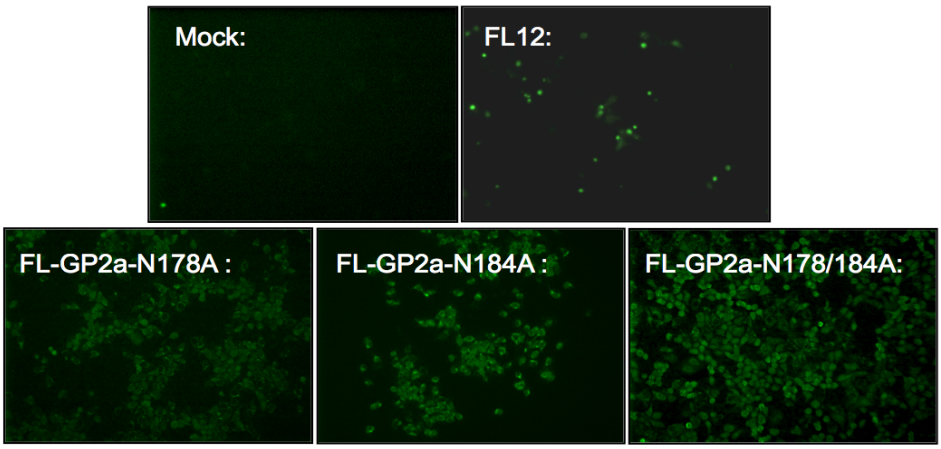

Figure 5.3 Expression of N proteins in GP2a N-glycosylation defective mutant viruses. MARC-145 cells were electroporated with in vitro transcripts derived from pFL12-Pol^{-} (mock), pFL12, pFL-GP2a-N178A, pFL-GP2a-N184A, and pFL-GP2a-N178/184A. At 48h after electroporation, cells were permeabilized and expression of N protein was examined using the monoclonal antibody SDOW17 and Alexa-488 conjugated anti-mouse IgG as secondary antibody.

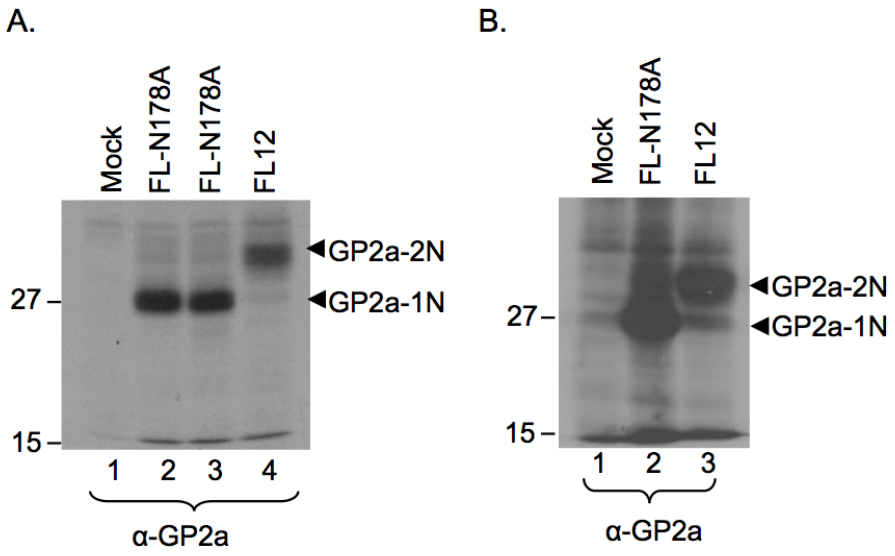

Figure 5.4 Protein expression of FL-GP2a-N178A virus. (A) MARC-145 cells were either left uninfected (lane 1) or infected with FL-GP2a-N178A virus of passage-1 (lane 2), FL-GP2a-N178A virus of passage-10 (lane 3), and FL12 virus (lane 4). Cells were radiolabeled for 4 h at 48 h post-infection, and the radiolabeled proteins were analyzed by immunoprecipitation with anti-GP2a antibody, resolved in SDS-12%PAGE and detected by fluorography. The extent of glycosylated forms of GP2a protein are identified on the right. Relative mobilities of molecular mass markers in kDa are shown on the left. (B) Fluorograph of immunoprecipitated GP2a-wild type and GP2a N-glycosylation mutant proteins synthesized in infected cells with virus recovered after 21 days post inoculation in piglets. The experiment was performed similarly as described in panel A except that sera collected from sham infected animal (lane 1), FL-GP2a-N178A virus infected animal (lane 2), and FL12 virus infected animal (lane 3) were used for infection of naïve MARC-145 cells. The relative mobilities of the molecular mass markers in kDa are shown on the left.

faster than the GP2a protein synthesized in FL12 virus-infected cells (Fig. 5.4A, lane 4), demonstrating the stability of the mutant virus under in vitro growth and passage conditions. Similarly, the cells infected with sera collected on 21 days post inoculation from FL-GP2a-N178A infected piglets also synthesize GP2a-N178A protein which migrated with a mobility that correlated with a loss of one glycan site (Fig. 5.4B, lane 2) in comparison to GP2a from FL12 virus inoculated piglets (Fig. 5.4B, lane 3). This indicated that the specific mutation in GP2a-N178A protein was stable in virus infected animals. To compare the growth characteristics of recovered FL-GP2a-N178A virus with the FL12 virus, multi step growth kinetics study was performed by infecting MARC-145 cells with 0.1 MOI of both wild type and mutant viruses as described in materials and methods. Subsequently, plaque assays were performed to measure the virus titers at different times post-infection. The growth characteristics of both FL-GP2a-N178A and FL12 virus were similar to that observed by multi step growth curve analysis (Fig. 5.5). My results show that glycan addition at amino acid position 184 of GP2a protein was important for infectious virus production in North American strain of PRRSV (FL12).

5.1.2 Role of individual N-glycosylation sites of GP4 on infectious virus production

GP4 protein of FL12 genome of PRRSV has four predicted sites at positions 37, 84, 120 and 130 (Fig. 5.6). To study the effect of N-glycosylation of GP4 protein on infectious virus production, I individually mutated N to A amino acid in all these four positions (N37A, N84A, N120A and N130A). All the mutant proteins were expressed at comparable levels to that of GP4 wild type protein (Fig. 5.7). The GP4-wild type protein migrated with a molecular weight of 29 kDa (Fig. 5.7, lane 2). All four N-glycosylation

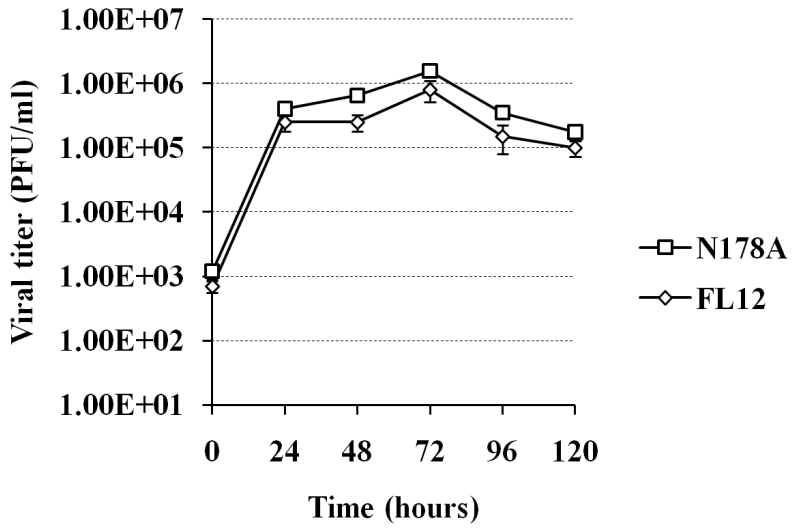

Figure 5.5 Multistep growth kinetics of FL12 and FL-GP2a-N178A recovered virus. MARC-145 cells were infected with FL12 and FL-GP2a-N178A viruses with 0.1 MOI and supernatant was collected in every 12 h interval up to 120 h. Plaque assay was performed as described in materials and methods. The viral titer was measured and expressed in $\log_{10}$ scale. The data points represent mean values from two independent experiments, and the error bars denote standard deviation.

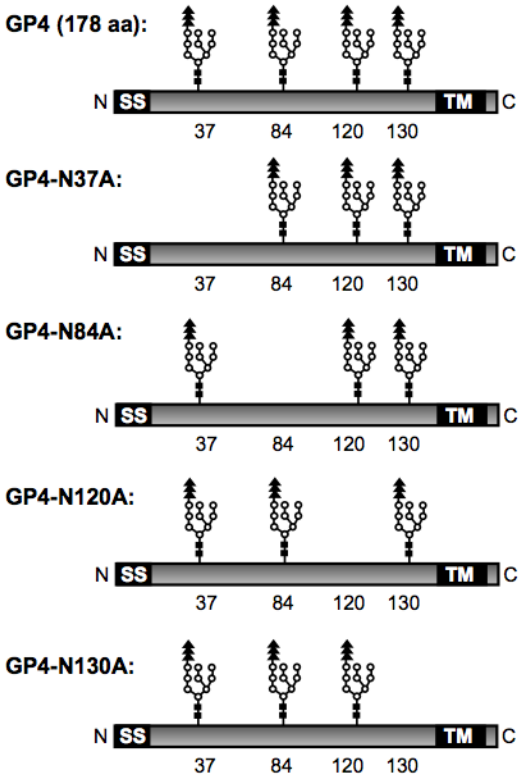

Figure 5.6 Schematic of GP4 single N-glycosylation defective mutants constructed. The size of the GP4 protein in amino acids is mentioned on the left. The amino acid position four predicted N-glycosylation sites were mentioned below each site. The signal cleavage site (SS) and transmembrane (TM) domain is indicated. The name of each of the mutant construct is shown on the left. The N to A mutation sites are left blank without any attached glycan moiety.

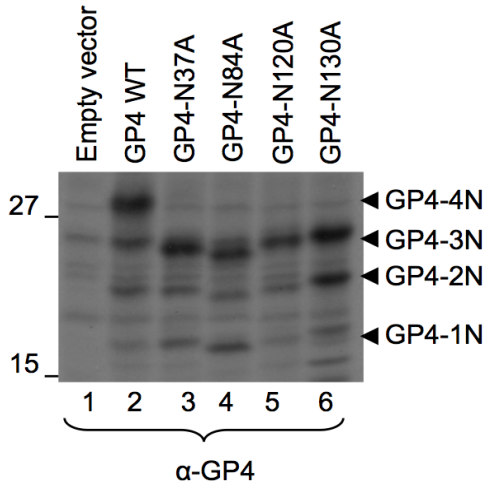

Figure 5.7 Protein expressions of GP4 single N-glycosylation mutant proteins. BHK-21 cells were infected with vTF7-3 and transfected with pGEM3 (Empty vector, lane 1) or GP4 (lane 2) and its N-glycosylation defective clones (lanes 3-6). Cells were radiolabeled for 4 h at 16 h post-transfection, and the radiolabeled proteins were analyzed by immunoprecipitation with anti-GP4 antibody, resolved in SDS-12%PAGE and detected by fluorography. The relative mobilities of the molecular mass markers in kDa are shown on the left.

mutant proteins migrated with a molecular weight of 26.5 kDa (Fig. 5.7, lanes 3-6). I observed a slight difference in electrophoretic mobility of the four GP4 mutant proteins. This may be due to the fact that mutations of N residues lead to further modification of GP4 protein folding. I introduced the N to A mutation of GP4 protein in full length genome of FL12 (FL-GP4-N37A, FL-GP4-N84A, FL-GP4-N120A, and FL-GP4-N130A). Forty-eight hours post electroporation, the N protein expression was observed in cells transfected with RNA derived from each of the GP4 mutant clones (data not shown). I was able to recover infectious viruses encoding the single glycosylation site mutations in GP4 protein. In the MARC-145 cells infected with the mutant viruses, the four single mutant GP4 proteins (GP4-N37A, GP4-N84A, GP4-N120A, and GP4-N130A) migrated with a mobility that correlated with the loss of one glycosylation site (Fig. 5.8A, lanes 2-5) and faster than GP4 protein (Fig. 5.8A, lane 6) . The intracellular protein expression profile for all these mutant viruses resembled that of transient protein expression assay results indicating the stability of the mutant viruses under in vitro growth and passage conditions (Fig. 5.8A). Similarly, in the cells infected with sera collected on 21 days post inoculation, the four GP4 single glycosylation mutant proteins migrated with mobility faster than that of GP4 protein (Fig. 5.8B). The multi- step growth curve analysis results indicated that all the mutant viruses had higher titer than the wild type virus (Fig. 5.9). I also observed a larger difference in viral titer in case of FL-GP4-120A and FL-GP4-130A virus in comparison to FL12 virus. While the FL12 virus had highest titer at 72 h post infection, the GP4 single mutant viruses achieved highest titer at 48 h post infection. FL-GP4-120A and FL-GP4-130A viruses seemed to have almost 10-50 fold higher titers than wild type FL12 virus at 48 h post infection. At

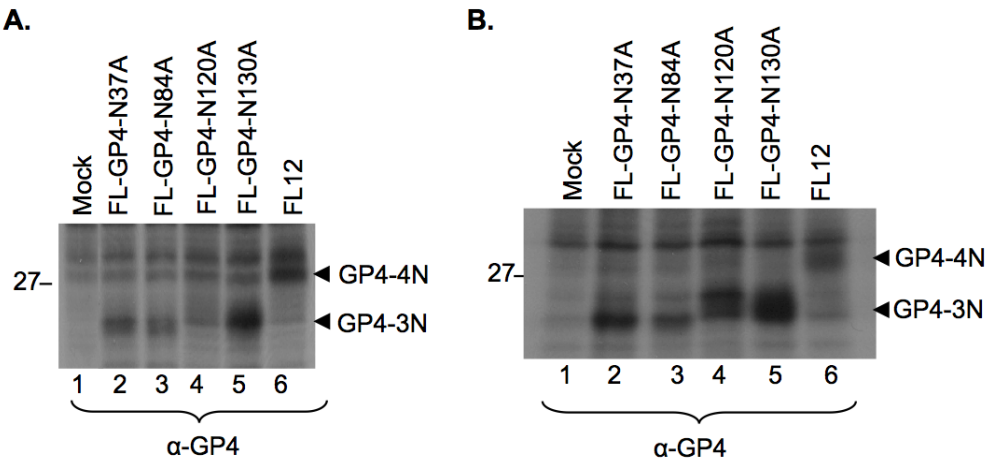

Figure 5.8 Protein expression profiles of recovered GP4 single mutant viruses. (A) MARC-145 cells were either left uninfected (Mock, lane 1) or infected with four single N-glycosylation defective mutant virus (lanes 2-5) of 10th passage and FL12 virus (lane 6). Cells were radiolabeled for 4 h at 48 h post-infection, and the radiolabeled proteins were analyzed by immunoprecipitation with anti-GP4 antibody, resolved in SDS-12%PAGE and detected by fluorography. Relative mobilities of molecular mass markers in kDa are shown on the left. (B) The experiment was performed similarly as described in panel A except sera collected from sham infected animals (lane 1), the single N-glycosylation defective mutant virus infected animals (lanes 2-5), and FL12 virus infected animals were used for infection of naïve MARC-145 cells. Relative mobilities of molecular mass markers in kDa are shown on the left.

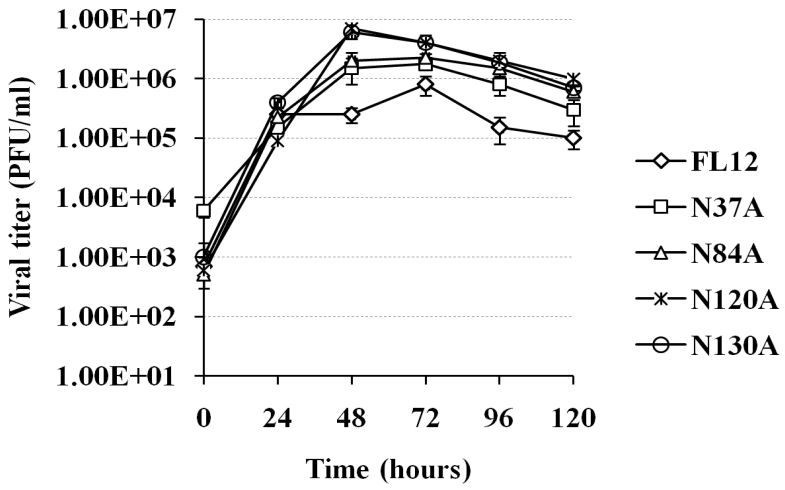

Figure 5.9 Multistep growth kinetics for recovered GP4-wild type and GP4 single N-deglycosylated mutant viruses. MARC-145 cells were infected with FL12 and GP4 single N-deglycosylated mutant viruses with 0.1 MOI and supernatant was collected in every 12 h interval up to 120 h. Plaque assay was performed as described in materials and methods. The viral titer was measured and expressed in $\log_{10}$ scale. The data points represent mean values from two independent experiments, and the error bars denote standard deviation.

most of the time points examined, the mutant viruses exhibited higher titers than the wild type FL12 virus. The reasons for better growth of the glycosylation mutant viruses are unknown at this time.

5.1.3 Simultaneous mutation of two N-glycosylation sites of GP4 is lethal for infectious virus production

To study the effect of double mutation of N-glycosylation sites of GP4 on infectious virus production, I generated six clones by simultaneously mutating two N residues of GP4 (N37/84A, N37/120A, N37/130A, N84/120A, N84/130A, and N120/130A) (Fig. 5.10). By losing two glycosylation sites, the transiently expressed proteins lost 5 kDa of molecular mass and migrated with a molecular weight of 24 kDa in transfected cells (Fig. 5.11, lanes 4-9). The GP4-N37/84A protein found to migrate slightly faster than the expected size. The same trend also observed for GP4-N120/130A mutation, in which case the protein migrated slower than its expected size. As observed for GP4 single N-glycosylation mutants, double mutations of GP4 protein probably affected the overall protein folding and hence the difference in protein migration. I further introduced these mutations in FL12 genome (FL-GP4-N37/84A, FL-GP4-N37/120A, FL-GP4-N37/130A, FL-GP4-N84/120A, FL-GP4-N84/130A, and FL-GP4-N120/130A and the mutation was confirmed by sequencing analysis (data not shown). Upon electroporation of in vitro transcribed RNA in MARC-145 cells, the N protein expression was observed in case of all the six mutant clones at 48 h post electroporation (Fig. 5.12). But, I was not able to successfully recover any of the six GP4 double mutant viruses. These results indicated that mutation of more than one glycosylation sites in GP4 was lethal for infectious virus particle formation.

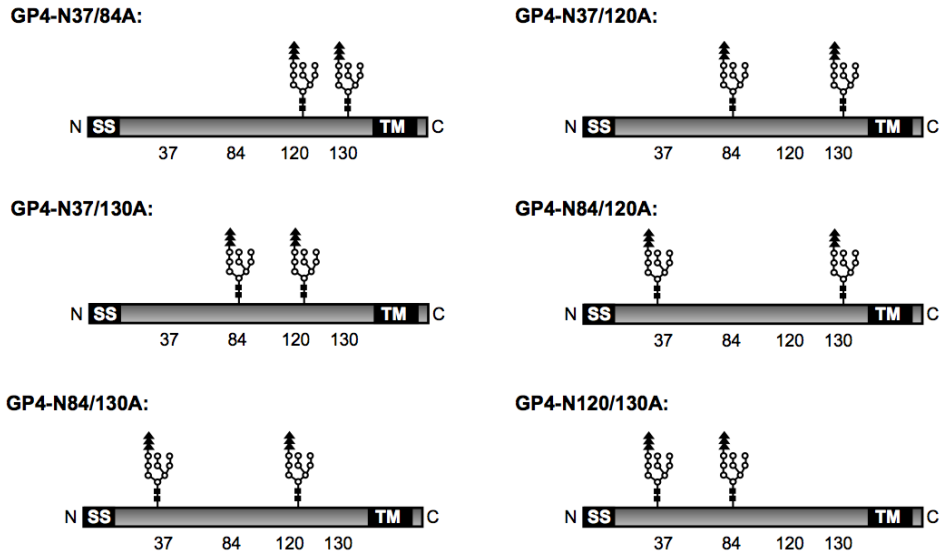

Figure 5.10 Schematic of GP4 double N-glycosylation defective mutants constructed. The name of each of the mutant construct is shown on the left. The signal cleavage site (SS) and transmembrane (TM) domain is indicated. The predicted N-glycosylation sites in amino acid numbers for GP4 are shown. The N to A mutation sites are left blank without any attached glycan moiety.

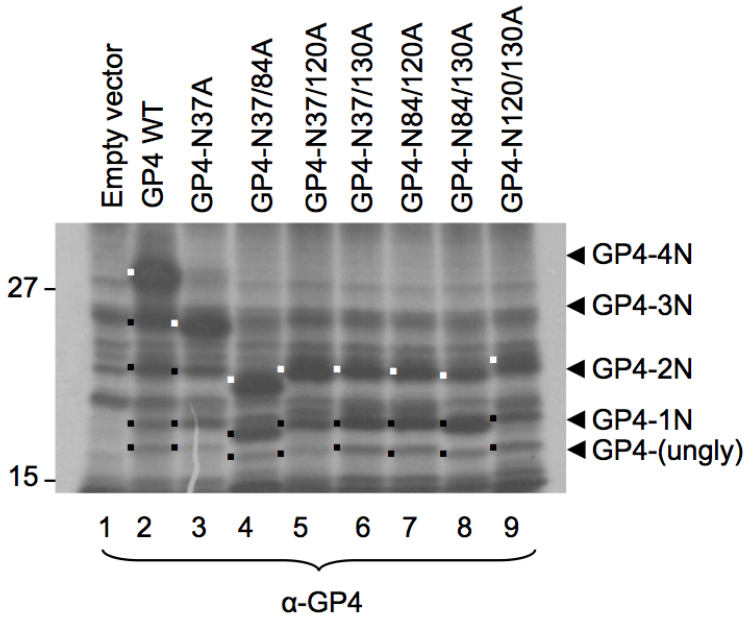

Figure 5.11 Protein expressions of GP4–double N-deglycosylated mutant proteins. BHK-21 cells were infected with vTF7-3 and transfected with pGEM3 (Empty vector, lane 1) or GP4 (lane 2), GP4-N37A (lane 3), and six double N-glycosylation defective clones of GP4 (lanes 4-9). Cells were radiolabeled for 4 h at 16 h post-transfection, and the radiolabeled proteins were analyzed by immunoprecipitation with anti-GP4 antibody, resolved in SDS-12%PAGE and detected by fluorography. The higher band intensities in different GP4 transfected constructs (lanes 2-9) in comparison to empty vector transfected construct (lane 1) is considered as specific proteins immunoprecipitated by anti-GP4 polyclonal antibody. The relative mobilities of the molecular mass markers in kDa are shown on the left.

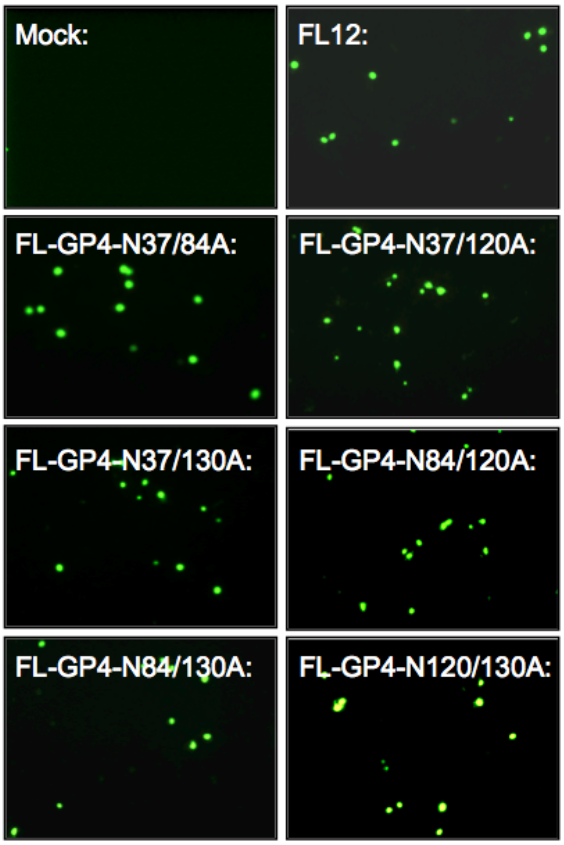

Figure 5.12 Expression of N protein in GP4 double N-glycosylation defective mutant viruses. MARC-145 cells were electroporated with in vitro transcripts derived from pFL12-Pol$^-$ (mock), pFL12, pFL-GP4-N37/84A, pFL-GP4-N37/120A, pFL-GP4-N37/130A, pFL-GP4-N84/120A, pFL-GP4-N84/130A, and pFL-GP4-N120/130A. At 48h after electroporation, cells were permeabilized and expression of N protein was examined using the monoclonal antibody SDOW17 and Alexa-488 conjugated anti-mouse IgG as secondary antibody.

5.2 Role of N-glycosylation of minor envelope glycoproteins on neutralizing antibody production in infected piglets

Twenty one days old weaned piglets were infected with FL12 as well as mutant viruses generated for the GP2a and GP4 proteins. For GP2a and GP4, only recovered single mutant viruses were used in these experiments. Groups of four 21 days old piglets were injected with the mutant viruses. All the different groups of piglets were housed separately. Sham infected piglets were included as negative control. The neutralizing antibody titer was measured by $TCID_{50}$ assay (Table 5.1). Since neutralizing antibody response is usually not detected before 21 days post infection, I normalized the titer of neutralizing antibody at day 7 as 1 for the wild type and mutant virus-infected sera from the animals. The FL12 infected piglet sera was tested against FL12 infected cells (homologous titer) and compared with sera collected from mutant virus infected piglets (heterologous titer). I did not observe any significant difference between neutralizing antibody response produced in case of FL12 virus or other mutant virus. These results indicated that hypoglycosylation of GP2a and GP4 did not influence neutralizing antibody response in infected piglets (Table 5.1). Overall, the results show that unlike GP5 (Ansari et al., 2006), hypoglycosylation of GP2a and GP4 did not induce higher neutralizing antibody response in infected pigs and the mutant viruses were not more sensitive to neutralization.

5.3 Role of N-glycosylation of GP2a and GP4 for their interaction with the receptor CD163

My previous study established that porcine CD163 interacts specifically with GP2a and GP4 proteins of PRRSV (Fig. 4.12). I further examined the role of N-

Table 5.1 Serum neutralization titer of animals infected with wild type or GP2a and GP4 glycosylation mutant PRRSVs.

Groups	Days post infection	
	7 days	46 days
FL12	1	32
GP2a FL-N178A	1	9.5
GP4 FL-N37A	1	13.5
GP4 FL-N84A	1	22.6
GP4 FL-N120A	1	26.9
GP4 FL-N130A	1	38.1

The serum neutralization value of both wild type and mutant viruses are made 1 for 7^{th} day for comparison. The results are shown as of average of four animals per each group.

glycosylation of GP2a and GP4 in their interaction with CD163 molecule by co-IP assay as described in the previous chapter. The receptor CD163 was individually co-expressed with GP2a-FLAG, GP2a-FLAG-N178A, GP2a-FLAG-N184A, or GP2a-FLAG-N178/184A mutant proteins and the protein complexes were co-immunoprecipitated with anti-FLAG polyclonal antibody (Fig. 5.13) or anti-CD163 monoclonal antibody (Fig. 5.14) and resolved in SDS-10% PAGE gel. By using anti-FLAG antibody, CD163 could be readily recovered by immunoprecipitation of cell lysate co-expressing GP2a-FLAG, GP2a-FLAG-N178A or GP2a-FLAG-N184A proteins (Fig. 5.13, lanes 9-11). But, CD163 molecule could not be co-immunoprecipitated when it was expressed with completely unglycosylated form of GP2a (GP2a-FLAG-N178/184A) protein (Fig. 5.13, lane 12). In a complementary experiment, I examined the interactions using anti-CD163 monoclonal antibody. The results (Fig. 5.14) showed that CD163 antibody could immunoprecipitate wild type GP2a and single glycosylation mutant GP2a proteins. However, little or no unglycosylated GP2a was detected by the antibody. These results suggest that glycosylation of at least one site in GP2a protein was necessary for efficient interaction with the receptor CD163.

A similar study was performed to determine the role of N-glycosylation of GP4 protein in its interaction with CD163 (Fig. 5.15). In these studies, I chose to use only one double mutant and the quadruple mutant (completely unglycosylated form) GP4 proteins for their interaction with CD163. I co-expressed GP4-wild type, GP4-partially double glycosylated protein (GP4-N37/84A), and fully unglycosylated GP4 protein (GP4-N37/84/120/130A) along with CD163 molecule and immunoprecipitated the protein

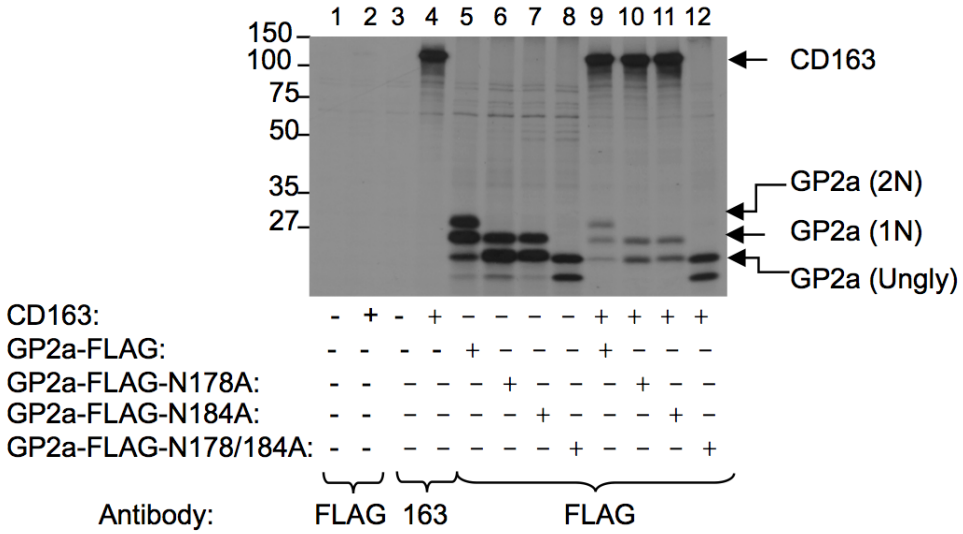

Figure 5.13 Examination of interaction of CD163 with GP2a N-glycosylation defective proteins using FLAG antibody. BHK-21 cells were infected with vTF7-3 virus and mock-transfected (lanes 1 and 3), transfected with both GP2a-FLAG or N-glycosylation defective GP2a-FLAG plasmids and CD163 plasmid as shown in the bottom of the panel. – and + indicate without or with the plasmid shown on the left. The cells were radiolabeled and immunoprecipitated with specific antibodies as shown below the lanes. The CD163 and GP2a (wild type and mutant) proteins were co-immunoprecipitated by anti FLAG antibody (lanes 9-12). Immunoprecipitated proteins were resolved in SDS-10% PAGE and detected by fluorography. CD163 and different glycosylated forms of GP2a proteins are identified on the right. The relative mobilities of the molecular mass markers in kDa are shown on the left.

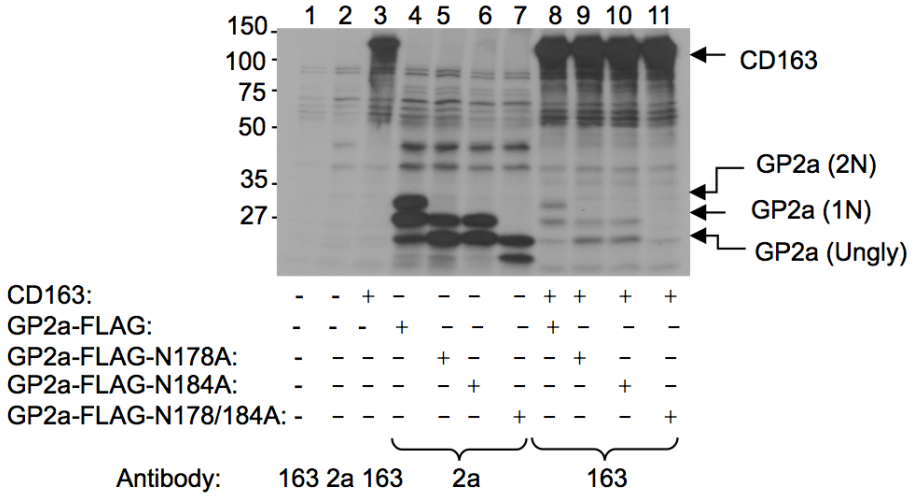

Figure 5.14 Examination of interaction of CD163 with GP2a N-glycosylation defective proteins using CD163 antibody. BHK-21 cells were infected with vTF7-3 virus and mock-transfected (lanes 1 and 2), transfected with both GP2a-FLAG or N-glycosylation defective GP2a-FLAG plasmids and CD163 plasmid as shown in the bottom of the panel. – and + indicate without or with the plasmid shown on the left. The cells were radiolabeled and immunoprecipitated with specific antibodies as shown below the lanes. The CD163 and GP2a (wild type and mutant) proteins were co-immunoprecipitated by anti CD163 antibody (lanes 8-11). Immunoprecipitated proteins were resolved in SDS-10% PAGE and detected by fluorography. CD163 and different glycosylated forms of GP2a proteins are identified on the right. The relative mobilities of the molecular mass markers in kDa are shown on the left.

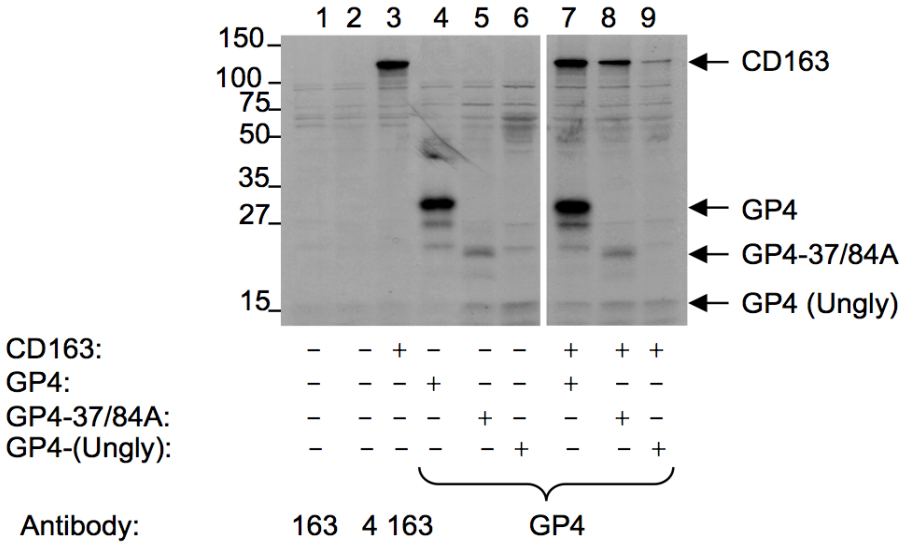

Figure 5.15 Examination of interaction of CD163 with double and completely unglycosylated GP4 proteins using GP4 antibody. BHK-21 cells were infected with vTF7-3 virus and mock-transfected (lanes 1 and 2), transfected with the plasmid encoding CD163 along with the plasmid encoding wild type GP4, double glycosylation mutant GP4 (N37/84A) or quadruple glycosylation mutant GP4 (unglycosylated) as shown in the bottom of the panel. – and + indicate without or with the plasmid shown on the left. The cells were radiolabeled and immunoprecipitated with specific antibodies as shown below the lanes. The CD163-GP4 (wild type and mutant) proteins were co-immunoprecipitated by anti GP4 antibody (lanes 7-9). Immunoprecipitated proteins were resolved in SDS-10% PAGE and detected by fluorography. CD163 and different GP4 proteins are identified on the right. The relative mobilities of the molecular mass markers in kDa are shown on the left.

complex by anti-GP4 polyclonal antibody. The results showed that the interaction between CD163 and GP4 was dependent on the extent of glycosylation of GP4. The wild type GP4 with glycans at all four sites interacted well with CD163 (Fig. 5.15, lane 7) whereas the GP4 mutant with only two glycan moieties interacted less well with CD163 (Fig. 5.15, lane 8). Further, interaction of unglycosylated GP4 with CD163 was very inefficient as only a very small amount of CD163 could be immunoprecipitated with GP4 antibody (Fig. 5.15, lane 9). Similar results were also observed with other glycosylation mutant GP4 proteins (data not shown). Upon repeated experiments, my results showed that an 8-to 10-fold reduction in the amount of CD163 was observed when unglycosylated GP4 was used whereas 2- to 3-fold reduction in CD163 was seen with double glycosylation mutant GP4 proteins. Overall, these studies suggest that glycosylation of GP2a and GP4 proteins was necessary for an optimal interaction with the receptor CD163.

5.4 Discussion

Viruses use host cell machinery for glycosylation of the viral envelope proteins (Vigerust & Shepherd, 2007). PRRSV has four envelope glycoproteins GP2a, GP3, GP4, and GP5. Our previous study on GP5 protein has shown the importance of N-glycosylation on viral immune evasion and infectivity (Ansari et al., 2006). My current study focused on the role of N-glycosylation of GP2a and GP4 proteins on virus infectivity, immune evasion and receptor interaction with CD163. My report concluded that (i) glycan addition at N184 of GP2a was individually required for infectious virus production. Glycan addition at a minimum two sites in GP4 was required for recovery of infectious PRRSV; (ii) N-glycosylation of GP2a and GP4 proteins do not play any

discernible role in viral immune evasion against host neutralizing antibody response or enhance host neutralizing antibody response; and (iii) Optimal interaction of GP2a and GP4 with CD163 molecule was dependent on glycosylation of GP2a and GP4 proteins.

Lelystad virus (European strain) and FL12 virus (North American strain) of PRRSV share approximately 60% nucleotide sequence homology. A previous study with GP2a protein of Lelystad virus had shown that both the N-glycosylation sites of GP2a at positions 173 and 179 are dispensable for infectious virus production (Wissink et al., 2004). But, my study with FL12 virus demonstrated that the N-glycosylation site at position 184 was required for infectious virus production. This result indicated that there were differences in the requirement of glycosylation of the viral glycoproteins for infectious virus production in these two viruses. It is also possible that these two genotypes of PRRSVs may have differences in their life cycle and/or pathogenic characteristics.

My study has shown that glycan addition at N184 of GP2a may be required for proper folding of the protein that is needed for infectious virus production. Defects in protein folding, virion assembly or egress have also observed for Dengue virus and Japanese encephalitis virus when their envelope glycoproteins were mutated at the glycosylation sites (Kim et al., 2008; Mondotte et al., 2007). The four N-glycosylation sequons of GP4 were found to be dispensable for infectious virus production. But, no virus was recovered upon double deglycosylation of any two of the four sequons. These results further corroborate my hypothesis that by mutating multiple glycosylation sites, proper folding of the mutant protein is impaired in such a manner that reduces infectious virus production or assembly. As observed for Sindbis virus (Knight et al., 2009), single

partially glycosylated mutant virus had slightly higher titer observed in comparison to parent virus. The FL12 virus achieved highest titer at 72 h post infection, whereas the GP4 single mutant viruses achieved highest titer at 48 h post infection. The reason for the growth advantage over parental virus was not clear. I speculate that the single glycosylation mutant GP4 proteins fold in a manner that was more favourable for infectious virus production at higher levels. This could potentially be achieved through increased interactions with other viral glycoproteins, incorporation into viral envelope, and/or interactions with the host cell receptor. Further studies will be needed to determine how the single glycosylation mutant GP4 proteins enhanced virus infectivity or virus production.

The GP5 of PRRSV was previously reported to be immunogenic and is required for conferring protection against host neutralizing antibody response (Ansari *et al.*, 2006; Pirzadeh & Dea, 1997). On the contrary, I did not observe any effect of N-glycosylation of GP2a and GP4 proteins on protection against neutralizing antibody response. It may be due to the fact that these two minor envelope glycoproteins are not abundantly expressed on the surface of the virion. There may be the existence of a 'malleable glycan shield' (Wei et al., 2003) in which case the glycan moities on GP5 may protect the minor envelope glycoprotein even if they are unglycosylated. Glycan shield generally requires co-operative packing of entire envelope protein to prevent antibody access (Wei et al., 2003). During glycan shielding, steric hindrance of epitope due to glycan addition at a nearby prevents its binding to a neutralizing antibody (Wei et al., 2003). It is possible that by partial deglycosylation, the potential neutralizing epitopes in these three glycoproteins have not been sufficiently exposed to permit binding of neutralizing antibody to each

protein. Alternatively, my results could suggest that these three glycoproteins do not contain PRRSV neutralizing epitopes or the glycan shielding mechanisms do not operate in these GPs. My studies have revealed that two out of the three minor envelope glycoproteins (GP2a and GP4) directly interact with CD163 (Fig. 4.12), which is an important receptor for PRRSV. Although the amino acid residues of GP2a and GP4 protein required for their binding with CD163 has not been completely mapped, it is plausible that interaction of these proteins with the receptor at the plasma membrane may sterically hinder the antibody binding as has been observed for gp120 protein of HIV-1 (Poon et al., 2007; Wyatt et al., 1998) and a favourable interaction may mask the exposure of neutralizing epitope on the surface of the virion.

Though I did not observe any significant defect in interaction of GP2a with CD163 upon individual mutation of its two glycosylation sites, abrogation of their interaction was observed when I mutated both the N residues of the sequons (Fig. 5.13 and 5.14). As observed for Hantaan virus (Shi & Elliott, 2004), the two sequons of GP2a may have different effect on protein folding and intracellular trafficking. It was also reported that upon complete deglycosylation of envelope proteins of HIV-1, its interaction with CD4 molecule was reduced, but was not completely abolished (Fenouillet *et al.*, 1990). Probably for PRRSV, glycan addition of GP2a has complementary roles on their functions in receptor interaction and that complete removal of the glycans abolishes or drastically reduces their receptor interaction functions. The glycan addition in GP4 may also have a similar role in its functions.

CHAPTER VI

ROLE OF N-GLYCOSYLATION OF GP3 OF PRRSV IN INFECTIOUS VIRUS PRODUCTION AND NEUTRALIZING ANTIBODY RESPONSE

Previous studies from our laboratory had shown that N-glycosylation of GP5 protein of PRRSV was required for protection against host neutralizing antibody response by glycan shielding mechanism (Ansari et al., 2006). Based on the presence on the envelope, the GP3 along with GP2a and GP4 are regarded as minor envelope glycoproteins. My other studies had also shown the importance of glycan moieties of GP2a and GP4 proteins on virus infectivity and interaction with receptor CD163 (chapter V). I further studied the role of glycan moieties of GP3 on virus infectivity and viral immune evasion.

6.1 N195 of GP3 is actually not glycosylated

The GP3 protein was predicted to have seven glycosylation sites (Fig. 6.1). I substituted A in place of N in all the seven predicted sites and cloned the wild type and mutant GP3 proteins in pGEM3 vector. The presence of each mutation was confirmed by sequencing all the clones (data not shown). The wild type as well as mutant proteins were transiently expressed in BHK-21 cells (Fig. 6.2). While the wild type protein migrated with a molecular weight of 42 kDa (Fig. 6.2, lane 2), the all single amino acid mutant clones (N29A, N42A, N50A, N131A, N152A, N160A) (Fig. 6.2, lanes 3-8) except N195A clone (Fig. 6.2, lane 9) migrated with a molecular weight of 39.5 kDa due to loss of one glycosylation site in each case. The substitution of N to A at position 195 of GP3 seemed to have no effect on protein glycosylation (Fig. 6.2, lane 9). This indicates that the N at position 195 was not used for glycan addition in GP3 protein.

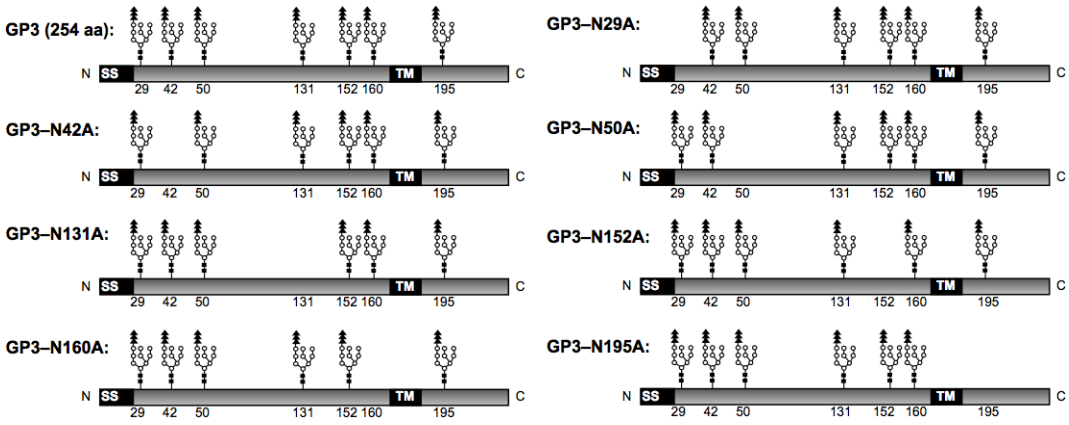

Figure 6.1 Schematic of GP3 and its single N-glycosylation defective mutant proteins. The predicted N-glycosylation sites in amino acid numbers for GP3 are shown. The size of the protein in amino acids, signal cleavage sites (SS) and transmembrane (TM) domains are indicated. The name of each of the mutant construct is shown on the left. The N to A mutation sites are left blank without any attached glycan moiety.

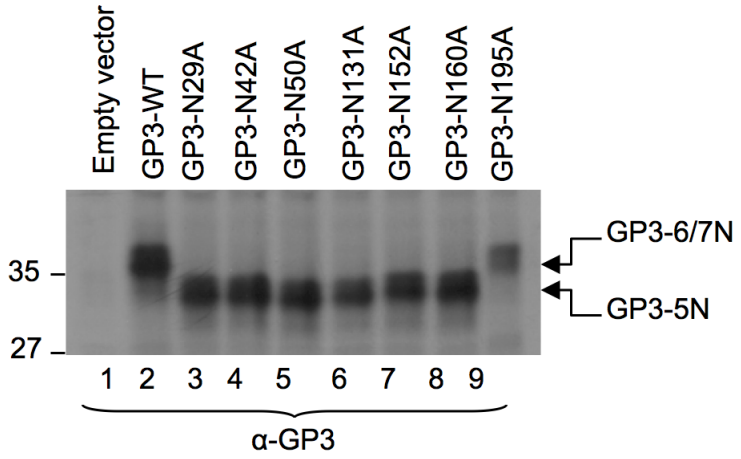

Figure 6.2 Protein expressions of GP3 and its single N-glycosylation defective mutants. BHK-21 cells were infected with vTF7-3 and transfected with pGEM3 (Empty vector, lane 1) or GP3 (lane 2) and its N-glycosylation defective clones (lanes 3-9). Cells were radiolabeled for 4 h at 16 h post-transfection, and the radiolabeled proteins were analyzed by immunoprecipitation with anti-GP3 antibody, resolved in SDS-12%PAGE and detected by fluorography. The extent of glycosylated forms of GP3 are shown on the right side. The relative mobilities of the molecular mass markers in kDa are shown on the left.

6.2 Glycosylation at N42, N50, and N131 of GP3 are crucial for infectious virus production

I subsequently introduced the glycosylation site mutations of GP3 into the FL12 infectious clone to generate various mutant viruses (pFL-GP3-N29A, pFL-GP3-N42A, pFL-GP3-N50A, pFL-GP3-N131A, pFL-GP3-N152A, and pFL-GP3-N160A). The presence of the above mutation was confirmed by sequencing the mutant FL12 genome (data not shown). The in vitro transcribed RNA of FL12 and single mutant GP3 proteins were electroporated in MARC-145 cells. The expression of N protein was confirmed by in immunofluorescence assay 48 h post-electroporation (Fig. 6.3). The CPE was observed in case of FL-GP3-N29A, FL-GP3-N152A and FL-GP3-N160A after five days of electroporation indicating successful recovery of respective viruses. However, even after multiple repeat experiments, viruses encoding mutations at the positions 42, 50 or 131 could not be recovered, indicating that glycan addition at these sites was essential for particle formation or infectivity. In MARC-145 cells infected with the GP3 single glycosylation defective mutant viruses after 10^{th} passage, the three GP3 single mutant proteins (GP3-N29A, GP3-N152A, and GP3-N160A) migrated with a mobility that correlated with loss of one glycosylation site (Fig. 6.4, lanes 3-5) and faster than GP3 wild type protein (Fig. 6.4, lane 2). This indicates that the recovered mutant viruses harboured the specific mutation after repeated passage in cell culture and the intracellular mutant viral proteins were stable. Two out of the three recovered GP3 single N-glycosylation defective viruses (FL-GP3-N29A and FL-GP3-N152A) were found to have similar or slightly higher growth characteristics in comparison to FL12 virus as observed by comparing their multi step growth kinetics (Fig. 6.7A). Whereas, FL-GP3-

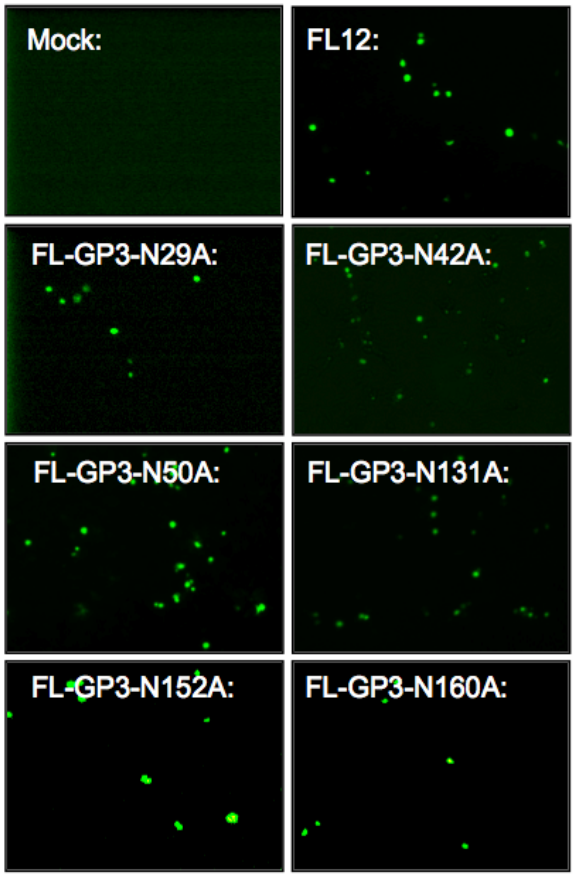

Figure 6.3 Expression of N protein in GP3 single N-glycosylation defective mutant viruses. MARC-145 cells were electroporated with in vitro transcripts derived from pFL12-Pol$^-$ (mock), pFL12, pFL-GP3-N29A, pFL-GP3-N42A, pFL-GP3-N50A, pFL-GP3-N131A, pFL-GP3-N152A, and pFL-GP3-N160A. At 48h after electorporation, cells were permeabilized and expression of N protein was examined using the monoclonal antibody SDOW17 and Alexa-488 conjugated anti-mouse IgG as secondary antibody.

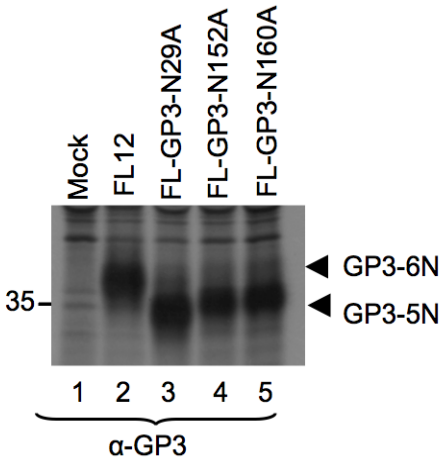

Figure 6.4 Protein expression of GP3 recovered single N-glycosylation defective mutant viruses. MARC-145 cells were either left uninfected (lane 1) or infected with FL12 virus (lane 2), FL-GP3-N29A virus (lane 3), FL-GP3-N152A virus (lane 4), and FL-GP3-N160A virus (lane 5) of passage-10. Cells were radiolabeled for 4 h at 48 h post-infection, and the radiolabeled proteins were analyzed by immunoprecipitation with anti-GP2a antibody, resolved in SDS-12%PAGE and detected by fluorography. The extent of glycosylated forms of GP3 are shown on the right. Relative mobilities of molecular mass markers in kDa are shown on the left.

N160A mutant virus yield after 120 h post-infection was about 8 fold less, indicating that this virus may be less stable or grows less efficiently compared to the wild type or other mutant viruses. These results show that glycosylation at amino acid positions 42, 50 and 131 of GP3 were important for infectious virus production or virus infectivity.

6.3 Triple mutations of N-glycosylation sites at N29, N152, and N160 positions of GP3 reduced the growth titer of mutant virus

To study the effect of mutation of two or more glycosylation sites at position 29, 152 and 160, I simultaneously mutated N to A in various combinations (N29/152A, N29/160A, and N152/160A, and N29/152/160A) of GP3 (Fig. 6.5). All four mutant proteins expressed similar levels of protein as observed in BHK-21 cells (Fig. 6.6A). The double mutant GP3 proteins (GP3-N29/152A, GP3-N29/160A, and GP3-N152/160A) lost approximately 5 kDa of molecular mass and had molecular weight of 37 kDa (Fig. 6.6A, lanes 4-6). Similarly, mutation of three glycosylation sites, the GP3-N29/152/160A mutant yielded a protein with molecular mass of 34.5 kDa (Fig. 6.6A, lane 7). I further introduced these specific double and triple mutations as mentioned for GP3 proteins in the FL12 genome of PRRSV (pFL-GP3-N29/152A, pFL-GP3-N29/160A, pFL-GP3-N152/160A, and pFL-GP3-N29/152/160A). The in vitro transcribed RNA was electroporated in MARC-145 cells. I was able to recover infectious viruses from each of these mutant RNA transfected cells. The recovered viruses were viable and found to retain the correct mutation even after 10^{th} passage in cell culture (data not shown). In MARC-145 cells infected with the mutant virus, the GP3-N29/152A, GP3-N29/160A, and GP3-N152/160A proteins migrated with a mobility that correlated with the loss of

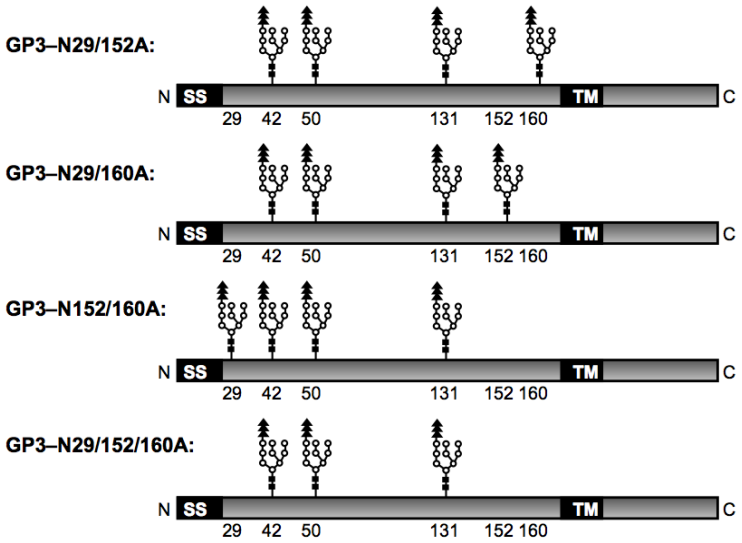

Figure 6.5 Schematics of GP3 double and triple N-glycosylation defective mutants constructed. The name of each of the mutant construct is shown on the left. The predicted N-glycosylation sites in amino acid numbers for GP3 are shown. The signal cleavage sites (SS) and transmembrane (TM) domains are indicated. The N to A mutation sites are left blank without any attached glycan moiety.

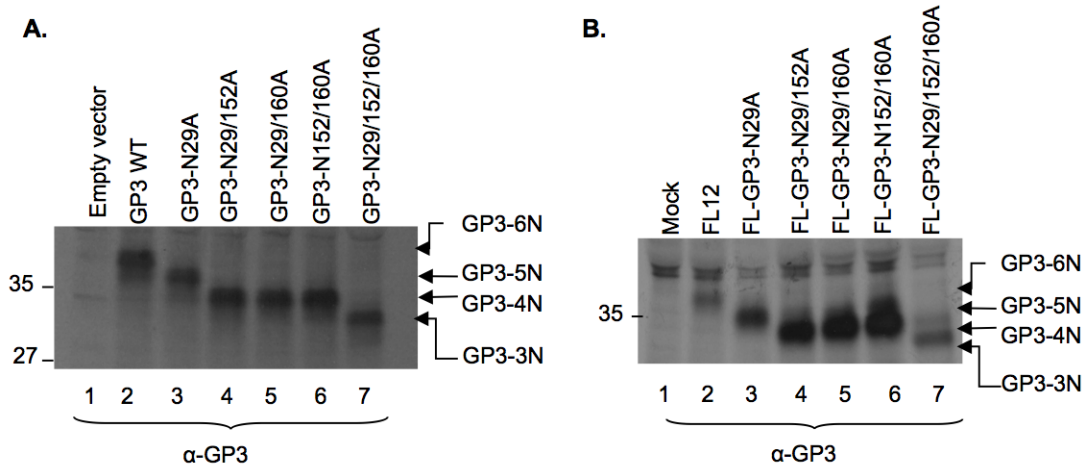

Figure 6.6 Protein expression of GP3 double and triple N-glycosylation defective mutants. (A) BHK-21 cells were infected with vTF7-3 and transfected with pGEM3 (Empty vector, lane 1) or GP3 (lane 2), GP3-N29A (lane 3), three double N-glycosylation defective clones of GP3 (lanes 4-6), and triple N-glycosylation defective clone (lane 7). Cells were radiolabeled for 4 h at 16 h post-transfection, and the radiolabeled proteins were analyzed by immunoprecipitation with anti-GP3 antibody, resolved in SDS-12%PAGE and detected by fluorography. The relative mobilities of the molecular mass markers in kDa are shown on the left. (B) MARC-145 cells were either left uninfected (Mock, lane 1) or infected with FL12 virus (lane 2), FL-GP3-N29A virus (lane 3), three double N-glycosylation defective mutant viruses of GP3 (lanes 4-6), and triple N-glycosylation defective mutant virus of GP3 (lane 7) after 10^{th} passage in cell culture. Cells were radiolabeled for 4 h at 48 h post-infection, and the radiolabeled proteins were analyzed by immunoprecipitation with anti-GP3 antibody, resolved in SDS-12%PAGE and detected by fluorography. Relative mobilities of molecular mass markers in kDa are shown on the left.

two glycosylation sites (Fig. 6.6B, lanes 4-6). Similarly, GP3-N29/152/160A protein migrated with a mobility that correlated with loss of three glycosylation sites (Fig. 6.6B, lane 7). The GP3 proteins synthesized in these mutant virus infected cells migrated faster than the GP3 protein synthesized in FL12 virus-infected cells (Fig. 6.6B, lane 2) and FL-GP3-N29A infected cells (Fig. 6.6B, lane 3), demonstrating the stability of the mutant virus under in vitro growth and passage conditions. The recovered double and triple mutant viruses were found to have different growth characteristics in comparison to wild type and single mutant GP3 proteins (Fig. 6.7B). They grew to a lower titer and in the case of the triple N-glycosylation defective mutant virus (FL-GP3-N29/152/160A), I observed a hundred fold decrease in virus titer in comparison to the FL12 virus (Fig. 6.7B). Also, in the case of FL-GP3-N29/152/160A virus infected MARC-145 cells, the time required for observable CPE was prolonged. These results suggested that simultaneous mutation of N to A at amino acid positions 29, 152 and 160 affected optimal virus growth and infectious virus production. Further, in cells infected with the mutant virus, the duration of appearance of CPE was prolonged.

6.4 Role of N-glycosylation of GP3 on neutralizing antibody production in infected piglets

Twenty one days old weaned piglets were infected with FL12 as well as mutant viruses generated for GP3 protein. For GP3 sites, I had generated seven mutant viruses out of which three have mutations in single amino acid position (FL-GP3-N29A, FL-GP3-N152A, and FL-GP3-N160A), three have mutation in two amino acid positions in different combinations (FL-GP3-N29/152A, FL-GP3-N29/160A, and FL-GP3-N152/160A) and one possessed mutations in three amino acid

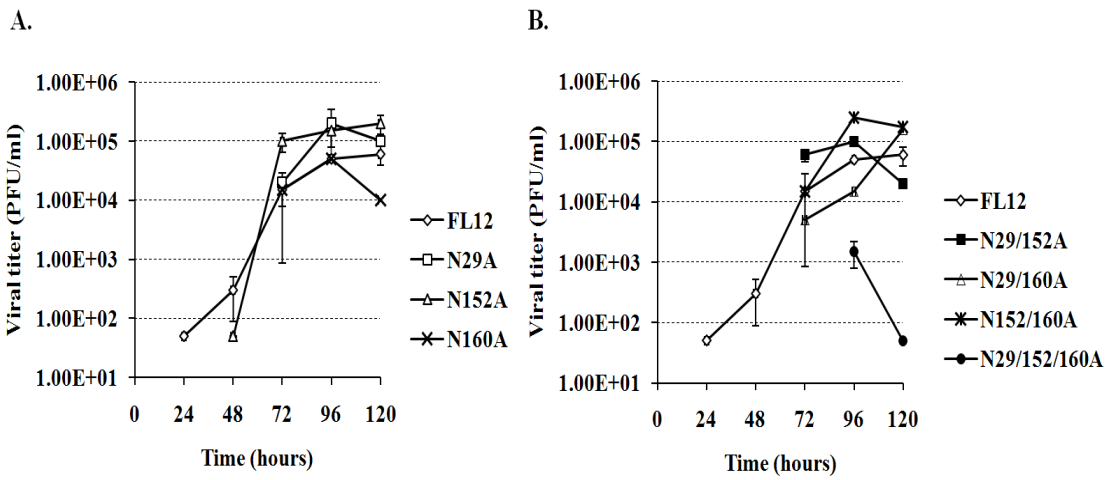

Figure 6.7 Multistep growth kinetics of recovered single, double, and triple N-glycosylation defective mutant viruses. (A) Multi step growth kinetics of recovered GP3 single N-glycosylation mutant viruses. MARC-145 cells were infected with wild type and mutant viruses (FL-GP3-N29A, FL-GP3-N152A, and FL-GP3-N160A) with 0.001 MOI and supernatant was collected in every 12 h interval up to 120 h. Plaque assay was performed as described in materials and methods. The viral titer was measured and expressed in $\log_{10}$ scale. The data points represent mean values from two independent experiments, and the error bars denote standard deviation. (B) Multi step growth kinetics of recovered GP3 double (FL-GP3-N29/152A, FL-GP3-N29/160A, and FL-GP3-N152/160A) and triple deglycosylation (FL-GP3-N29/152/160A) mutant viruses. The experiment was performed similarly as described for panel A.

positions (FL-GP3-N29/152/160A). Based on the previous report (Wei et al., 2003) on cumulative effect of N-glycosylation sites of a protein on glycan shielding, I used one of recovered double deglycosylated mutant virus (FL-GP3-N29/152A) and triple deglycosylated mutant virus (FL-GP3-29/152/160A) for inoculation in piglets. Groups of four 21 days old piglets were injected with the mutant viruses. All the different groups of piglets were housed separately. Sham infected piglets were included as negative control. The neutralizing antibody titer was measured by $TCID_{50}$ assay (Table 6.1). Since neutralizing antibody response is usually not detected before 21 days post infection, I normalized the titer of neutralizing antibody at day 7 as 1 for the wild type and GP3 mutant virus-infected sera from the animals. The FL12 infected piglet sera was tested against FL12 infected cells (homologous titer) and compared with sera collected from mutant virus infected piglets (heterologous titer). I did not observe any significant difference between neutralizing antibody response produced in case of FL12 virus or other GP3 mutant virus. These results indicated that hypoglycosylation of GP3 did not influence neutralizing antibody response in infected piglets (Table 6.1). Overall, the results show that unlike GP5 (Ansari et al., 2006), hypoglycosylation of GP3 did not induce higher neutralizing antibody response in infected pigs and the mutant viruses were not more sensitive to neutralization by neutralizing antibodies in the infected animals.

6.5 Discussion

PRRSV has four envelope glycoproteins GP2a, GP3, GP4, and GP5. Our previous study on GP5 protein has shown the importance of N-glycosylation on viral immune evasion and infectivity (Ansari et al., 2006). The N-glycosylation of GP2a and GP4 protein was also shown to be required for infectious virus production and interaction with

Table 6.1 Serum neutralization titer of animals infected with wild type or GP3 glycosylation defective mutant PRRSVs.

Groups	Days post infection	
	7 days	46 days
FL12	1	32
GP3 FL-N29/152A	1	13.5
GP3 FL-N29/152/160A	1	16

The serum neutralization value of both wild type and mutant viruses are made 1 for 7th day for comparison. The results are shown as of average of four animals per each group.

receptor CD163 (chapter V). My current study focused on the role of N-glycosylation of GP3 on virus infectivity and immune evasion. My report concluded that (i) glycan addition at N42, N50, and N131 of GP3 were individually required for infectious virus production and (ii) N-glycosylation of GP3 did not play any discernible role in viral immune evasion against host neutralizing antibody response or enhancement of host neutralizing antibody response.

My study had shown that N195 of GP3 proteins is not glycosylated. The bioinformatics analysis of the protein showed that residue has intracytoplasmic orientation, perhaps making it unavailable for glycosylation by host enzymes. Studies with the prototype foamy virus revealed that 14 out of 15 predicted glycosylation sites of its envelope protein were actually glycosylated in the virion and the glycan addition site present on the signal peptide is not glycosylated (Luftenegger et al., 2005). The N42, N50, and N131 of GP3 protein of PRRSV are individually required for infectious virus production. It is possible that without glycan addition at these positions, the synthesized GP3 adopted a protein conformation that was not favorable for generation of infectious particle formation. Although I recovered a PRRSV encoding GP3 with mutations at glycan addition sites N29, N152, and N160, this mutant virus was found to have lower titers than wild type, single, or double mutant viruses. These results imply that by mutating multiple glycosylation sites, proper folding of the mutant protein was impaired in such a manner that reduced infectious virus production or assembly.

The GP5 of PRRSV was previously reported to be immunogenic and was required for conferring protection against host neutralizing antibody response (Pirzadeh & Dea, 1997). As reported for GP2a and GP4 (chapter V), I did not observe any effect of N-

glycosylation of GP3 on protection against neutralizing antibody response. It may be due to the fact that these three minor envelope glycoproteins (GP2a, GP3, and GP4) are not abundantly expressed on the surface of the virion. There may be the existence of a 'malleable glycan shield' (Wei et al., 2003) in which case the glycan moities on GP5 may protect the minor envelope glycoprotein even if they are unglycosylated. Glycan shield generally requires co-operative packing of entire envelope protein to prevent antibody access (Wei et al., 2003). During glycan shielding, steric hindrance of epitope due to glycan addition at a nearby position prevents its binding to a neutralizing antibody (Wei et al., 2003). It is possible that by partial deglycosylation, the potential neutralizing epitopes in these three glycoproteins have not been sufficiently exposed to permit binding of neutralizing antibody to each protein. Alternatively, my results could suggest that these three glycoproteins do not contain PRRSV neutralizing epitopes or the glycan shielding mechanisms do not operate in these GPs. It should be noted that GP3 of North American strain seems to possess neutralizing epitopes (Yang et al., 2000). So the later possibility appears to be more likely.

CONCLUSION

PRRSV encodes one major envelope glycoprotein (GP5) and three minor envelope glycoproteins (GP2a, GP3, and GP4). The studies reported in this dissertation focused on examining interactions of these minor glycoproteins amongst themselves and also with the PRRSV receptor CD163. Further, the role of glycan addition at various sites in these glycoproteins in GP-receptor interactions, neutralizing antibody response, and generation of infectious virus production were examined. The following conclusions were derived from these studies:

1. Individually expressed envelope glycoproteins are localized in the ER

By the use of monospecific antibodies to the individual GPs or tagged antibodies, I was able to demonstrate expression of both mature as well as partially glycosylated form of the proteins in BHK-21, HeLa, and MARC-145 cells (Fig. 3.1, 3.2, and 3.3). By immunofluorescence microscopy and endo H digestion studies, I have also shown that upon ectopic expression, the individual glycoproteins remained in the ER and were not transported to the plasma membrane (Fig. 3.4 and 3.5).

2. GP2a, GP3, and GP4 are co-translationally glycosylated, whereas GP5 is post-translationally glycosylated

Previously, it was reported that STT3A ad STT3B subunits of OST enzyme complex were required for co-translational and post-translational glycosylation of glycoproteins in the cell. Though most the glycoproteins are co-translationally glycosylated, post-translational glycosylation of some proteins including coagulation factor VII and L protein of hepatitis B virus were reported. In my attempt to decipher whether viral GPs are co-translationally or post-translationally glycosylated, I employed

short pulse labelling of the proteins and subsequent examination of the proteins during various lengths of chase periods. My results show that GP2a, GP3, and GP4 proteins are co-translationally glycosylated whereas; GP5 protein is post-translationally glycosylated (Fig. 3.7, 3.8, 3.9, and 3.10). The significance of post-translational glycosylation of GP5 in the viral life cycle is not clear.

3. GP4 interacts with GP5 and mediates formation of multiprotein complex

Co-expression of multiple proteins and co-IP studies revealed that GP2a interacts strongly with GP3 and GP4 proteins, but not with GP5 (Fig. 4.1). The GP3 interacts strongly with GP2a and GP4 proteins, but not with GP5 (Fig. 4.2). The GP4 interacts with GP2a, GP3, and GP5 proteins (Fig. 4.3). The GP5 interacts primarily with GP4 and this interaction was required for multiprotein complex formation of the glycoproteins (Fig. 4.4 and 4.5). Previously it was reported that GP5 and M proteins interact with each other and form a heterodimer. Based on these results (Table 4.1), I speculate that GP4 acts as a bridge between the three minor envelope glycoproteins and GP5 and this is important for virus assembly.

4. Both GP2a and GP4 interact with PRRSV receptor CD163

The porcine CD163 receptor was the major receptor for PRRSV in PAM cells. I had also independently cloned and characterized porcine CD163 molecule (Fig. 4.9, 4.10, and 4.11). Expression of this receptor in non-susceptible BHK-21 cells conferred permissivity to PRRSV infection. I also obtained a truncated form of the receptor protein (CD163ΔTM) which lacked the 9^{th} SRCR domain and transmembrane domain of CD163. Expression of this mutant protein in BHK-21 cells did not confer permissivity to PRRSV infection because this protein was not expressed on the plasma membrane due to the

absence of the transmembrane domain (Fig. 4.11). The CD163 molecule was found to interact specifically with GP2a and GP4 proteins of PRRSV (Fig. 4.12). The CD163ΔTM protein was also found to interact with both GP2a and GP4 (Fig. 4.14) indicating that the 9th SRCR domain was not required for this interaction. I have concluded that porcine CD163 interacts with GP2a and GP4 proteins of PRRSV.

5. Specific regions of GP2a and GP4 that interact with CD163

By generating a series of deletion mutants of GP2a as well as GP4 and examining their interactions with CD163, it was observed that GP2a region spanning amino acids residues 76-112 are critical for its interaction with CD163 (Fig. 4.16). Similarly, amino acid regions 141-177 of GP4 are required for its efficient interaction with CD163 (Fig. 4.17).

6. N-glycosylation of GP2a and GP4 protein of PRRSV is required for their interaction with receptor CD163

To study the effect of N-glycosylation of GP2a and GP4 with their interaction with receptor CD163, I co-expressed the mutant proteins with the receptor and performed co-IP assays. Although single site N-glycosylation mutations of GP2a had no negative effect on interactions with CD163, completely unglycosylated GP2a was defective in interaction with CD163 molecule (Fig. 5.13 and 5.14). A similar co-IP study for CD163-GP4 interaction showed that mutation of individual N-glycosylation sites of GP4 had no effect for this interaction. But, upon deglycosylation of two or more sites, significant reduction in the interaction with CD163 was observed (Fig. 5.15). Based on these observations, I conclude that the N-glycosylation sites of GP2a and GP4 proteins of PRRSV are required for their optimal interaction with receptor CD163.

7. N-glycosylation of minor envelope glycoproteins of PRRSV is required for infectious virus production

The N-glycan moieties of GP5 for both European and North American strains of PRRSV are required for virus infectivity. But, the glycan moieties of GP2a of European strain (Lelystad virus) are dispensable for virus production. To study the role of N-glycosylation of GP2a, GP3, and GP4 proteins on virus infectivity, I mutated N residue of predicted glycan moities of the proteins to A residue in infectious clone FL12 of PRRSV. Of the two glycan addition sites (N178 and N184) of GP2a, N184 is required for virus production. GP3 has seven potential glycosylation sites at positions N29, N42, N50, N131, N152, N160, and N195. My studies have revealed that N195 site is not glycosylated (Fig. 6.2). Furthermore, glycan addition at sites N42, N50, and N131 is required for infectious virus production. GP4 has four N-glycosylation sites at positions N37, N84, N120, and N130. Although individual glycosylation site mutations at any of these sites did not affect infectious virus production, introduction of double site mutations of various combinations was lethal for infectious virus recovery. Taken together, my data suggest that addition of glycan moities at several sites in the three minor envelope glycoproteins of PRRSV is required for virus infectivity.

8. N-glycosylation of minor envelope glycoproteins of PRRSV is not required for glycan shielding against host neutralizing antibody response

The N-glycosylation of GP5 was important for protection against host neutralizing antibody response by glycan shielding mechanism. To further address the role of glycan moities of GP2a, GP3, and GP4 proteins in glycan shielding mechanism, I

performed animal studies using various recovered glycosylation mutant viruses. Neutralizing antibody titers in piglets infected with various mutant viruses revealed no significant increase in neutralizing antibody production (Tables 5.1 and 6.1). These results indicate that N-glycosylation sites of GP2a, GP3, and GP4 protein of PRRSV are not required for protection of the virus against host neutralizing antibody response and that hypoglycosylation of the minor glycoproteins do not induce higher neutralizing antibody titers. Considering the fact that GP2a, GP3, and GP4 are minor envelope proteins it is possible that the virus does not use glycan moities of these proteins for protection against host neutralizing antibody response. This is in contrast to GP5 in which hypoglycosylation of the protein induces higher neutralizing antibody response and the virus containing hypoglycosylated forms of GP5 are readily neutralized by neutralizing antibodies. Also, GP2a and GP4 protein apparently interact with receptor CD163 (Fig. 4.12). Based on these observations, I hypothesize that PRRSV mobilizes the different envelope proteins for different functions for successful viral infection and immune evasion.

OVERVIEW

My dissertation research involves study of interactions among the four glycoproteins of PRRSV, the interaction of the glycoproteins with one of the PRRSV receptor CD163, and the role of N-glycosylation of three minor glycoproteins (GP2a, GP3, and GP4) in receptor interactions, infectious virus production, and protection against host neutralizing antibody response. Specific interaction patterns between different glycoproteins have been demonstrated by my study. I hypothesize that the GP4 and GP5 interaction probably helps in viral particle formation. Similarly, I also observed that GP2a and GP4 proteins of PRRSV interact with the receptor CD163. This specific interaction is probably required for virus entry and uncoating inside the infected cells.

Studies from our laboratory and other laboratories have indicated that certain N-glycosylation sites of PRRSV envelope proteins are required for infectious virus production. While the glycan moieties of GP5 are required for protection against host neutralizing antibody response, N-glycosylation of GP2a, GP3, and GP4 is not required for protection against host neutralizing antibody response. Out of four glycoproteins, GP2a, GP3, and GP4 are co-translationally glycosylated whereas, GP5 is post-translationally glycosylated. The significance of the different mechanism for glycosylation in the biology and/or pathogenesis of PRRSV are unknown at this time and further investigation in these lines will be required.

Overall, my dissertation research has provided an understanding of the role and requirement of glycosylation of envelope proteins of PRRSV and their interactions in particle formation, host-cell interactions, and immune response.

REFERENCES

Albina, E., Carrat, C. & Charley, B. (1998). Interferon-alpha response to swine arterivirus (PoAV), the porcine reproductive and respiratory syndrome virus. *J Interferon Cytokine Res* **18**, 485-490.

Ansari, I. H., Kwon, B., Osorio, F. A. & Pattnaik, A. K. (2006). Influence of N-linked glycosylation of porcine reproductive and respiratory syndrome virus GP5 on virus infectivity, antigenicity, and ability to induce neutralizing antibodies. *J Virol* **80**, 3994-4004.

Balasuriya, U. B. & MacLachlan, N. J. (2004). The immune response to equine arteritis virus: potential lessons for other arteriviruses. *Vet Immunol Immunopathol* **102**, 107-129.

Baric, R. S., Stohlman, S. A. & Lai, M. M. (1983). Characterization of replicative intermediate RNA of mouse hepatitis virus: presence of leader RNA sequences on nascent chains. *J Virol* **48**, 633-640.

Batista, L., Pijoan, C., Dee, S., Olin, M., Molitor, T., Joo, H. S., Xiao, Z. & Murtaugh, M. (2004). Virological and immunological responses to porcine reproductive and respiratory syndrome virus in a large population of gilts. *Can J Vet Res* **68**, 267-273.

Bautista, E. M. & Molitor, T. W. (1999). IFN gamma inhibits porcine reproductive and respiratory syndrome virus replication in macrophages. *Arch Virol* **144**, 1191-1200.

Bautista, E. M., Suarez, P. & Molitor, T. W. (1999). T cell responses to the structural polypeptides of porcine reproductive and respiratory syndrome virus. *Arch Virol* **144**, 117-134.

Beasley, D. W., Whiteman, M. C., Zhang, S., Huang, C. Y., Schneider, B. S., Smith, D. R., Gromowski, G. D., Higgs, S., Kinney, R. M. & Barrett, A. D. (2005). Envelope protein glycosylation status influences mouse neuroinvasion phenotype of genetic lineage 1 West Nile virus strains. *J Virol* **79**, 8339-8347.

Ben-Dor, S., Esterman, N., Rubin, E. & Sharon, N. (2004). Biases and complex patterns in the residues flanking protein N-glycosylation sites. *Glycobiology* **14**, 95-101.

Benfield, D., Collins, J., Dee, S., Halbu, P., Joo, H. & Larger, K. (1999). *Porcine reproductive and respiratory syndrome*. Ames, Iowa: Iowa State University Press.

Beura, L. K., Sarkar, S. N., Kwon, B., Subramaniam, S., Jones, C., Pattnaik, A. K. & Osorio, F. A. (2010). Porcine reproductive and respiratory syndrome virus nonstructural protein 1beta modulates host innate immune response by antagonizing IRF3 activation. *J Virol* **84**, 1574-1584.

Bolt, G., Kristensen, C. & Steenstrup, T. D. (2005). Posttranslational N-glycosylation takes place during the normal processing of human coagulation factor VII. *Glycobiology* **15**, 541-547.

Butler, J. E., Wertz, N., Weber, P. & Lager, K. M. (2008). Porcine reproductive and respiratory syndrome virus subverts repertoire development by

proliferation of germline-encoded B cells of all isotypes bearing hydrophobic heavy chain CDR3. *J Immunol* **180**, 2347-2356.

Calvert, J. G., Slade, D. E., Shields, S. L., Jolie, R., Mannan, R. M., Ankenbauer, R. G. & Welch, S. K. (2007). CD163 expression confers susceptibility to porcine reproductive and respiratory syndrome viruses. *J Virol* **81**, 7371-7379.

Cancel-Tirado, S. M., Evans, R. B. & Yoon, K. J. (2004). Monoclonal antibody analysis of porcine reproductive and respiratory syndrome virus epitopes associated with antibody-dependent enhancement and neutralization of virus infection. *Vet Immunol Immunopathol* **102**, 249-262.

Chandran, K., Sullivan, N. J., Felbor, U., Whelan, S. P. & Cunningham, J. M. (2005). Endosomal proteolysis of the Ebola virus glycoprotein is necessary for infection. *Science* **308**, 1643-1645.

Chang, C. C., Yoon, K. J., Zimmerman, J. J., Harmon, K. M., Dixon, P. M., Dvorak, C. M. & Murtaugh, M. P. (2002). Evolution of porcine reproductive and respiratory syndrome virus during sequential passages in pigs. *J Virol* **76**, 4750-4763.

Chang, H. C., Peng, Y. T., Chang, H. L., Chaung, H. C. & Chung, W. B. (2008). Phenotypic and functional modulation of bone marrow-derived dendritic cells by porcine reproductive and respiratory syndrome virus. *Vet Microbiol* **129**, 281-293.

Chen, Z., Lawson, S., Sun, Z., Zhou, X., Guan, X., Christopher-Hennings, J., Nelson, E. A. & Fang, Y. (2010). Identification of two auto-cleavage products of nonstructural protein 1 (nsp1) in porcine reproductive and respiratory syndrome virus infected cells: nsp1 function as interferon antagonist. *Virology* **398**, 87-97.

Cho, J. G. & Dee, S. A. (2006). Porcine reproductive and respiratory syndrome virus. *Theriogenology* **66**, 655-662.

Costers, S., Delputte, P. L. & Nauwynck, H. J. (2006). Porcine reproductive and respiratory syndrome virus-infected alveolar macrophages contain no detectable levels of viral proteins in their plasma membrane and are protected against antibody-dependent, complement-mediated cell lysis. *J Gen Virol* **87**, 2341-2351.

Costers, S., Lefebvre, D. J., Delputte, P. L. & Nauwynck, H. J. (2008). Porcine reproductive and respiratory syndrome virus modulates apoptosis during replication in alveolar macrophages. *Arch Virol* **153**, 1453-1465.

Daniels, R., Kurowski, B., Johnson, A. E. & Hebert, D. N. (2003). N-linked glycans direct the cotranslational folding pathway of influenza hemagglutinin. *Mol Cell* **11**, 79-90.

Das, P. B., Dinh, P. X., Ansari, I. H., de Lima, M., Osorio, F. A. & Pattnaik, A. K. (2010). The minor envelope glycoproteins GP2a and GP4 of porcine reproductive and respiratory syndrome virus interact with the receptor CD163. *J Virol* **84**, 1731-1740.

Das, S. C., Nayak, D., Zhou, Y. & Pattnaik, A. K. (2006). Visualization of intracellular transport of vesicular stomatitis virus nucleocapsids in living cells. *J Virol* **80**, 6368-6377.

Das, S. C. & Pattnaik, A. K. (2005). Role of the hypervariable hinge region of phosphoprotein P of vesicular stomatitis virus in viral RNA synthesis and assembly of infectious virus particles. *J Virol* **79**, 8101-8112.

de Lima, M., Ansari, I. H., Das, P. B., Ku, B. J., Martinez-Lobo, F. J., Pattnaik, A. K. & Osorio, F. A. (2009). GP3 is a structural component of the PRRSV type II (US) virion. *Virology* **390**, 31-36.

de Lima, M., Pattnaik, A. K., Flores, E. F. & Osorio, F. A. (2006). Serologic marker candidates identified among B-cell linear epitopes of Nsp2 and structural proteins of a North American strain of porcine reproductive and respiratory syndrome virus. *Virology* **353**, 410-421.

Dea, S., Gagnon, C. A., Mardassi, H., Pirzadeh, B. & Rogan, D. (2000). Current knowledge on the structural proteins of porcine reproductive and respiratory syndrome (PRRS) virus: comparison of the North American and European isolates. *Arch Virol* **145**, 659-688.

Delputte, P. L., Costers, S. & Nauwynck, H. J. (2005). Analysis of porcine reproductive and respiratory syndrome virus attachment and internalization: distinctive roles for heparan sulphate and sialoadhesin. *J Gen Virol* **86**, 1441-1445.

Delputte, P. L., Meerts, P., Costers, S. & Nauwynck, H. J. (2004). Effect of virus-specific antibodies on attachment, internalization and infection of porcine reproductive and respiratory syndrome virus in primary macrophages. *Vet Immunol Immunopathol* **102**, 179-188.

Delputte, P. L. & Nauwynck, H. J. (2004). Porcine arterivirus infection of alveolar macrophages is mediated by sialic acid on the virus. *J Virol* **78**, 8094-8101.

Delputte, P. L., Van Breedam, W., Delrue, I., Oetke, C., Crocker, P. R. & Nauwynck, H. J. (2007). Porcine arterivirus attachment to the macrophage-specific receptor sialoadhesin is dependent on the sialic acid-binding activity of the N-terminal immunoglobulin domain of sialoadhesin. *J Virol* **81**, 9546-9550.

Delputte, P. L., Vanderheijden, N., Nauwynck, H. J. & Pensaert, M. B. (2002). Involvement of the matrix protein in attachment of porcine reproductive and respiratory syndrome virus to a heparinlike receptor on porcine alveolar macrophages. *J Virol* **76**, 4312-4320.

Delrue, I., Delputte, P. L. & Nauwynck, H. J. (2009). Assessing the functionality of viral entry-associated domains of porcine reproductive and respiratory syndrome virus during inactivation procedures, a potential tool to optimize inactivated vaccines. *Vet Res* **40**, 62.

den Boon, J. A., Faaberg, K. S., Meulenberg, J. J., Wassenaar, A. L., Plagemann, P. G., Gorbalenya, A. E. & Snijder, E. J. (1995). Processing and evolution of the N-terminal region of the arterivirus replicase ORF1a protein: identification of two papainlike cysteine proteases. *J Virol* **69**, 4500-4505.

Dobbe, J. C., van der Meer, Y., Spaan, W. J. & Snijder, E. J. (2001). Construction of chimeric arteriviruses reveals that the ectodomain of the major glycoprotein is not the main determinant of equine arteritis virus tropism in cell culture. *Virology* **288**, 283-294.

Du, L., He, Y., Zhou, Y., Liu, S., Zheng, B. J. & Jiang, S. (2009). The spike protein of SARS-CoV--a target for vaccine and therapeutic development. *Nat Rev Microbiol* **7**, 226-236.

Duan, X., Nauwynck, H. J. & Pensaert, M. B. (1997). Effects of origin and state of differentiation and activation of monocytes/macrophages on their susceptibility to porcine reproductive and respiratory syndrome virus (PRRSV). *Arch Virol* **142**, 2483-2497.

Faaberg, K. S., Even, C., Palmer, G. A. & Plagemann, P. G. (1995). Disulfide bonds between two envelope proteins of lactate dehydrogenase-elevating virus are essential for viral infectivity. *J Virol* **69**, 613-617.

Fang, L., Jiang, Y., Xiao, S., Niu, C., Zhang, H. & Chen, H. (2006). Enhanced immunogenicity of the modified GP5 of porcine reproductive and respiratory syndrome virus. *Virus Genes* **32**, 5-11.

Fang, Y., Christopher-Hennings, J., Brown, E., Liu, H., Chen, Z., Lawson, S. R., Breen, R., Clement, T., Gao, X., Bao, J., Knudsen, D., Daly, R. & Nelson, E. (2008). Development of genetic markers in the non-structural protein 2 region of a US type 1 porcine reproductive and respiratory syndrome virus: implications for future recombinant marker vaccine development. *J Gen Virol* **89**, 3086-3096.

Fenouillet, E., Gluckman, J. C. & Bahraoui, E. (1990). Role of N-linked glycans of envelope glycoproteins in infectivity of human immunodeficiency virus type 1. *J Virol* **64**, 2841-2848.

Fitter, S., Sincock, P. M., Jolliffe, C. N. & Ashman, L. K. (1999). Transmembrane 4 superfamily protein CD151 (PETA-3) associates with beta 1 and alpha IIb beta 3 integrins in haemopoietic cell lines and modulates cell-cell adhesion. *Biochem J* **338 (Pt 1)**, 61-70.

Flores-Mendoza, L., Silva-Campa, E., Resendiz, M., Osorio, F. A. & Hernandez, J. (2008). Porcine reproductive and respiratory syndrome virus infects mature porcine dendritic cells and up-regulates interleukin-10 production. *Clin Vaccine Immunol* **15**, 720-725.

Forsberg, R. (2005). Divergence time of porcine reproductive and respiratory syndrome virus subtypes. *Mol Biol Evol* **22**, 2131-2134.

Fournillier, A., Wychowski, C., Boucreux, D., Baumert, T. F., Meunier, J. C., Jacobs, D., Muguet, S., Depla, E. & Inchauspe, G. (2001). Induction of hepatitis C virus E1 envelope protein-specific immune response can be enhanced by mutation of N-glycosylation sites. *J Virol* **75**, 12088-12097.

Frias-Staheli, N., Giannakopoulos, N. V., Kikkert, M., Taylor, S. L., Bridgen, A., Paragas, J., Richt, J. A., Rowland, R. R., Schmaljohn, C. S., Lenschow, D. J., Snijder, E. J., Garcia-Sastre, A. & Virgin, H. W. t. (2007). Ovarian tumor

domain-containing viral proteases evade ubiquitin- and ISG15-dependent innate immune responses. *Cell Host Microbe* **2**, 404-416.

Fuerst, T. R., Niles, E. G., Studier, F. W. & Moss, B. (1986). Eukaryotic transient-expression system based on recombinant vaccinia virus that synthesizes bacteriophage T7 RNA polymerase. *Proc Natl Acad Sci U S A* **83**, 8122-8126.

Gaudreault, N., Rowland, R. R. & Wyatt, C. R. (2009). Factors affecting the permissiveness of porcine alveolar macrophages for porcine reproductive and respiratory syndrome virus. *Arch Virol* **154**, 133-136.

Gavel, Y. & von Heijne, G. (1990). Sequence differences between glycosylated and non-glycosylated Asn-X-Thr/Ser acceptor sites: implications for protein engineering. *Protein Eng* **3**, 433-442.

Glabe, C. G., Hanover, J. A. & Lennarz, W. J. (1980). Glycosylation of ovalbumin nascent chains. The spatial relationship between translation and glycosylation. *J Biol Chem* **255**, 9236-9242.

Godeny, E. K., Chen, L., Kumar, S. N., Methven, S. L., Koonin, E. V. & Brinton, M. A. (1993). Complete genomic sequence and phylogenetic analysis of the lactate dehydrogenase-elevating virus (LDV). *Virology* **194**, 585-596.

Goldberg, T. L., Lowe, J. F., Milburn, S. M. & Firkins, L. D. (2003). Quasispecies variation of porcine reproductive and respiratory syndrome virus during natural infection. *Virology* **317**, 197-207.

Gonin, P., Mardassi, H., Gagnon, C. A., Massie, B. & Dea, S. (1998). A nonstructural and antigenic glycoprotein is encoded by ORF3 of the IAF-Klop strain of porcine reproductive and respiratory syndrome virus. *Arch Virol* **143**, 1927-1940.

Han, J., Liu, G., Wang, Y. & Faaberg, K. S. (2007). Identification of nonessential regions of the nsp2 replicase protein of porcine reproductive and respiratory syndrome virus strain VR-2332 for replication in cell culture. *J Virol* **81**, 9878-9890.

Hanada, K., Suzuki, Y., Nakane, T., Hirose, O. & Gojobori, T. (2005). The origin and evolution of porcine reproductive and respiratory syndrome viruses. *Mol Biol Evol* **22**, 1024-1031.

Hanna, S. L., Pierson, T. C., Sanchez, M. D., Ahmed, A. A., Murtadha, M. M. & Doms, R. W. (2005). N-linked glycosylation of west nile virus envelope proteins influences particle assembly and infectivity. *J Virol* **79**, 13262-13274.

Hasegawa, H., Nomura, T., Kishimoto, K., Yanagisawa, K. & Fujita, S. (1998). SFA-1/PETA-3 (CD151), a member of the transmembrane 4 superfamily, associates preferentially with alpha 5 beta 1 integrin and regulates adhesion of human T cell leukemia virus type 1-infected T cells to fibronectin. *J Immunol* **161**, 3087-3095.

Hashiguchi, T., Kajikawa, M., Maita, N., Takeda, M., Kuroki, K., Sasaki, K., Kohda, D., Yanagi, Y. & Maenaka, K. (2007). Crystal structure of measles virus hemagglutinin provides insight into effective vaccines. *Proc Natl Acad Sci U S A* **104**, 19535-19540.

Horter, D. C., Pogranichniy, R. M., Chang, C. C., Evans, R. B., Yoon, K. J. & Zimmerman, J. J. (2002). Characterization of the carrier state in porcine reproductive and respiratory syndrome virus infection. *Vet Microbiol* **86**, 213-228.

Jiang, W., Jiang, P., Li, Y., Wang, X. & Du, Y. (2007a). Analysis of immunogenicity of minor envelope protein GP3 of porcine reproductive and respiratory syndrome virus in mice. *Virus Genes* **35**, 695-704.

Jiang, W., Jiang, P., Wang, X., Li, Y. & Du, Y. (2007b). Influence of porcine reproductive and respiratory syndrome virus GP5 glycoprotein N-linked glycans on immune responses in mice. *Virus Genes* **35**, 663-671.

Jusa, E. R., Inaba, Y., Kouno, M. & Hirose, O. (1997). Effect of heparin on infection of cells by porcine reproductive and respiratory syndrome virus. *Am J Vet Res* **58**, 488-491.

Kaletsky, R. L., Simmons, G. & Bates, P. (2007). Proteolysis of the Ebola virus glycoproteins enhances virus binding and infectivity. *J Virol* **81**, 13378-13384.

Kapur, V., Elam, M. R., Pawlovich, T. M. & Murtaugh, M. P. (1996). Genetic variation in porcine reproductive and respiratory syndrome virus isolates in the midwestern United States. *J Gen Virol* **77 (Pt 6)**, 1271-1276.

Katz, J. B., Shafer, A. L., Eernisse, K. A., Landgraf, J. G. & Nelson, E. A. (1995). Antigenic differences between European and American isolates of porcine reproductive and respiratory syndrome virus (PRRSV) are encoded by the carboxyterminal portion of viral open reading frame 3. *Vet Microbiol* **44**, 65-76.

Kelleher, D. J. & Gilmore, R. (2006). An evolving view of the eukaryotic oligosaccharyltransferase. *Glycobiology* **16**, 47R-62R.

Kim, H. S., Kwang, J., Yoon, I. J., Joo, H. S. & Frey, M. L. (1993). Enhanced replication of porcine reproductive and respiratory syndrome (PRRS) virus in a homogeneous subpopulation of MA-104 cell line. *Arch Virol* **133**, 477-483.

Kim, J. K., Fahad, A. M., Shanmukhappa, K. & Kapil, S. (2006). Defining the cellular target(s) of porcine reproductive and respiratory syndrome virus blocking monoclonal antibody 7G10. *J Virol* **80**, 689-696.

Kim, J. M., Yun, S. I., Song, B. H., Hahn, Y. S., Lee, C. H., Oh, H. W. & Lee, Y. M. (2008). A single N-linked glycosylation site in the Japanese encephalitis virus prM protein is critical for cell type-specific prM protein biogenesis, virus particle release, and pathogenicity in mice. *J Virol* **82**, 7846-7862.

Kim, O., Sun, Y., Lai, F. W., Song, C. & Yoo, D. (2010). Modulation of type I interferon induction by porcine reproductive and respiratory syndrome virus and degradation of CREB-binding protein by non-structural protein 1 in MARC-145 and HeLa cells. *Virology*.

Kim, W. I. & Yoon, K. J. (2008). Molecular assessment of the role of envelope-associated structural proteins in cross neutralization among different PRRS viruses. *Virus Genes* **37**, 380-391.

Kimman, T. G., Cornelissen, L. A., Moormann, R. J., Rebel, J. M. & Stockhofe-Zurwieden, N. (2009). Challenges for porcine reproductive and respiratory syndrome virus (PRRSV) vaccinology. *Vaccine* **27**, 3704-3718.

Knight, R. L., Schultz, K. L., Kent, R. J., Venkatesan, M. & Griffin, D. E. (2009). Role of N-linked glycosylation for sindbis virus infection and replication in vertebrate and invertebrate systems. *J Virol* **83**, 5640-5647.

Kreutz, L. C. & Ackermann, M. R. (1996). Porcine reproductive and respiratory syndrome virus enters cells through a low pH-dependent endocytic pathway. *Virus Res* **42**, 137-147.

Kroese, M. V., Zevenhoven-Dobbe, J. C., Bos-de Ruijter, J. N., Peeters, B. P., Meulenberg, J. J., Cornelissen, L. A. & Snijder, E. J. (2008). The nsp1alpha and nsp1 papain-like autoproteinases are essential for porcine reproductive and respiratory syndrome virus RNA synthesis. *J Gen Virol* **89**, 494-499.

Lai, M. M., Baric, R. S., Brayton, P. R. & Stohlman, S. A. (1984). Characterization of leader RNA sequences on the virion and mRNAs of mouse hepatitis virus, a cytoplasmic RNA virus. *Proc Natl Acad Sci U S A* **81**, 3626-3630.

Lai, M. M., Patton, C. D., Baric, R. S. & Stohlman, S. A. (1983). Presence of leader sequences in the mRNA of mouse hepatitis virus. *J Virol* **46**, 1027-1033.

Lai, M. M., Patton, C. D. & Stohlman, S. A. (1982). Further characterization of mRNA's of mouse hepatitis virus: presence of common 5'-end nucleotides. *J Virol* **41**, 557-565.

Lambert, C. & Prange, R. (2007). Posttranslational N-glycosylation of the hepatitis B virus large envelope protein. *Virol J* **4**, 45.

Lamontagne, L., Page, C., Larochelle, R. & Magar, R. (2003). Porcine reproductive and respiratory syndrome virus persistence in blood, spleen, lymph nodes, and tonsils of experimentally infected pigs depends on the level of CD8high T cells. *Viral Immunol* **16**, 395-406.

Lawson, S. R., Rossow, K. D., Collins, J. E., Benfield, D. A. & Rowland, R. R. (1997). Porcine reproductive and respiratory syndrome virus infection of gnotobiotic pigs: sites of virus replication and co-localization with MAC-387 staining at 21 days post-infection. *Virus Res* **51**, 105-113.

Le Bon, A., Schiavoni, G., D'Agostino, G., Gresser, I., Belardelli, F. & Tough, D. F. (2001). Type i interferons potently enhance humoral immunity and can promote isotype switching by stimulating dendritic cells in vivo. *Immunity* **14**, 461-470.

Lee, C., Calvert, J. G., Welch, S. K. & Yoo, D. (2005). A DNA-launched reverse genetics system for porcine reproductive and respiratory syndrome virus reveals that homodimerization of the nucleocapsid protein is essential for virus infectivity. *Virology* **331**, 47-62.

Lee, C., Hodgins, D., Calvert, J. G., Welch, S. K., Jolie, R. & Yoo, D. (2006). Mutations within the nuclear localization signal of the porcine reproductive and respiratory syndrome virus nucleocapsid protein attenuate virus replication. *Virology* **346**, 238-250.

Lee, C. & Yoo, D. (2005). Cysteine residues of the porcine reproductive and respiratory syndrome virus small envelope protein are non-essential for virus infectivity. *J Gen Virol* **86**, 3091-3096.

Lee, C. & Yoo, D. (2006). The small envelope protein of porcine reproductive and respiratory syndrome virus possesses ion channel protein-like properties. *Virology* **355**, 30-43.

Lee, S. M. & Kleiboeker, S. B. (2007). Porcine reproductive and respiratory syndrome virus induces apoptosis through a mitochondria-mediated pathway. *Virology* **365**, 419-434.

Lim, A. P., Chan, C. E., Wong, S. K., Chan, A. H., Ooi, E. E. & Hanson, B. J. (2008). Neutralizing human monoclonal antibody against H5N1 influenza HA selected from a Fab-phage display library. *Virol J* **5**, 130.

Lin, G., Simmons, G., Pohlmann, S., Baribaud, F., Ni, H., Leslie, G. J., Haggarty, B. S., Bates, P., Weissman, D., Hoxie, J. A. & Doms, R. W. (2003). Differential N-linked glycosylation of human immunodeficiency virus and Ebola virus envelope glycoproteins modulates interactions with DC-SIGN and DC-SIGNR. *J Virol* **77**, 1337-1346.

Loemba, H. D., Mounir, S., Mardassi, H., Archambault, D. & Dea, S. (1996). Kinetics of humoral immune response to the major structural proteins of the porcine reproductive and respiratory syndrome virus. *Arch Virol* **141**, 751-761.

Loh, P. C., Oie, H. K. & Ratnayake, R. M. (1970). Accelerated Cytopathology in HeLa Cells Induced by Reovirus and Cycloheximide. *Infect Immun* **2**, 705-712.

Lopez, O. J. & Osorio, F. A. (2004). Role of neutralizing antibodies in PRRSV protective immunity. *Vet Immunol Immunopathol* **102**, 155-163.

Loving, C. L., Brockmeier, S. L. & Sacco, R. E. (2007). Differential type I interferon activation and susceptibility of dendritic cell populations to porcine arterivirus. *Immunology* **120**, 217-229.

Loving, C. L., Brockmeier, S. L., Vincent, A. L., Lager, K. M. & Sacco, R. E. (2008). Differences in clinical disease and immune response of pigs challenged with a high-dose versus low-dose inoculum of porcine reproductive and respiratory syndrome virus. *Viral Immunol* **21**, 315-325.

Lowe, J. E., Husmann, R., Firkins, L. D., Zuckermann, F. A. & Goldberg, T. L. (2005). Correlation of cell-mediated immunity against porcine reproductive and respiratory syndrome virus with protection against reproductive failure in sows during outbreaks of porcine reproductive and respiratory syndrome in commercial herds. *J Am Vet Med Assoc* **226**, 1707-1711.

Luftenegger, D., Picard-Maureau, M., Stanke, N., Rethwilm, A. & Lindemann, D. (2005). Analysis and function of prototype foamy virus envelope N glycosylation. *J Virol* **79**, 7664-7672.

Madsen, M., Moller, H. J., Nielsen, M. J., Jacobsen, C., Graversen, J. H., van den Berg, T. & Moestrup, S. K. (2004). Molecular characterization of the haptoglobin.hemoglobin receptor CD163. Ligand binding properties of the

scavenger receptor cysteine-rich domain region. *J Biol Chem* **279**, 51561-51567.

Mardassi, H., Gonin, P., Gagnon, C. A., Massie, B. & Dea, S. (1998). A subset of porcine reproductive and respiratory syndrome virus GP3 glycoprotein is released into the culture medium of cells as a non-virion-associated and membrane-free (soluble) form. *J Virol* **72**, 6298-6306.

Mardassi, H., Massie, B. & Dea, S. (1996). Intracellular synthesis, processing, and transport of proteins encoded by ORFs 5 to 7 of porcine reproductive and respiratory syndrome virus. *Virology* **221**, 98-112.

Mardassi, H., Mounir, S. & Dea, S. (1995). Molecular analysis of the ORFs 3 to 7 of porcine reproductive and respiratory syndrome virus, Quebec reference strain. *Arch Virol* **140**, 1405-1418.

Maric, M. A., Taylor, M. D. & Blum, J. S. (1994). Endosomal aspartic proteinases are required for invariant-chain processing. *Proc Natl Acad Sci U S A* **91**, 2171-2175.

Mascola, J. R. & Montefiori, D. C. (2003). HIV-1: nature's master of disguise. *Nat Med* **9**, 393-394.

Meier, W. A., Galeota, J., Osorio, F. A., Husmann, R. J., Schnitzlein, W. M. & Zuckermann, F. A. (2003). Gradual development of the interferon-gamma response of swine to porcine reproductive and respiratory syndrome virus infection or vaccination. *Virology* **309**, 18-31.

Meng, X. J., Paul, P. S., Halbur, P. G. & Lum, M. A. (1995). Phylogenetic analyses of the putative M (ORF 6) and N (ORF 7) genes of porcine reproductive and respiratory syndrome virus (PRRSV): implication for the existence of two genotypes of PRRSV in the U.S.A. and Europe. *Arch Virol* **140**, 745-755.

Meulenberg, J. J. (2000). PRRSV, the virus. *Vet Res* **31**, 11-21.

Meulenberg, J. J., Hulst, M. M., de Meijer, E. J., Moonen, P. L., den Besten, A., de Kluyver, E. P., Wensvoort, G. & Moormann, R. J. (1993). Lelystad virus, the causative agent of porcine epidemic abortion and respiratory syndrome (PEARS), is related to LDV and EAV. *Virology* **192**, 62-72.

Meulenberg, J. J., Petersen-den Besten, A., De Kluyver, E. P., Moormann, R. J., Schaaper, W. M. & Wensvoort, G. (1995). Characterization of proteins encoded by ORFs 2 to 7 of Lelystad virus. *Virology* **206**, 155-163.

Meulenberg, J. J., van Nieuwstadt, A. P., van Essen-Zandbergen, A., Bos-de Ruijter, J. N., Langeveld, J. P. & Meloen, R. H. (1998). Localization and fine mapping of antigenic sites on the nucleocapsid protein N of porcine reproductive and respiratory syndrome virus with monoclonal antibodies. *Virology* **252**, 106-114.

Meulenberg, J. J., van Nieuwstadt, A. P., van Essen-Zandbergen, A. & Langeveld, J. P. (1997). Posttranslational processing and identification of a neutralization domain of the GP4 protein encoded by ORF4 of Lelystad virus. *J Virol* **71**, 6061-6067.

Misinzo, G. M., Delputte, P. L. & Nauwynck, H. J. (2008). Involvement of proteases in porcine reproductive and respiratory syndrome virus uncoating upon internalization in primary macrophages. *Vet Res* **39**, 55.

Mondotte, J. A., Lozach, P. Y., Amara, A. & Gamarnik, A. V. (2007). Essential role of dengue virus envelope protein N glycosylation at asparagine-67 during viral propagation. *J Virol* **81**, 7136-7148.

Munday, J., Floyd, H. & Crocker, P. R. (1999). Sialic acid binding receptors (siglecs) expressed by macrophages. *J Leukoc Biol* **66**, 705-711.

Murtaugh, M. P., Elam, M. R. & Kakach, L. T. (1995). Comparison of the structural protein coding sequences of the VR-2332 and Lelystad virus strains of the PRRS virus. *Arch Virol* **140**, 1451-1460.

Murtaugh, M. P., Xiao, Z. & Zuckermann, F. (2002). Immunological responses of swine to porcine reproductive and respiratory syndrome virus infection. *Viral Immunol* **15**, 533-547.

Nauwynck, H. J., Duan, X., Favoreel, H. W., Van Oostveldt, P. & Pensaert, M. B. (1999). Entry of porcine reproductive and respiratory syndrome virus into porcine alveolar macrophages via receptor-mediated endocytosis. *J Gen Virol* **80 (Pt 2)**, 297-305.

Nedialkova, D. D., Ulferts, R., van den Born, E., Lauber, C., Gorbalenya, A. E., Ziebuhr, J. & Snijder, E. J. (2009). Biochemical characterization of arterivirus nonstructural protein 11 reveals the nidovirus-wide conservation of a replicative endoribonuclease. *J Virol* **83**, 5671-5682.

Nelson, E. A., Christopher-Hennings, J., Drew, T., Wensvoort, G., Collins, J. E. & Benfield, D. A. (1993). Differentiation of U.S. and European isolates of porcine reproductive and respiratory syndrome virus by monoclonal antibodies. *J Clin Microbiol* **31**, 3184-3189.

Ostrowski, M., Galeota, J. A., Jar, A. M., Platt, K. B., Osorio, F. A. & Lopez, O. J. (2002). Identification of neutralizing and nonneutralizing epitopes in the porcine reproductive and respiratory syndrome virus GP5 ectodomain. *J Virol* **76**, 4241-4250.

Pasternak, A. O., Spaan, W. J. & Snijder, E. J. (2006). Nidovirus transcription: how to make sense...? *J Gen Virol* **87**, 1403-1421.

Pasternak, A. O., van den Born, E., Spaan, W. J. & Snijder, E. J. (2001). Sequence requirements for RNA strand transfer during nidovirus discontinuous subgenomic RNA synthesis. *EMBO J* **20**, 7220-7228.

Paton, D. J., Brown, I. H., Edwards, S. & Wensvoort, G. (1991). 'Blue ear' disease of pigs. *Vet Rec* **128**, 617.

Pirzadeh, B. & Dea, S. (1997). Monoclonal antibodies to the ORF5 product of porcine reproductive and respiratory syndrome virus define linear neutralizing determinants. *J Gen Virol* **78 (Pt 8)**, 1867-1873.

Plagemann, P. G. (2006). Neutralizing antibody formation in swine infected with seven strains of porcine reproductive and respiratory syndrome virus as measured by indirect ELISA with peptides containing the GP5 neutralization epitope. *Viral Immunol* **19**, 285-293.

Plagemann, P. G., Rowland, R. R. & Faaberg, K. S. (2002). The primary neutralization epitope of porcine respiratory and reproductive syndrome virus strain VR-2332 is located in the middle of the GP5 ectodomain. *Arch Virol* **147**, 2327-2347.

Poon, A. F., Lewis, F. I., Pond, S. L. & Frost, S. D. (2007). Evolutionary interactions between N-linked glycosylation sites in the HIV-1 envelope. *PLoS Comput Biol* **3**, e11.

Ran, Z. G., Chen, X. Y., Guo, X., Ge, X. N., Yoon, K. J. & Yang, H. C. (2008). Recovery of viable porcine reproductive and respiratory syndrome virus from an infectious clone containing a partial deletion within the Nsp2-encoding region. *Arch Virol* **153**, 899-907.

Rawlings, N. D. & Barrett, A. J. (1995). Families of aspartic peptidases, and those of unknown catalytic mechanism. *Methods Enzymol* **248**, 105-120.

Reitter, J. N., Means, R. E. & Desrosiers, R. C. (1998). A role for carbohydrates in immune evasion in AIDS. *Nat Med* **4**, 679-684.

Roberts, J. J., Rodgers, S. E., Drury, J., Ashman, L. K. & Lloyd, J. V. (1995). Platelet activation induced by a murine monoclonal antibody directed against a novel tetra-span antigen. *Br J Haematol* **89**, 853-860.

Rodriguez, M. J., Sarraseca, J., Garcia, J., Sanz, A., Plana-Duran, J. & Ignacio Casal, J. (1997). Epitope mapping of the nucleocapsid protein of European and North American isolates of porcine reproductive and respiratory syndrome virus. *J Gen Virol* **78 (Pt 9)**, 2269-2278.

Rowland, R. R., Schneider, P., Fang, Y., Wootton, S., Yoo, D. & Benfield, D. A. (2003). Peptide domains involved in the localization of the porcine reproductive and respiratory syndrome virus nucleocapsid protein to the nucleolus. *Virology* **316**, 135-145.

Rowland, R. R., Steffen, M., Ackerman, T. & Benfield, D. A. (1999). The evolution of porcine reproductive and respiratory syndrome virus: quasispecies and emergence of a virus subpopulation during infection of pigs with VR-2332. *Virology* **259**, 262-266.

Rowland, R. R. & Yoo, D. (2003). Nucleolar-cytoplasmic shuttling of PRRSV nucleocapsid protein: a simple case of molecular mimicry or the complex regulation by nuclear import, nucleolar localization and nuclear export signal sequences. *Virus Res* **95**, 23-33.

Ruiz-Canada, C., Kelleher, D. J. & Gilmore, R. (2009). Cotranslational and posttranslational N-glycosylation of polypeptides by distinct mammalian OST isoforms. *Cell* **136**, 272-283.

Russell, J. S. a. D. W. (2001). *Molecular Cloning: A Laboratory Manual*. Cold Spring Harbor, New York: Cold Spring Harbor Laboratory Press.

Sanchez-Torres, C., Gomez-Puertas, P., Gomez-del-Moral, M., Alonso, F., Escribano, J. M., Ezquerra, A. & Dominguez, J. (2003). Expression of porcine CD163 on monocytes/macrophages correlates with permissiveness to African swine fever infection. *Arch Virol* **148**, 2307-2323.

Sarkar, G. & Sommer, S. S. (1990). The "megaprimer" method of site-directed mutagenesis. *Biotechniques* **8**, 404-407.

Sastradipura, D. F., Nakanishi, H., Tsukuba, T., Nishishita, K., Sakai, H., Kato, Y., Gotow, T., Uchiyama, Y. & Yamamoto, K. (1998). Identification of cellular compartments involved in processing of cathepsin E in primary cultures of rat microglia. *J Neurochem* **70**, 2045-2056.

Sawicki, D., Wang, T. & Sawicki, S. (2001). The RNA structures engaged in replication and transcription of the A59 strain of mouse hepatitis virus. *J Gen Virol* **82**, 385-396.

Sawicki, S. G. & Sawicki, D. L. (1995). Coronaviruses use discontinuous extension for synthesis of subgenome-length negative strands. *Adv Exp Med Biol* **380**, 499-506.

Sawicki, S. G. & Sawicki, D. L. (2005). Coronavirus transcription: a perspective. *Curr Top Microbiol Immunol* **287**, 31-55.

Scanlan, C. N., Offer, J., Zitzmann, N. & Dwek, R. A. (2007). Exploiting the defensive sugars of HIV-1 for drug and vaccine design. *Nature* **446**, 1038-1045.

Shanmukhappa, K., Kim, J. K. & Kapil, S. (2007). Role of CD151, A tetraspanin, in porcine reproductive and respiratory syndrome virus infection. *Virol J* **4**, 62.

Shen, S., Kwang, J., Liu, W. & Liu, D. X. (2000). Determination of the complete nucleotide sequence of a vaccine strain of porcine reproductive and respiratory syndrome virus and identification of the Nsp2 gene with a unique insertion. *Arch Virol* **145**, 871-883.

Shi, X., Brauburger, K. & Elliott, R. M. (2005). Role of N-linked glycans on bunyamwera virus glycoproteins in intracellular trafficking, protein folding, and virus infectivity. *J Virol* **79**, 13725-13734.

Shi, X. & Elliott, R. M. (2004). Analysis of N-linked glycosylation of hantaan virus glycoproteins and the role of oligosaccharide side chains in protein folding and intracellular trafficking. *J Virol* **78**, 5414-5422.

Sincock, P. M., Fitter, S., Parton, R. G., Berndt, M. C., Gamble, J. R. & Ashman, L. K. (1999). PETA-3/CD151, a member of the transmembrane 4 superfamily, is localised to the plasma membrane and endocytic system of endothelial cells, associates with multiple integrins and modulates cell function. *J Cell Sci* **112 (Pt 6)**, 833-844.

Snijder, E. J., Dobbe, J. C. & Spaan, W. J. (2003). Heterodimerization of the two major envelope proteins is essential for arterivirus infectivity. *J Virol* **77**, 97-104.

Snijder, E. J. & Meulenberg, J. J. (1998). The molecular biology of arteriviruses. *J Gen Virol* **79 (Pt 5)**, 961-979.

Snijder, E. J. & Spaan, W. J. M. (2007). *Fields' Virology*: Lippincott Williams & Wolters Kluwer Business.

Snijder, E. J., Wassenaar, A. L. & Spaan, W. J. (1994). Proteolytic processing of the replicase ORF1a protein of equine arteritis virus. *J Virol* **68**, 5755-5764.

Snijder, E. J., Wassenaar, A. L., Spaan, W. J. & Gorbalenya, A. E. (1995). The arterivirus Nsp2 protease. An unusual cysteine protease with primary structure similarities to both papain-like and chymotrypsin-like proteases. *J Biol Chem* **270**, 16671-16676.

Spaan, W., Delius, H., Skinner, M., Armstrong, J., Rottier, P., Smeekens, S., van der Zeijst, B. A. & Siddell, S. G. (1983). Coronavirus mRNA synthesis involves fusion of non-contiguous sequences. *EMBO J* **2**, 1839-1844.

Spilman, M. S., Welbon, C., Nelson, E. & Dokland, T. (2009). Cryo-electron tomography of porcine reproductive and respiratory syndrome virus: organization of the nucleocapsid. *J Gen Virol* **90**, 527-535.

Stadejek, T., Stankevicius, A., Storgaard, T., Oleksiewicz, M. B., Belak, S., Drew, T. W. & Pejsak, Z. (2002). Identification of radically different variants of porcine reproductive and respiratory syndrome virus in Eastern Europe: towards a common ancestor for European and American viruses. *J Gen Virol* **83**, 1861-1873.

Sun, Y., Xue, F., Guo, Y., Ma, M., Hao, N., Zhang, X. C., Lou, Z., Li, X. & Rao, Z. (2009). Crystal structure of porcine reproductive and respiratory syndrome virus leader protease Nsp1alpha. *J Virol* **83**, 10931-10940.

Tarr, A. W., Owsianka, A. M., Timms, J. M., McClure, C. P., Brown, R. J., Hickling, T. P., Pietschmann, T., Bartenschlager, R., Patel, A. H. & Ball, J. K. (2006). Characterization of the hepatitis C virus E2 epitope defined by the broadly neutralizing monoclonal antibody AP33. *Hepatology* **43**, 592-601.

Thanawongnuwech, R., Young, T. F., Thacker, B. J. & Thacker, E. L. (2001). Differential production of proinflammatory cytokines: in vitro PRRSV and Mycoplasma hyopneumoniae co-infection model. *Vet Immunol Immunopathol* **79**, 115-127.

Truong, H. M., Lu, Z., Kutish, G. F., Galeota, J., Osorio, F. A. & Pattnaik, A. K. (2004). A highly pathogenic porcine reproductive and respiratory syndrome virus generated from an infectious cDNA clone retains the in vivo virulence and transmissibility properties of the parental virus. *Virology* **325**, 308-319.

van Aken, D., Zevenhoven-Dobbe, J., Gorbalenya, A. E. & Snijder, E. J. (2006). Proteolytic maturation of replicase polyprotein pp1a by the nsp4 main proteinase is essential for equine arteritis virus replication and includes internal cleavage of nsp7. *J Gen Virol* **87**, 3473-3482.

Van Breedam, W., Van Gorp, H., Zhang, J. Q., Crocker, P. R., Delputte, P. L. & Nauwynck, H. J. (2010). The M/GP(5) glycoprotein complex of porcine reproductive and respiratory syndrome virus binds the sialoadhesin receptor in a sialic acid-dependent manner. *PLoS Pathog* **6**, e1000730.

Van Gorp, H., Van Breedam, W., Delputte, P. L. & Nauwynck, H. J. (2008). Sialoadhesin and CD163 join forces during entry of the porcine reproductive and respiratory syndrome virus. *J Gen Virol* **89**, 2943-2953.

Van Gorp, H., Van Breedam, W., Van Doorsselaere, J., Delputte, P. L. & Nauwynck, H. J. (2010). Identification of the CD163 protein domains

involved in infection of the porcine reproductive and respiratory syndrome virus. *J Virol* **84**, 3101-3105.

van Marle, G., Dobbe, J. C., Gultyaev, A. P., Luytjes, W., Spaan, W. J. & Snijder, E. J. (1999). Arterivirus discontinuous mRNA transcription is guided by base pairing between sense and antisense transcription-regulating sequences. *Proc Natl Acad Sci U S A* **96**, 12056-12061.

van Nieuwstadt, A. P., Meulenberg, J. J., van Essen-Zanbergen, A., Petersen-den Besten, A., Bende, R. J., Moormann, R. J. & Wensvoort, G. (1996). Proteins encoded by open reading frames 3 and 4 of the genome of Lelystad virus (Arteriviridae) are structural proteins of the virion. *J Virol* **70**, 4767-4772.

Van Reeth, K., Labarque, G., Nauwynck, H. & Pensaert, M. (1999). Differential production of proinflammatory cytokines in the pig lung during different respiratory virus infections: correlations with pathogenicity. *Res Vet Sci* **67**, 47-52.

Vanderheijden, N., Delputte, P., Nauwynck, H. & Pensaert, M. (2001). Effects of heparin on the entry of porcine reproductive and respiratory syndrome virus into alveolar macrophages. *Adv Exp Med Biol* **494**, 683-689.

Vanderheijden, N., Delputte, P. L., Favoreel, H. W., Vandekerckhove, J., Van Damme, J., van Woensel, P. A. & Nauwynck, H. J. (2003). Involvement of sialoadhesin in entry of porcine reproductive and respiratory syndrome virus into porcine alveolar macrophages. *J Virol* **77**, 8207-8215.

Vashisht, K., Goldberg, T. L., Husmann, R. J., Schnitzlein, W. & Zuckermann, F. A. (2008). Identification of immunodominant T-cell epitopes present in glycoprotein 5 of the North American genotype of porcine reproductive and respiratory syndrome virus. *Vaccine* **26**, 4747-4753.

Verheije, M. H., Welting, T. J., Jansen, H. T., Rottier, P. J. & Meulenberg, J. J. (2002). Chimeric arteriviruses generated by swapping of the M protein ectodomain rule out a role of this domain in viral targeting. *Virology* **303**, 364-373.

Vigerust, D. J. & Shepherd, V. L. (2007). Virus glycosylation: role in virulence and immune interactions. *Trends Microbiol* **15**, 211-218.

Wang, X., Eaton, M., Mayer, M., Li, H., He, D., Nelson, E. & Christopher-Hennings, J. (2007). Porcine reproductive and respiratory syndrome virus productively infects monocyte-derived dendritic cells and compromises their antigen-presenting ability. *Arch Virol* **152**, 289-303.

Wassenaar, A. L., Spaan, W. J., Gorbalenya, A. E. & Snijder, E. J. (1997). Alternative proteolytic processing of the arterivirus replicase ORF1a polyprotein: evidence that NSP2 acts as a cofactor for the NSP4 serine protease. *J Virol* **71**, 9313-9322.

Wei, X., Decker, J. M., Wang, S., Hui, H., Kappes, J. C., Wu, X., Salazar-Gonzalez, J. F., Salazar, M. G., Kilby, J. M., Saag, M. S., Komarova, N. L., Nowak, M. A., Hahn, B. H., Kwong, P. D. & Shaw, G. M. (2003). Antibody neutralization and escape by HIV-1. *Nature* **422**, 307-312.

Wesley, R. D., Lager, K. M. & Kehrli, M. E., Jr. (2006). Infection with Porcine reproductive and respiratory syndrome virus stimulates an early gamma interferon response in the serum of pigs. *Can J Vet Res* **70**, 176-182.

Wesley, R. D., Mengeling, W. L., Lager, K. M., Vorwald, A. C. & Roof, M. B. (1999). Evidence for divergence of restriction fragment length polymorphism patterns following in vivo replication of porcine reproductive and respiratory syndrome virus. *Am J Vet Res* **60**, 463-467.

Whitley, P., Nilsson, I. M. & von Heijne, G. (1996). A nascent secretory protein may traverse the ribosome/endoplasmic reticulum translocase complex as an extended chain. *J Biol Chem* **271**, 6241-6244.

Wieringa, R., de Vries, A. A., van der Meulen, J., Godeke, G. J., Onderwater, J. J., van Tol, H., Koerten, H. K., Mommaas, A. M., Snijder, E. J. & Rottier, P. J. (2004). Structural protein requirements in equine arteritis virus assembly. *J Virol* **78**, 13019-13027.

Wissink, E. H., Kroese, M. V., Maneschijn-Bonsing, J. G., Meulenberg, J. J., van Rijn, P. A., Rijsewijk, F. A. & Rottier, P. J. (2004). Significance of the oligosaccharides of the porcine reproductive and respiratory syndrome virus glycoproteins GP2a and GP5 for infectious virus production. *J Gen Virol* **85**, 3715-3723.

Wissink, E. H., Kroese, M. V., van Wijk, H. A., Rijsewijk, F. A., Meulenberg, J. J. & Rottier, P. J. (2005). Envelope protein requirements for the assembly of infectious virions of porcine reproductive and respiratory syndrome virus. *J Virol* **79**, 12495-12506.

Wojczyk, B. S., Takahashi, N., Levy, M. T., Andrews, D. W., Abrams, W. R., Wunner, W. H. & Spitalnik, S. L. (2005). N-glycosylation at one rabies virus glycoprotein sequon influences N-glycan processing at a distant sequon on the same molecule. *Glycobiology* **15**, 655-666.

Wootton, S., Yoo, D. & Rogan, D. (2000). Full-length sequence of a Canadian porcine reproductive and respiratory syndrome virus (PRRSV) isolate. *Arch Virol* **145**, 2297-2323.

Wootton, S. K., Rowland, R. R. & Yoo, D. (2002). Phosphorylation of the porcine reproductive and respiratory syndrome virus nucleocapsid protein. *J Virol* **76**, 10569-10576.

Wootton, S. K. & Yoo, D. (2003). Homo-oligomerization of the porcine reproductive and respiratory syndrome virus nucleocapsid protein and the role of disulfide linkages. *J Virol* **77**, 4546-4557.

Wu, W. H., Fang, Y., Rowland, R. R., Lawson, S. R., Christopher-Hennings, J., Yoon, K. J. & Nelson, E. A. (2005). The 2b protein as a minor structural component of PRRSV. *Virus Res* **114**, 177-181.

Wyatt, R., Kwong, P. D., Desjardins, E., Sweet, R. W., Robinson, J., Hendrickson, W. A. & Sodroski, J. G. (1998). The antigenic structure of the HIV gp120 envelope glycoprotein. *Nature* **393**, 705-711.

Xue, F., Sun, Y., Yan, L., Zhao, C., Chen, J., Bartlam, M., Li, X., Lou, Z. & Rao, Z. (2010). The Crystal Structure of the PRRSV Nonstructural Protein Nsp1{beta} Reveals a Novel Metal-dependent Nuclease. *J Virol*.

Yang, L., Frey, M. L., Yoon, K. J., Zimmerman, J. J. & Platt, K. B. (2000). Categorization of North American porcine reproductive and respiratory syndrome viruses: epitopic profiles of the N, M, GP5 and GP3 proteins and susceptibility to neutralization. *Arch Virol* **145**, 1599-1619.

Yoo, D., Wootton, S. K., Li, G., Song, C. & Rowland, R. R. (2003). Colocalization and interaction of the porcine arterivirus nucleocapsid protein with the small nucleolar RNA-associated protein fibrillarin. *J Virol* **77**, 12173-12183.

Ziebuhr, J., Snijder, E. J. & Gorbalenya, A. E. (2000). Virus-encoded proteinases and proteolytic processing in the Nidovirales. *J Gen Virol* **81**, 853-879.

Zuniga, S., Sola, I., Alonso, S. & Enjuanes, L. (2004). Sequence motifs involved in the regulation of discontinuous coronavirus subgenomic RNA synthesis. *J Virol* **78**, 980-994.